UNIVERSITÀ DEGLI STUDI DI PADOVA

Dipartimento di Fisica e Astronomia "Galileo Galilei"

Master Degree in Physics

Final Dissertation

On UV Sensitivities of Non-renormalizable Operators for Freeze-In Production of Dark Matter in Modified Cosmologies

Thesis supervisor

Dr. Francesco D'Eramo

Candidate

Emanuele Copello

Academic Year 2018/2019

Contents

Introduction

Dark Matter (DM) has become more than a suggestion nowadays: it is an experimental evidence. However, we still know little or nothing about its nature and the most wanted candidate, a weakly interacting massive particle (WIMP) is challenged by experimental data, since no conclusive signals, despite considerable search campaigns, have been observed[1]. New models to explain DM nature are continuously emerging and, along the theoretical particle physics side, an increasing attention is being paid on modifications of the standard cosmological scenario. The reason is simple; if after cosmic inflation the Universe was not merely radiation-dominated up to Big Bang Nucleosynthesis (BBN), potential alterations could have had an important impact on both particle production (hence on particle phenomenology) and cosmological signatures.

Among the possible way to produce a DM particle candidate in the early Universe, one of the most appealing is certainly the freeze-in mechanism, which was originally proposed[2] as a non-thermal alternative to the standard thermal freeze-out. Basically, some particle X is supposed to be negligibly abundant at the beginning and to have very feeble renormalizable interactions with the hot plasma, so that it had never had the chance to be in thermal equilibrium with the visible sector (it is called FIMP, Feebly Interacting Massive Particle).

Yet, these interactions (e.g. decay of a particle of the visible sector heat bath, or single and pair productions via scatterings or annihilations of bath particles) are enough to provide some X production, which becomes increasingly efficient as the temperature lowers towards the heaviest mass involved in the process. Once the temperature drops below this value, the abundance of the parent particle(s) is Maxwell-Boltzmann-suppressed and the number density of X freezes to a constant value. Therefore, X production is IR-dominated by low temperatures of order the dominating physical scale and is independent of unknown UV quantities, such as the reheat temperature T_{RH} after inflation. Once produced, the X particles simply red-shift away with the expanding Universe and are still present today as a cosmic relic.

[1] G. Arcadi et al. "The waning of the WIMP? A review of models, searches, and constraints" Eur.Phys.J. C78 (2018) no.3, 203 arXiv:1703.07364

[2] L. J. Hall, K. Jedamzik, J. March-Russell, S. T. West "Freeze-In Production of FIMP Dark Matter" JHEP **1003** (2010) 080 arXiv:0911.1120

However, if one considers modified cosmological histories or interactions mediated by non-renormalizable operators, this IR-domination needs to be revisited. The first ones are motivated by a variety of theoretical frameworks and do not encounter experimental exclusion, since no stringent bounds on the physics of the Universe at temperatures above $1 - 20$ MeV exist, where, instead, we know that the BBN theory has proved to be successful. The latter find many inspirations in Beyond the Standard Model (BSM) scenarios and in Effective Field Theory (EFT) approaches.

In fact, as recently demonstrated[3], if one accounts for a modified, pre-BBN expansion history in which the energy density of a new scalar species ϕ scales as $\rho_\phi \propto a^{-(4+n)}$, with $n > 0$, then the relic DM density is significantly lower than the one obtained in a standard scenario (the difference can span ten orders of magnitude), as a result of the equality between the (faster) expansion rate and the thermal processes rates occurring at earlier times. Therefore, in order to provide the observed relic abundance, larger couplings between dark matter and the visible sector are needed, predicting a strong enhancement in potential signals for FIMPs detection.

Moreover, multi-production of DM through scattering processes is IR-dominated only for operators whose mass dimension satisfies $d < 4.5 + n/4$. Hence, some non-standard cosmologies allow for the contribution of non-renormalizable interactions even at low temperatures. In addition to this, the freeze-in mechanism mediated by irrelevant operators has the advantage that the very tiny couplings required in the original scheme become somewhat more natural, because the suppression is already provided by the UV-cutoff mass scale in the effective lagrangian.

In this thesis work we mainly study two motivated scenarios: kination-dominated (KD) and non-adiabatic matter-dominated (MD_{NA}) regimes. The first ones can be seen as cosmological theories with $n = 2$, with an energy density red-shifting as $\rho_\phi \propto a^{-6}$; scenarios of this kind are those driven by quintessential fluids, inspired by the discovery of the accelerated expansion of the universe. The KD phase happens when the kinetic energy density dominates over the potential, which then evolves towards a potential energy density dominated phase, mimicking a cosmological constant. One possible scalar potential leading to this behavior is the exponential form $V(\phi) = V_0 \exp[-\lambda\phi]$, where ϕ is the quintessential scalar field. Regarding DM production, this scenario has already been addressed in the context of thermal WIMPs[4] and neutralino dark matter in particular[5].

Furthermore, when operators have dimensions greater than four, a crucial point regards the reheating phase after Inflation. It has already been studied how particle

[3]F. D'Eramo, N. Fernandez, S. Profumo "Dark Matter Freeze-in Production in Fast-Expanding Universes" JCAP **1802** (2018) no.02, 046 arXiv:1712.07453

[4]C. Pallis "Quintessential kination and cold dark matter abundance" JCAP **0510** (2005) 015 arXiv:hep-ph/0503080.

[5]S. Profumo, P. Ullio "SUSY dark matter and quintessence" JCAP **0311** (2003) 006 arXiv:hep-ph/0309220.

production could be affected if happened during a prolonged matter-dominated phase, such as the non-adiabatic epoch of coherent oscillations of the decaying inflaton[6] [7]. In this respect, a pivotal feature to be considered is the duration of this stage, since a low reheating temperature scenario would seriously affect the final relic abundance, either through the faster expanding background, or with the large entropy release after decays, both depleting the comoving number density of DM particles.

This thesis aims at studying how non-renormalizable operators and modifications of the standard cosmological scenarios affect FIMP production, which we choose to be a TeV-scale Dirac fermion, stabilised by some internal symmetry. The main focus is on dimension-5 operators and we choose a simple fermionic Higgs portal operator as a case study, without the presumption of digging into the details of the EFT of BSM physics. FIMP production occurs through annihilations of the massless Higgs complex scalars in the thermal bath: this interaction is determined by the reheating temperature in standard RD scenarios, while for KD or faster cosmologies it shifts towards an IR production. The behavior during an non-adiabatic MD epoch, instead, is scrambled by an extreme IR-dominance due to the non-conservation of entropy.

An interesting feature of the kination configuration is that both the rate of interaction Γ and the Hubble parameter H scale with the temperature as T^3, providing a nearly constant ratio $\Gamma/H \sim const.$ This means that the information on the relevant physical scale involved in the process gets lost and implications of this behavior needs to be studied.

The thesis is subdivided into five chapters. In *Chapter 1*, we introduce the concept of particle production in the early Universe and we provide some examples of relevant processes; *Chapter 2* is wholly dedicated to the development of the Boltzmann equation formalism; in *Chapter 3*, we review and analyze some modifications of the standard early cosmological scenario; in *Chapter 4*, we study the role of the fermionic Higgs portal during an early, non-adiabatic, matter-dominated epoch; finally, *Chapter 5* regards the UV sensitivity of non-renormalizable operators in (adiabatic) faster-than-radiation cosmologies, where we provide both semi-analytical and numerical solutions for generic scalar fields and for a quintessential kination scenario. Appendix A provides a short compendium of pivotal cosmological quantities, while Appendix B includes the notation and the calculations of matrix elements and cross-sections.

[6] G. F. Giudice, E. W. Kolb, A. Riotto "Largest temperature of the radiation era and its cosmological implications" Phys.Rev. D64 (2001) 023508 arXiv:hep-ph/0005123.

[7] R. T. Co, F. D'Eramo, L. J. Hall, D. Pappadopulo "Freeze-In Dark Matter with Displaced Signatures at Colliders" JCAP **1512** (2015) no.12, 024 arXiv:1506.07532.

Chapter 1

Particle Production in the Early Universe

The Standard Model of Particle Physics (SM) is the best theory we have to describe the nature and the behavior of all up-to-now discovered elementary particles and three of their four fundamental interactions: the electromagnetic, the weak nuclear and the strong nuclear forces. As we witness the hierarchical nature of the energy scale at which these interactions become important, it turns to be natural to think that all the SM particles must have been produced at a given moment in the early history of the Universe. However, there are many aspects of observed Physics that have no place in the SM picture; for example, an explanation for neutrino masses, Dark Matter (DM) and Dark Energy (DE), the nature of Inflation and other important shortcomings which call for broad extensions of well-established paradigms to a more complete "Beyond the Standard Model" (BSM) theory.

Evidences of these elusive phenomena come from a variety of direct and indirect discoveries, among which the observation of the percentage of the total energy budget of the Universe retained by each species i, measured by the *density parameter* Ω_i, defined as the ratio ρ_i/ρ_c between the energy density of the species i and the *critical energy density* of the Universe (the one which would make it spatially flat). Two macroscopic ingredients compose it: non-relativistic matter ($\Omega_m = 0.315 \pm 0.007$) and dark energy ($\Omega_\Lambda = 0.6847 \pm 0.0073$, where Λ indicates the contribution of DE in the form of a cosmological constant). The first one is divided into a non-baryonic content, cold dark matter (CDM) ($\Omega_c h^2 = 0.120 \pm 0.001$) and baryonic matter ($\Omega_b h^2 = 0.0224 \pm 0.0001$), where $h \simeq 0.7$. The remaining contribution is in the form of neutrinos ($\Omega_\nu h^2 \lesssim 0.016$) and a completely negligible photon component ($\Omega_r h^2 \sim 10^{-5}$). These results are in agreement with the fact that we observe a Universe which is almost perfectly flat in space, that is to say $\Omega_{TOT} = \sum_i \Omega_i = 1$ (spatial curvature number density amounts to $\Omega_K = 0.001 \pm 0.002$) [1]. The standard model of modern cosmology is thus called "the ΛCDM model" and we refer to Appendix A for a short review.

Another important result is the nice compatibility of SM and ΛCDM predictions on the number of light degrees of freedom with data from the CMB, BBN and LSS;

deviations of this observable would imply an evidence for the presence of particles not included in the SM picture, and/or a modifications of the standard cosmological scenario. The way this effect is historically parameterized is by measuring alterations of the energy density of neutrinos from that of photons, which are related by $\rho_\nu/\rho_\gamma \simeq 0.2N_{eff.}$, with the SM+$\Lambda$CDM models predicting $N_{eff} = 3.045$. Again, Planck data show that $N_{eff} = 2.99^{+0.34}_{-0.33}$, in good agreement with theory, but leaving still for a narrow open window of values (see Section 1.4 for a discussion).

Among the others, the way new exotic particles might have been created at early times is crucial to investigate their properties. In short, the overall picture is that after Inflation the Universe was an extremely hot soup of relativistic particles, each of which created with some mechanism, whose classification is commonly divided into two broad categories:

- Production at thermal equilibrium;
- Non-thermal production.

The "thermal equilibrium" condition refers to the ability of the particles to interact quickly enough to attain an average collective temperature; this situation is quite common at very high temperatures, but gets jeopardized by the expansion of the Universe, which tends to physically separate the particles, making their number density smaller while cooling down the system. Eventually, at some temperature T the rate of interaction $\Gamma(T)$ becomes smaller than the rate of expansion of the Universe $H(T)$, so that a net amount of particles *decouples* from the hot plasma and remains as a relic throughout the entire history of the Universe, unless it gets involved in other processes (e.g. nucleosynthesis). We say that these particles have undergone to *freeze-out*.

However, in the recent literature, an increasing attention has been paid to *non-thermal* mechanisms, by which the produced particles never had the chance to attain a tight coupling with the background medium and reach thermal equilibrium; alternatively, its genesis goes along in a non-trivial way. Concretely, some non-equilibrium processes are baryogenesis [2], some types of axion generation [3, 4], the freeze-in mechanism [5], asymmetric dark matter [6] and production of superheavy particles [7]. This thesis is mainly focused on out-of-equilibrium mechanisms and we will postpone to Section 1.3 the explanation of how could a relic abundance be formed in these situations.

As a last comment, we stress that particle production reduces to a careful balance between Γ and H; the dynamical, quantitative and precise way to characterize the evolution of the properties of particles involved in the various processes is with the resolution of the Boltzmann equations in the expanding Universe. We leave this discussion to Chapter 2. In this chapter, we will give just a qualitative description and we will outline some cases of interest for the physical contextualization of this thesis work.

1.1 A primordial plasma of SM particles

In order to make a precise classification of the nature of the particles in the Early Universe, we say that, when they are at thermal equilibrium, sharing a certain temperature T, they are considered as

relativistic if their mass is $m < T$,

non-relativistic if their mass is $m > T$.

Hence, well above the scale of electroweak symmetry breaking (EWSB), $\Lambda_{EW} \sim 246$ GeV, all the fermions and bosons of the SM can be treated as ultra-relativistic. They form a hot, highly-interacting plasma, with a rate of interaction typically given by

$$\Gamma \equiv n\langle\sigma v\rangle, \tag{1.1}$$

where n is the number density of some particle species, σ its interaction cross section with the background plasma, v the relative velocity and the angular parentheses indicate a thermal average over some distribution of interest. In this environment, the only relevant physical scale is the temperature T, so that $n \sim T^3$ by dimensional analysis. The cross section (see Appendix B for a resume on notation and formulae for particle interactions) is given by $|\mathcal{M}|^2/T^2$, where $|\mathcal{M}|^2$ is the amplitude squared of the involved interaction.

For example, if this is mediated by a massless gauge boson, we roughly have $|\mathcal{M}|^2 \sim \alpha^2$, where $\alpha \sim g^2/4\pi$ is a generalized structure constant and g a gauge coupling. Hence, we obtain

$$\sigma \sim \frac{\alpha^2}{T^2}.$$

Therefore, the interaction rate reads

$$\Gamma = n\sigma v \sim T^3\frac{\alpha^2}{T^2} \sim \alpha^2 T. \tag{1.2}$$

As we said, this needs to be compared with the Hubble rate, given by (see Appendix A)

$$H = \frac{\sqrt{\rho}}{\sqrt{3}M_P} \sim \frac{T^2}{M_P}, \tag{1.3}$$

where we assumed a radiation-dominated era and used $\rho \sim T^4$ from dimensional analysis and $M_P = (8\pi G)^{-1/2} \simeq 2.4 \times 10^{18}$ GeV, the reduced Planck mass. Hence,

$$\frac{\Gamma}{H} \sim \frac{\alpha^2 M_P}{T}, \tag{1.4}$$

so that for $\Lambda_{EW} < T \lesssim \alpha^2 M_P \sim 10^{16}$ GeV, reactions are fast enough, while in the opposite case they are "frozen".

We refer to Appendix A for a better treatment of the Thermodynamics in the early Universe; the main result is that *at thermal equilibrium* we can describe all the relevant variables in terms of integrals over the occupation number per unit volume in phase space, or *distribution function*, of a given species,

$$f(E,T) = \frac{1}{e^{E/T} \pm 1}, \tag{1.5}$$

where the + is for fermionic species (Fermi-Dirac distribution) and − is for bosonic species (Bose-Einstein distribution) [8]. This is translated into a Maxwell-Boltzmann form, $f \sim e^{-E/T}$, when the energy of the involved particles are extremely high. As a consequence, relativistic particles, also called *radiation*, are the ones that dominate the primordial plasma. In particular, the important aspect to bear in mind is the asymptotic behavior of the number density, which is roughly given by

$$\begin{aligned} n_{rel} &\sim T^3 \quad \text{if} \quad m \ll T, \\ n_{non-rel} &\sim (mT)^{3/2} \exp(-m/T) \quad \text{if} \quad m \gg T. \end{aligned}$$

We notice the so-called *Boltzmann suppression factor*, which enhances the depletion of the number density of non-relativistic particles that remain in equilibrium as soon as the temperatures drops beneath their masses; these particles are gradually washed out by the cooling of the Universe and become soon negligible, unless they manage to escape the coupling with the thermal bath.

In general, as the Universe expands, H overtakes the interaction rate at some freeze-out temperature $T_{f.o.}$. From that moment, the decoupled particles and the plasma behave as two distinct, disconnected fluids. This decoupling could have happened either if the involved particles were still relativistic at $T_{f.o.}$, or if they had already become non-relativistic. The crucial difference between the two cases is that, in the latter, particles may had tracked their equilibrium abundances for a long period, having already been exponentially suppressed. The first type of relic is called *hot*, the second *cold*.

Probably, the most famous hot relics are neutrinos, whose freeze-out temperature is around 1 MeV, much greater than their mass, smaller than $\sim$ eV [9] (see next Section). Other pivotal predictions of particle production in the early Universe is the formation of the first nuclei and atoms, theorized with Big Bang Nucleosynthesis and Recombination and confirmed with an outstanding accuracy [1, 2, 8, 9]. We will not discuss them here.

A common crucial feature of almost all the relevant epochs in the standard scenario is that entropy is conserved in a comoving volume, that is to say

$$\dot{S} = \frac{\mathrm{d}}{\mathrm{d}t}(sa^3) = 0 \implies s \propto a^{-3}, \tag{1.6}$$

where we have defined the entropy density as $s = S/a^3$, with a the scale factor. This allows us to use entropy as a "tracker" for the expansion of the Universe, letting us

define comoving quantities simply dividing by s. For example, it is customary to introduce a *comoving number density* as

$$Y = \frac{n}{s}. \tag{1.7}$$

Examples in which entropy is not conserved are discussed in [10–12] and refer to the period after conventional inflation, the reheating phase, during which the inflaton decays, emitting lots of radiation and entropy in the Universe.

To sum up, the central point to have in mind is that, in the earliest epochs, SM particles behave as a single highly-relativistic hot plasma, a kind of extremely interacting *background medium* from which, eventually, some particle will departure, depending on its characteristics and its couplings with the thermal bath. Dark matter and other BSM particles may or may not have been in thermal contact with this ancestral plasma, but all good DM candidates require a (at least not very large) coupling with something that certainly already existed, like radiation. The possibility that they may have been produced gravitationally, or directly from the inflaton decay (see Section 1.3.1) is not excluded a priori, but a primordial "ocean" of relativistic particles (with an essentially zero chemical potential) is a much more likely initial situation for the generation of the first seeds.

1.2 Thermal decoupling: freeze-out mechanism

We still do not know how SM (or BSM) particles were exactly produced in the Early Universe. For instance, the commonly accepted hypothesis is that at the very high energies ($E \gtrsim 1$ TeV) new physics must enter the game and all the particles and interactions we know might come from a common picture, ruled by some large symmetry which has the SM as its low-energy effective description (e.g. GUT, Supersymmetry, String Theory, etc.) [9]. The breaking of these symmetries, if any, differentiates the particle zoo and the precise mechanism by which this happens is a matter of wild discussion and speculation among theoretical physicists. Nevertheless, important paradigms have been reached so far and in this section we want to discuss probably the most common one: thermal freeze-out.

As we said previously, with this mechanism we essentially look for situations in which

$$\begin{aligned} \Gamma \gtrsim H &\implies \text{thermal equilibrium}, \\ \Gamma \lesssim H &\implies \text{thermal decoupling}. \end{aligned}$$

When $\Gamma \sim H$, the typical timescale of the interactions is comparable with the age of the Universe. From that moment on, a net amount of particles leaves the thermal bath and forms a relic species, which evolves throughout the history of the Universe, simply by redshifting away. We want to use this rule of thumb to give a glimpse of the idea behind thermal decoupling, leaving the formal (and correct) discussion to Chapter 2.

1.2.1 Hot relics

To estimate the freeze-out temperature $T_{f.o.}$, we simply demand

$$n(T_{f.o,})\,\sigma(T_{f.o.}) = H(T_{f.o.}) \implies T_{f.o.}^3\sigma(T_{f.o.}) \simeq T_{f.o.}^2/M_p,$$

where we put $v = 1$ and we supposed to be fully inside the radiation era; in a standard cosmological scenario, this is a reasoned hypothesis, since the production of every elementary particle must have happened before the BBN, in order not to disrupt the excellent agreement we have between theoretical predictions and observations up to $T_{BBN} \sim 1$ MeV, hence well before the matter era[1]. A modification of the standard scheme would imply a careful study of when radiation dominated and when not before BBN.

Therefore, the freeze-out temperature crucially depends on the cross section of the particular process we are considering. As an example, if we consider neutrinos, we can think of $T_{f.o.}$ much lower than the mass of the gauge bosons of electroweak interactions ($M_W \lesssim 100$ GeV) and use Fermi's effective theory. The cross section is $\sigma \sim T^2 G_F^2$, with $G_F \sim 10^{-5}$ GeV^{-2} the Fermi constant. Neutrino decoupling is thus efficient at

$$T_\nu^3\, G_F^2\, T_\nu^2 \simeq 1/M_P \implies T_\nu \sim (G_F^2 M_P)^{-1/3} \sim 1\,\mathrm{MeV},$$

which confirms the validity of Fermi's effective description[2].

If the expansion of the Universe proceed adiabatically, the comoving number density is a conserved quantity, meaning that $Y_0 = Y_{f.o.}$, where the subscript "0" means "today". Accordingly, we can derive the energy density of neutrinos today as

$$\rho_{\nu,0} = m_\nu n_{\nu 0} = m_\nu Y_{\nu 0}\, s_0 = m_\nu Y_{\nu,f.o.}\, s_0$$

and compare it with the critical energy density. The density parameter of neutrinos is thus

$$\Omega_\nu h^2 = \frac{\rho_{\nu,0}}{\rho_c} h^2 \simeq \frac{m_\nu}{91.5\,\mathrm{eV}}. \tag{1.8}$$

We know from cosmological observations that the current value for the dark matter density parameter is $\Omega_{DM} h^2 = 0.120 \pm 0.001$ and that neutrino masses are constrained by $\sum m_\nu < 0.12$ eV [1]. This is one of the most stringent arguments that exclude neutrinos among the candidates for dark matter. In addition to this, SM neutrinos cannot constitute a significant part of dark matter because this upper limit on their mass implies that they would freely stream on scales of many Mpc and hence wash out the density fluctuations observed at these scales.

[1] The temperature of matter-radiation equality is around 1 eV.

[2] Actually, the temperature for neutrino decoupling is slightly higher, $T_\nu \sim 2$ MeV.

1.2.2 Cold relics: a WIMP miracle

For non-relativistic relics we need to use the equilibrium number density

$$n = g\left(\frac{m\,T}{2\pi}\right)^{3/2} e^{-m/T}.$$

Hence, the freeze-out condition now reads

$$n_{f.o.}\sigma \simeq T_{f.o.}^2/M_p \implies (m\,T_{f.o.})^{3/2}\, e^{-m/T_{f.o.}}\,\sigma \simeq T_{f.o.}^2/M_p. \tag{1.9}$$

By defining the "time variable" $x = m/T$, we obtain the transcendental equation

$$\sqrt{x}\, e^{-x} = \frac{1}{m\, M_P\, \sigma}. \tag{1.10}$$

Clearly, we are in the situation with $x > 1$ and typical values for freeze-out temperatures entail a range $x_{f.o.} \simeq 20 - 50$, depending on the r.h.s of the equation. The values vary in a small interval because the dependence of $x_{f.o.}$ on the microphysics, namely the mass and the cross section, is only logarithmic.

The most famous cold thermal relics are Weakly Interacting Massive Particles (WIMPs) [2, 13], historically the most promising candidates for cold dark matter.

Basically, if χ is a WIMP, from the density parameter

$$\Omega_\chi = \frac{m_\chi n_{\chi,0}}{\rho_c} = \frac{m_\chi T_0^3}{\rho_c}\frac{n_{f.o.}}{T_{f.o.}^3} = \left(\frac{T_0^3}{\rho_c M_P}\right)\frac{x_{f.o.}}{\sigma},$$

we have

$$\Omega_\chi \simeq 0.2\left(\frac{x_{f.o.}}{20}\right)\left(\frac{10^{-8}\,\mathrm{GeV}^{-2}}{\sigma}\right). \tag{1.11}$$

This is what in literature is called the "WIMP miracle": the cross section needed to provide the observed DM relic abundance is typical of the electroweak interactions. Hence, a particle electroweak-interacting, with masses around the electroweak scale, $\Lambda_{EW} \sim 200$ GeV, might be a good cold dark matter candidate, hence the name WIMP. The fact that not far from this scale we do expect the rise of new physics, makes this setup very attractive, with several hypothetical signatures from terrestrial and space experiments. Among the most important sources of their popularity is the fact that solutions to the Higgs hierarchy problem typically require new weakly-interacting particles not much above the electroweak scale [9, 14–16]. In addition to this, one obviously requires this candidate to be stable (at least with a lifetime of order the age of the Universe) and electrically neutral (the Universe is neutral on average and we do not observe electromagnetic signatures of DM, hence the name "dark").

This "golden" number can also be written as the average of the cross-section times velocity, a quantity that appears in the r.h.s of the Boltzmann equation for the number density of DM particles. Accounting for a typical WIMP velocity of $v \sim c/3$ at the time of freeze-out, one finds the following very famous quantity

$$\langle\sigma v\rangle \sim 3 \times 10^{-26}\ \mathrm{cm}^3/s, \tag{1.12}$$

usually referred to as a benchmark for WIMP searches experiments.

To contain the excitement for this peculiarity, we notice that this "miracle" is a consequence of having required $x \gg 1 \implies m\,\sigma\,M_P \gg 1$ and $\sigma \sim 10^{-8}$ GeV^{-2}. If we take the most general cross section for a cold relic, $\sigma \sim g^4/m_\chi^2$, the relic abundance reads as [17]

$$\Omega \sim \sigma^{-1} \sim \frac{m_\chi^2}{g^4},$$

from which we see that the combination (g_{EW}, m_{EW}) is only one of the infinite possible combinations of couplings and masses that give the right number.

In principle, one may take masses as low as a fraction of an electronvolt, but in fact there exists a couple of famous limits on the masses of cold relics. For WIMPs one has the *Lee-Weinberg* limit [18], which states that in a standard Hot Big Bang cosmology, one has $m_\chi \gtrsim 5 - 10$ GeV in order to provide the right dark matter abundance (in the original paper, the authors looked for a heavy neutrino with an energy density compatible with the limits on the critical density at that time). In general, many different WIMPless scenarios [17] could be taken into account, for example a scalar dark matter candidate may have a mass well lying in the MeV-GeV range [19].

What about an upper bound on m_χ? In a historical paper [20], the authors calculated what is the maximum mass compatible with the partial-wave unitarity limits for the annihilation cross section of non-relativistic particles. They found that for scalars and Majorana fermions there is an upper bound of $m_\chi \lesssim 340$ TeV, while for Dirac fermions $m_\chi \lesssim 240$ TeV.

1.3 The Freeze-in mechanism

The fact that we still do not know what dark matter is, despite observing its effects on cosmological scales [1], and the surprising (and somehow depressing) absence of any experimental signals of well-grounded BSM theories, like supersymmetry, paints the WIMP paradigm and many other speculated particles into a corner [21–25].

Importantly, there is no compelling reason for thermal production to be the only or the dominant way to generate particles in the Early Universe and other solutions might be viable as well. In fact, in recent years, more and more mechanisms have been cooked up, such as those invoking scenarios in which particles arise without being in thermal contact with the radiation plasma: we call them *non-thermal relics*. The attraction in this kind of mechanisms grew in the last decades thanks to the increasing interest in some processes, like out-of-equilibrium decays of gravitinos [26], axion cosmology [3, 4], baryogenesis and leptogenesis [2, 27, 28] and alternative dark matter scenarios, such as superheavy dark matter [7, 29].

A well-motivated production mechanism is provided by the *freeze-in* of Feebly Interacting Massive Particles (FIMPs) [5, 16]. In this scenario, the FIMP has a zero or negligible initial abundance and a very tiny coupling λ with the thermal bath, making it essentially decoupled from SM particles. The genesis of FIMPs is usually

IR-dominated by $1 \to 2$ decay or $2 \to 2$ annihilations of SM particles, which are assumed to be mediated by renormalizable operators. Let us name with LOSP (Lightest Observable Sector Particle) the lightest particle that is in thermal equilibrium with the visible sector heat bath and that shares with the FIMP an unbroken symmetry (which makes the FIMP stable) and that participates in the interaction vertex with a coupling λ; we will indicate this particle with the letter ζ and the FIMP with a χ. The freeze-in production goes ahead until the bath temperature reaches $T \sim m_\zeta$, while the LOSP decouples following a standard freeze-out mechanism at $T \sim m_\zeta/20$. Up to that time, for a $\zeta \to \chi\chi$ decay, the comoving number density of the FIMP grows in a radiation-dominated Universe as

$$Y(T) = \frac{n_\chi}{s} \simeq \Gamma_{\zeta\to\chi\chi}(T)t(T) \simeq \lambda^2\, T\frac{M_P}{T^2} = \lambda^2\frac{M_P}{T}, \tag{1.13}$$

freezing-in at $T \sim m$:

$$Y_{f.i.} \simeq \lambda^2\frac{M_P}{m}. \tag{1.14}$$

We can compare this result with the analog of the freeze-out mechanism,

$$Y_{f.o.} \simeq \frac{n_{f.o.}}{s_{f.o.}} \simeq \frac{T^2_{f.o.}}{\sigma' M_P s_{f.o.}} \simeq \frac{T}{\sigma' M_P T^3_{f.o.}} \simeq \frac{1}{\sigma' M_P m'},$$

where we used $T_{f.o.} \sim m'$; by assigning $\sigma' \sim \lambda^2 m'^2$, we obtain the yield

$$Y_{f.o.} \simeq \frac{1}{\lambda'^2}\frac{m'}{M_P} \tag{1.15}$$

and we observe the interesting fact that $Y_{f.i.}$ and $Y_{f.o.}$ are inverses of each other.

The reason is simple: a bigger coupling would enhance the depletion of the equilibrium number density before freeze-out, whereas in the freeze-in scheme it would increase the rate of production of FIMPs. Eq. (1.14) implies that, in order to have the correct DM relic abundance for a weak-scale mass, $m \sim v$, we would need

$$\lambda \sim \frac{v}{M_P}, \quad Y_{f.i.} \simeq \frac{v}{M_P},$$

resulting in a very suppressed coupling. The two different behaviors are sketched in Fig. 1.1, where it can be appreciated how, in the thermal case, the larger interaction rate delays the departure from the equilibrium tail and set lower relic densities, while in the freeze-in scheme it gives the opposite result, yielding a greater abundance.

In the original paper [5], the authors considered three examples of interactions giving a frozen-in abundance during a radiation-dominated era: direct freeze-in of FIMP dark matter $B_1 \to B_2\chi$, where B_1 and B_2 are two bath particles, inverse decays of unstable frozen-in FIMPs to dark matter $\chi \to B_1 B_2$ (assuming that its vertex is the same responsible for the freeze-in interaction producing χ), scatterings $B_1 B_2 \to B_3\chi$ (and the other two permutations of the bath particles).

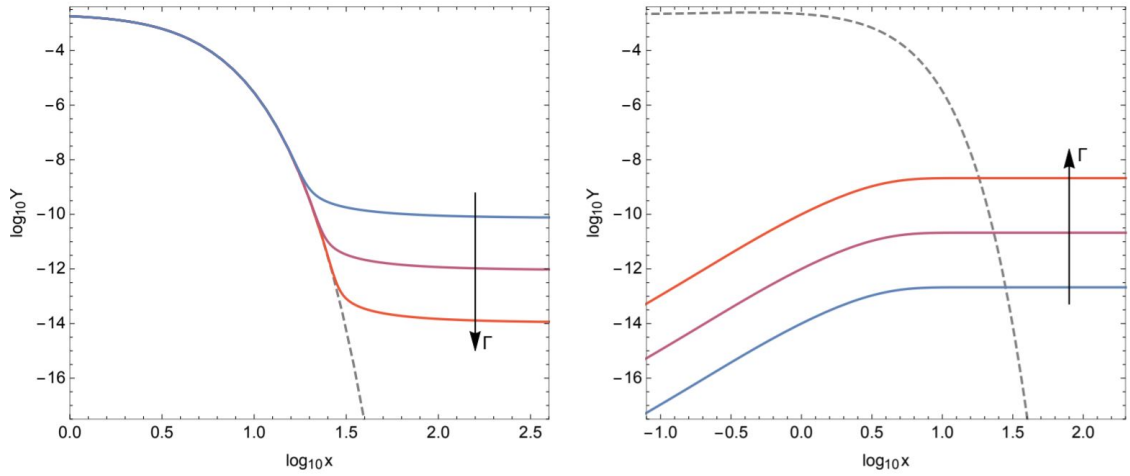

Figure 1.1: Freeze-out (left panel) and freeze-in (right panel) production mechanisms. The interaction rate Γ increases along the direction of the arrow, making the final yield smaller (larger) in the freeze-out (freeze-in) scheme. The shaded grey line represents the equilibrium abundance, which gets exponentially damped as the temperature lowers. *Source*: Picture from [16].

In the first case, the interaction vertex is $\lambda\chi B_1 B_2$ and the comoving abundance is approximately given by

$$Y_{1\to 2} \simeq \frac{M_p m_{B_1} \Gamma_{B_1}}{T^3}.$$

Integrating the Boltzmann equation (see Chapter 3) and using $\Gamma_{1\to 2} = \lambda^2 m_{B_1}/8\pi$, one finds

$$\begin{aligned} \Omega_\chi h^2 &\simeq 1.08 \times 10^{27} \frac{g_{B_1}}{g_{*S}\sqrt{g_*}} \frac{m_\chi \Gamma_{1\to 2}}{m_{B_1}^2} \\ &\Downarrow \\ \lambda &\simeq 1.5 \times 10^{-13} \left(\frac{m_B}{m_\chi}\right)^{1/2} \left(\frac{g_*(m_B)}{100}\right)^{3/4} \left(\frac{g_B}{100}\right)^{-1/2}, \end{aligned} \tag{1.16}$$

where g_* and g_{*S} are respectively the energy density and entropy number of relativistic degrees of freedom. In the second passage, we have considered a common mass m_B for all the bath particles and we have approximated $g_{*S} = g_*$. A very similar result is found for the inverse scattering, with

$$\lambda \simeq 1.5 \times 10^{-12} \left(\frac{m_\chi}{m_{B_1}}\right)^{1/2} \left(\frac{g_*(m_\chi)}{100}\right)^{3/4}. \tag{1.17}$$

In both cases we notice the smallness of the coupling needed to provide the observed number density and the strong IR-domination of the yield, which is basically determined at temperatures around the mass of the decaying particle.

Regarding the $2 \to 2$ scattering, the interaction vertex with four scalars can be taken as $\lambda\chi B_1 B_2 B_3$ and the yield is

$$Y_{2\to 2} \simeq \lambda^2 \frac{M_P}{T}.$$

Integrating the Boltzmann equation and accounting for all the permutations of the bath particles, one finds

$$\begin{aligned} \Omega_\chi h^2 &\simeq 1.01 \times 10^{24} \frac{\lambda^2}{g_{*S}\sqrt{g_*}} \\ &\Downarrow \\ \lambda &\simeq 1{\times}10^{-11} \left(\frac{g_*(m_\chi)}{100}\right)^{3/4}, \end{aligned} \tag{1.18}$$

a bit larger than in decay processes.

It needs to be emphasized that in these calculations the initial abundance of χ particles is zero and that in the scattering process one assumes the masses of the bath particles much lighter than m_χ. Moreover, despite a possible early injection of DM particles, the process is almost totally IR-dominated for renormalizable operators, with most of the abundance frozen-in at $x_{f.i.} = m/T_{f.i.} \sim 2-5$, m being the relevant scale of the interaction (in contrast with the freeze-out scenario, where $x_{f.o.} \sim 20-50$). In any case, a general prediction of this mechanism is that the final yield should not depend (or at least it could in a very mild way) on the DM particle mass.

Requiring such tiny coupling constants may seem very unnatural, since one usually expect, from theoretical naturalness, that an adimensional coupling is of order the unities, $\lambda \sim \mathcal{O}(1)$. The solution, which will be thoroughly discussed in Chapter 4, involve the assumption of a dominant contribution to the yield given by non-renormalizable operators at some UV scale [5, 30, 31]. In this scenario, a small coupling arises naturally from the UV-suppressed interaction vertex, but one may pay the price that, in a standard RD cosmology, the yield is dominated by the maximum temperature reached during the production era, which can be the reheating temperature after inflation, or the maximum temperature of the reheating phase [11, 12], depending on the type of operator involved. As a consequence, knowing the particular UV physics and the initial conditions becomes crucial, whereas in both IR freeze-in and IR freeze-out this was not necessary. We will come back to this point in next chapters.

In addition to this, we stress again the fact that all these calculations were carried out in a standard radiation-dominated era, but nothing prevents us to explore other possibilities, as soon as we do not ruin the excellent agreement with cosmological data on the abundances of light nuclei, the formation of structures and the CMB. Again, we will fully discuss this possibility and its implication in the next chapters.

1.3.1 Superheavy dark matter freeze-in

Is the bound on dark matter mass found for WIMPs in Section 1.2.2 an absolute upper limit for all the possible dark matter candidates [20]? Actually, it is not. Another very interesting theory for DM is the unconventional hypothesis that it might have been gravitationally generated in the context of inflationary cosmology, within a non-thermal scenario; the result is known as *superheavy dark matter*, also renamed with the fancy name *WIMPzillas* [7, 29, 32]. In order for this type of particles to be nice DM candidates, they certainly need to have a lifetime longer than the age of the Universe and undergo tiny interactions in order to never reach thermal equilibrium, otherwise they would have an overly large relic abundance.

This last condition implies that we must *always* have $\Gamma < H$, or $n_X \sigma |v| < H$, with X the WIMPzilla particle. This becomes automatic as long as the X mass is very heavy; in fact, in a standard radiation-dominated era, we have

$$\Omega_X h^2 = \frac{\rho_{X0}}{\rho_{c0}} h^2 = \Omega_\gamma h^2 \frac{\rho_{X0}}{\rho_{\gamma 0}} = \Omega_\gamma h^2 \frac{m_X n_X(T_0)}{\rho_\gamma(T_0)} = \Omega_\gamma h^2 \frac{T_*}{T_0} m_X \frac{n_X(T_*)}{\rho_\gamma(T_*)}, \tag{1.19}$$

where in the last passage we used $n_X \propto T^3$ and $\rho_\gamma \propto T^4$. Replacing $\rho_\gamma(T_*)$ with the Hubble parameter at T_*, $\rho_\gamma(T_*) = H(T_*) M_P T_*^2$, we obtain

$$\frac{n_X(T_*)}{H(T_*)} = \frac{\Omega_X}{\Omega_\gamma} \frac{T_0 \, M_P \, T_*}{m_X}, \tag{1.20}$$

and by demanding that $\sigma |v| \lesssim m_X^{-2}$, we obtain

$$\left. \frac{\Gamma}{H} \right|_{T_*} = \frac{n_X(T_*) \sigma |v|}{H(T_*)} \lesssim \frac{n_X(T_*)}{H(T_*) m_X^2} = \frac{\Omega_X}{\Omega_\gamma} \frac{T_0 \, M_P \, T_*}{m_X^3} < 1, \tag{1.21}$$

which is achieved as long as $\Omega_X h^2 \lesssim 1$ and

$$\left(\frac{200 \, \text{TeV}}{m_X} \right)^2 \left(\frac{T_*}{m_X} \right) < 1. \tag{1.22}$$

Thus, if the WIMPzillas are produced at $T_* < m_X$ with low densities to provide $\Omega_X h^2 \lesssim 1$, then the stability condition $\tau_X / \tau_{Universe} \simeq H/\Gamma > 1$ and the out-of-equilibrium request are given for free.

The real task is to explain how to provide such low X densities in the early Universe; it turns out that gravitational production during or after inflation with direct coupling to the Ricci scalar, i.e. $\xi R X^2$ for scalars, is one of the most attractive answers [7, 29], with implications on particle production during or after reheating [10, 11].

However, viewing the WIMPzilla in the context of effective field theory, there is at least another way to produce non-thermal superheavy DM and it is as intriguing as a purely gravitational genesis: an effective thermal interaction, such as a direct Higgs-WIMPzilla coupling for the freeze-in pair production of WIMPzilla DM

through Higgs annihilations [33]. The interaction may be mediated either by renormalizable or non-renormalizable operators, depending on the Lorentz nature of the WIMPzilla. For instance, scalars would be linked via marginal couplings $\sim \phi^2 H^\dagger H$, while fermions and vectors would interact with irrelevant operators, e.g. $\sim \frac{1}{M_P}\overline{\psi}\psi H^\dagger H$ and $\sim \frac{m^2}{M_P^2} g_{\mu\nu} A^\mu A^\nu H^\dagger H$, with the latter vanishing in the massless limit, in order to preserve gauge invariance. These operators are very general and one would expect their presence in any motivated UV effective field theory of some new physics at the Planck scale (despite some particular symmetry that might forbid them). At temperatures of our interest, the Higgs doublet is present with all its four states and can annihilate via $H^0\bar{H}^0 \to XX$ and $H^+H^- \to XX$. This is a concrete example of a *UV-dominated freeze-in* process, as we will discuss in detail in Chapter 4 and Chapter 5.

It can be shown [33] that the relic number density today of X particles is given by

$$\Omega_X h^2 = 0.12 \times 10^7 \left(\frac{H_e}{10^{13}\,\text{GeV}}\right)^2 \left(\frac{T_{RH}}{10^9\,\text{GeV}}\right) \left(\frac{m}{H_e}\right) \left(\frac{a^3 n}{a_e^3 H_e^3}\right), \tag{1.23}$$

where the e subscript stands for "end of inflation" and the measured relic density is $\Omega_{cdm} h^2 \simeq 0.12$.

In the same paper, it is argued that freeze-in production is always more efficient than gravitational production for masses $m > H_e \simeq 10^{13}$ GeV, while, for fermions, a sufficient thermal abundance survives even if $m \sim T_{RH} < H_e$. The general picture (with differences among minimally or non-minimally coupled scalars, fermions and vectors), shows an increasing upper bound on T_{RH} up to $T_{RH} \lesssim 10^{15}$ GeV as long as m increases, with higher values for shrunk coupling constants. In fact, at a given mass, having a lower reheating temperature would delay the radiation domination era, leaving room for a prolonged faster expansion epoch and a higher dilution of the number density; hence the requirement of a larger coupling. Conversely, once the reheating temperature is fixed, bigger masses imply an exponentially higher Boltzmann suppression in the number densities and therefore the need for enhanced couplings becomes more dramatic.

1.4 Light invisible species

One of the most remarkable achievement of modern cosmology is the precision reached in constraining the properties of neutrinos. For example, the recent data release of the Planck satellite [1] enforces the limits on neutrino masses, with a very stringent bound of

$$\sum m_\nu < 0.12 \text{ eV} \quad \begin{array}{l}(95\%\ \textit{Planck},\ \text{TT,TE,EE} \\ +\text{lowE} +\text{lensing}+\text{BAO}).\end{array} \tag{1.24}$$

This number puts tension on the inverted hierarchy scheme, which requires $\sum m_\nu \gtrsim 0.1$ eV, in contrast to the normal scheme where $\sum m_\nu \lesssim 0.1$ eV.

In addition to this, we have now precise constraints on the possible existence of new light invisible species in extensions of the Standard Model (e.g. sterile neutrinos, light

thermal axions, dark photons etc.). This possibility is traditionally parameterized by an effective number of relativistic neutrino species N_{eff}, which is defined in such a way that the neutrino-to-photon energy density ratio after electron-positron annihilation is

$$\frac{\rho_\nu}{\rho_\gamma} = \frac{7}{8} N_{eff} \left(\frac{4}{11}\right)^{4/3}, \tag{1.25}$$

where the 7/8 factor comes from the fermionic nature of neutrinos and the last factor arises because neutrinos decouples slightly earlier ($T \sim 2$ MeV) than electron-positron annihilation ($T \sim 1$ MeV), yielding $T_\nu/T_\gamma = (4/11)^{1/3}$. If one assumes that neutrinos were completely decoupled by the time of electron-positron annihilation, $T_{e^-e^+} \sim 1$ MeV, we have $N_{eff} = 3$ as one would expect in the SM. Instead, a more precise calculation must include several effects like the non-complete neutrino decoupling at the onset of e^+e^- annihilations, neutrino oscillations and finite-temperature QED corrections. The correct number is $N_{eff} = 3.045$. Eventually, even a low-reheating temperature scenario might affect this number, because if $T_{RH} \sim$ few MeV, neutrinos would not have time to thermalize, affecting their role in the total radiation energy density. In this scenario, one could potentially have N_{eff} close to zero, but actual experimental bounds tell us that the accepted values are certainly above $2.7 - 2.8$ [34, 35].

This simple reasoning allows us to think of two implications: any additional light species that is present before recombination is a contributor to N_{eff}, viewing ρ_ν as the relativistic energy density of the Universe without that of photons. Moreover, a non-standard cosmological scenario can provide significant deviations from the canonical value. This deviance is measured by

$$\Delta N_{eff} \equiv N_{eff} - 3.045, \tag{1.26}$$

which in turn translates into a variation on the number of relativistic degrees of freedom

$$g_*^{eff} = 5.5 + \frac{7}{4} N_{eff} \implies \Delta g_* = \frac{7}{4} \Delta N_{eff}, \tag{1.27}$$

with critical consequences on the CMB, BBN, recombination and the matter power spectrum, via both background and perturbation effects [9]. The direct transfer from N_{eff} to g_*^{eff} is straightforward if the particles can be considered effectively massless, that is to say they need to have $m \ll$ eV in order to be ultra-relativistic during and short after Recombination. Non-zero masses modify the relation between energy density and pressure, so that we cannot relate these particles to an effective g_*, but we need to rely upon mass-dependent effects [35].

Within the ΛCDM model, current CMB measurements from Planck 2018 analyses [1] show

$$N_{eff} = 2.99^{+0.34}_{-0.33} \quad \begin{array}{l}(95\%\ \textit{Planck},\ \text{TT,TE,EE} \\ +\text{lowE} +\text{lensing}+\text{BAO}),\end{array} \tag{1.28}$$

while, accounting for the 3σ tension on H_0 between Planck 2018 and [37], they find

$$N_{eff} = 3.27 \pm 0.30 \quad \begin{array}{l}(95\%\ \textit{Planck},\ \text{TT,TE,EE} \\ +\text{lowE} +\text{lensing}+\text{BAO}+H_0).\end{array} \tag{1.29}$$

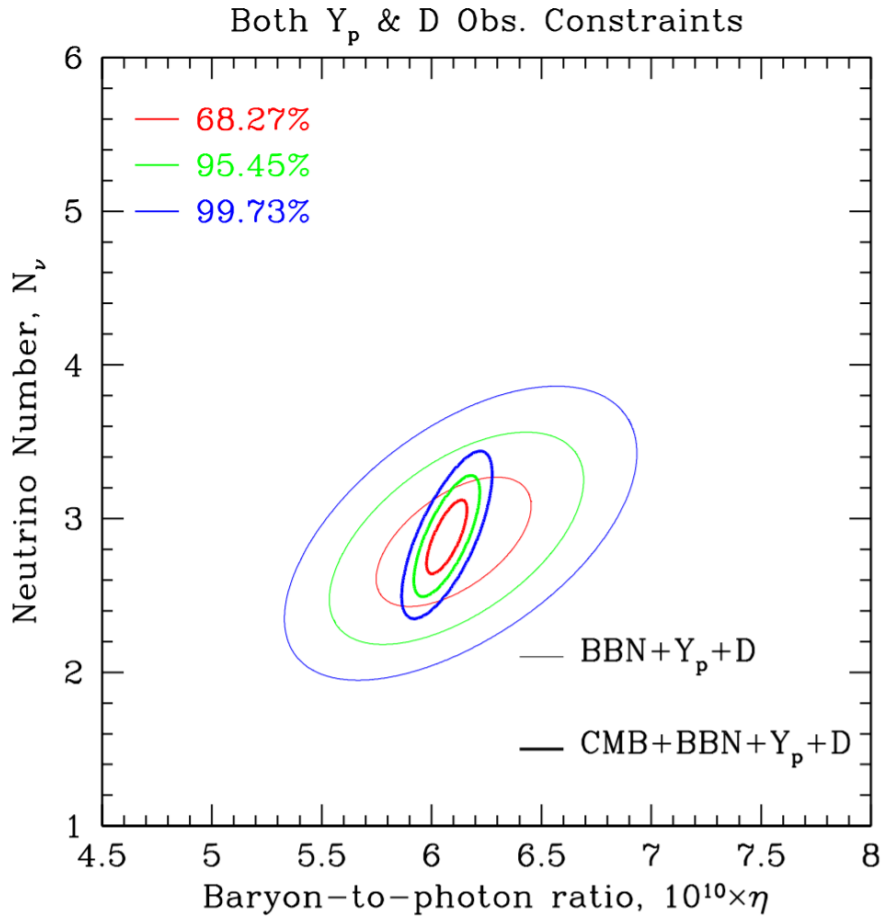

Figure 1.2: Constraints on the number of neutrino species from experimental data on the abundances of ^{4}He and D/H. The bounds $2.3 < N_{eff} < 3.4$ we employ are those highlighted by the inner blue ellipsis (comprising CMB data), corresponding to a C.L. of 3σ. *Source*: Image taken from [36].

As discussed in [34], a conservative bound is given by $2.66 < N_{eff} < 3.57$, otherwise it is ruled out at the level of 2σ. Further, taking into account variations of the primordial Helium abundance, Planck data result in $N_{eff} = 2.99^{+0.43}_{-0.40}$, much the same as Eq. (1.28).

Another popular bound is the one calculated in [36] and shown in Fig. 1.2, where the authors find $2.3 < N_{eff} < 3.4$ at 99.7% C.L., hence $\Delta N_{eff} \lesssim 1.1$, only based on ^{4}He and D abundances and the CMB results from Planck 2015. In this thesis, we will take care of avoiding the disruption of BBN results when new BSM phenomena will be included, therefore we will follow the analyses in [38–40] and we will be as much conservative as we can, using the latter bound on N_{eff}.

Chapter 2

The Boltzmann equation formalism

In this thesis, we will extensively make use of the Boltzmann equation. As Dodelson's book affirms, *"The Boltzmann equation formalizes the statement that the rate of change in the abundance of a given particle is the difference between the rates for producing and eliminating that species"*, that is to say it describes the statistical behavior of a thermodynamical system at or out of the equilibrium. Much of the notation in this chapter and in this thesis has been taken from the evergreen books of Kolb and Turner [2] and Dodelson [8], but it has been also reworked for the specific context of this thesis work.

After giving an idea of how the Boltzmann equation arises in statistical physics (Section 2.1), we construct its generalization within a FLRW metric (Section 2.2), we review the freeze-out of WIMPs in Section 2.3, historically the production mechanism par excellence and we develop the formalism usually employed for particle interaction in the freeze-in context (Section 2.4). Many technicalities of the computations here presented are left to Appendix B.

2.1 Statistical physics framework

Let us suppose to have a physical process where particles are created and destroyed, and we wish to compute the evolution of the total number of one of the species. This is given by the integral of its distribution function $f(\mathbf{q}, \mathbf{p}, t)$ over all the phase space $\mathrm{d}^3\mathbf{q}\,\mathrm{d}^3\mathbf{p}$,

$$N = \int f(\mathbf{q}, \mathbf{p}, t)\,\mathrm{d}^3\mathbf{q}\,\mathrm{d}^3\mathbf{p} \tag{2.1}$$

Let us also assume that an instantaneous force acts on an infinitesimal phase space volume; exploiting the Liouville's theorem, which affirms that in absence of collisions the phase space distribution is constant, we have [41]

$$f\left(\mathbf{q} + \frac{\mathbf{p}}{m}\Delta t, \mathbf{p} + \mathbf{F}\Delta t, t + \Delta t\right)\,\mathrm{d}^3\mathbf{q}\,\mathrm{d}^3\mathbf{p} = f(\mathbf{q}, \mathbf{p}, t)\,\mathrm{d}^3\mathbf{q}\,\mathrm{d}^3\mathbf{p}. \tag{2.2}$$

However, we are mainly interested in collisional systems; hence, the change in the number of particles in an infinitesimal volume will be

$$\begin{aligned} \mathrm{d}N_{coll} &= \left\{ f\left(\mathbf{q} + \frac{\mathbf{p}}{m}\Delta t, \mathbf{p} + \mathbf{F}\Delta t, t + \Delta t\right) - f(\mathbf{q}, \mathbf{p}, t) \right\} \mathrm{d}^3\mathbf{q}\, \mathrm{d}^3\mathbf{p} = \\ &= \left(\frac{\partial f}{\partial t}\right)_{coll} \mathrm{d}t\, \mathrm{d}^3\mathbf{q}\, \mathrm{d}^3\mathbf{p}. \end{aligned} \tag{2.3}$$

Differentiating this expression with respect to $\mathrm{d}^3\mathbf{q}\, \mathrm{d}^3\mathbf{p}\, \mathrm{d}t$, we obtain

$$\frac{\mathrm{d}N_{coll}}{\mathrm{d}^3\mathbf{q}\, \mathrm{d}^3\mathbf{p}\, \mathrm{d}t} = \left(\frac{\partial f}{\partial t}\right)_{coll} = \frac{\mathrm{d}f}{\mathrm{d}t}, \tag{2.4}$$

which makes clear how the total derivative of f rules the net change of particles per unit time and unit phase space volume. The total derivative of f reads

$$\begin{aligned} \frac{\mathrm{d}f}{\mathrm{d}t} &= \frac{\partial f}{\partial t} + \nabla_{\mathbf{q}} f \cdot \frac{\mathrm{d}\mathbf{q}}{\mathrm{d}t} + \nabla_{\mathbf{p}} f \cdot \frac{\mathrm{d}\mathbf{p}}{\mathrm{d}t} = \\ &= \frac{\partial f}{\partial t} + \frac{\mathbf{p}}{m} \cdot \nabla_{\mathbf{q}} f + \mathbf{F} \cdot \nabla_{\mathbf{p}} f \\ &\overset{!}{=} \left(\frac{\partial f}{\partial t}\right)_{coll}. \end{aligned} \tag{2.5}$$

This is the *classical Boltzmann equation.*

2.2 Boltzmann equation in a FLRW Universe

The whole argument works well in a flat spacetime. However, in a generic metric we cannot neglect spacetime curvature and the fact that particle dynamics is governed by the covariant generalization of classical mechanics laws, ruled by General Relativity.

Let us introduce the classical Liouville (or kinematic) operator [2],

$$\hat{\mathbb{L}}[\cdot] = \partial_t + \frac{\mathbf{p}}{m} \cdot \nabla_{\mathbf{q}} + \mathbf{F} \cdot \nabla_{\mathbf{p}} \tag{2.6}$$

where $\mathbf{p} = \mathrm{d}\mathbf{v}/\mathrm{d}t$ and $\mathbf{F} = \mathrm{d}\mathbf{p}/\mathrm{d}t$. We can generalize this operator to the covariant form[1]

$$\hat{\mathbb{L}}[\cdot] = P^\mu \frac{\partial}{\partial P_\mu} - \Gamma^\mu_{\nu\sigma} P^\nu P^\sigma \frac{\partial}{\partial P_\mu}. \tag{2.7}$$

The Boltzmann equation, Eq. (2.5), can be reformulated in a very general way as

$$\hat{\mathbb{L}}[f] = \hat{\mathbb{C}}[f] \tag{2.8}$$

[1] Use $\partial_t + \frac{p^i}{m}\partial_{x^i} = P^\mu \partial_\mu$, with $P^\mu = \frac{\mathrm{d}x^\mu}{\mathrm{d}\lambda}$, λ affine parameter, and use the geodesic equation.

where $\hat{\mathbb{C}}[f]$ is the collision operator, to be specified case by case.

In a FLRW expanding Universe (see Appendix A for further details), we need to specify the relevant Christoffel symbols. Exploiting the homogeneity and isotropy of this metric, we know that the distribution function must depend only on energy and time, so that $\partial_{x^i} f = 0$. This simplifies our Liouville operator, since we only need

$$\Gamma^0{}_{00} = 0, \qquad \Gamma^0{}_{ij} = \frac{\dot{a}}{a} g_{ij}$$

and we are left with

$$\Gamma^0{}_{ij} P^i P^j = \frac{\dot{a}}{a} g_{ij} p^i p^j = \frac{\dot{a}}{a} |\mathbf{p}|^2.$$

Hence,

$$\hat{\mathbb{L}}[f] = E \frac{\partial f}{\partial t} - \frac{a}{\dot{a}} |\mathbf{p}|^2 \frac{\partial f}{\partial E}. \tag{2.9}$$

We can easily rearrange the Boltzmann equation, multiplying by the number of internal degrees of freedom g, dividing by the energy E and integrating on the Lorentz-invariant phase space measure (LIPS) (see Appendix B for more details),

$$d\Pi = \frac{d^3\mathbf{p}}{(2\pi)^3\, 2E}, \tag{2.10}$$

obtaining

$$\frac{g}{(2\pi)^3 E} \int \mathrm{d}^3\mathbf{p}\, \hat{\mathbb{L}}[f] = \frac{g}{(2\pi)^3} \int \frac{\mathrm{d}^3\mathbf{p}}{E}\, \hat{\mathbb{C}}[f]. \tag{2.11}$$

Simplifying the l.h.s of this equation gives

$$\begin{aligned} \frac{g}{(2\pi)^3 E} \int \mathrm{d}^3\mathbf{p}\, \hat{\mathbb{L}}[f] &= \frac{g}{(2\pi)^3 E} \int d^3\mathbf{p} \left[E \frac{\partial f}{\partial t} - \frac{\dot{a}}{a} |\mathbf{p}|^2 \frac{\partial f}{\partial E} \right] = \\ &= \dot{n} - \frac{\dot{a}}{a} \frac{g}{2\pi^2} \int_0^\infty \mathrm{d}p\, p^4 \frac{\partial f}{\partial E} = \dot{n} - \frac{\dot{a}}{a} \frac{g}{2\pi^2} \int_0^\infty \mathrm{d}p\, p^3 \frac{\partial f}{\partial p} = \\ &= \dot{n} - \frac{\dot{a}}{a} \frac{g}{2\pi^2} \left[f p^3 \big|_0^\infty - 3 \int_0^\infty \mathrm{d}p\, p^2 f \right] = \\ &= \dot{n} + 3 \frac{\dot{a}}{a} n. \end{aligned} \tag{2.12}$$

In the second passage we used the definition of *number density*, given by

$$n(t) = \frac{g}{(2\pi)^3} \int \mathrm{d}^3\mathbf{p}\, f(E,t)\,, \tag{2.13}$$

in the third we used the fact that, thanks to $E^2 = p^2 + m^2$, we have $\frac{1}{E}\frac{\partial}{\partial E} = \frac{1}{p}\frac{\partial}{\partial p}$, in the fourth we integrated by parts and in the last one we used the assumption that at the boundary we do expect the distribution function to vanish very rapidly.

To sum up, our final Boltzmann equation is

$$\boxed{\dot{n}(t) + 3Hn(t) = \frac{g}{(2\pi)^3}\int \frac{\mathrm{d}^3\mathbf{p}}{E}\,\hat{\mathbb{C}}[f]} \tag{2.14}$$

where we introduced the Hubble parameter $H = \dot{a}/a$. This equation is the starting point of every discussion on particle production in the early Universe. Of course, one needs to specify the collision operator on a case by case basis. In this respect, beautiful discussions can be found in [2], [42] and [43]. We will use some of the results therein. Notice also the behavior of a non collisional system, i.e. one where $\hat{\mathbb{C}}[f] = 0$: the number density scales as $n(t) \propto a(t)^{-3}$, meaning that the number of particles in a comoving volume is conserved.

2.2.1 Master equation for the comoving density

The Boltzmann equation Eq. (2.14), can be rewritten as

$$\dot{n} + 3Hn = \mathcal{C}_\alpha \tag{2.15}$$

where we have used $\mathcal{C}_\alpha$ to indicate the generic integral collision operator of a certain process α (e.g scattering, decay, etc.). We can rewrite Eq. (2.15) in comoving coordinates, by introducing the comoving density $Y_X = n_X/s$, with $s = \frac{2\pi^2}{45}g_{*s}(T)T^3$ the entropy density of the primordial plasma:

$$\dot{Y}_X = -\frac{\dot{s}}{3H}\mathcal{C}_\alpha. \tag{2.16}$$

Another useful way to express it is to exploit the conservation of the total entropy $S = sa^3$, by which we can write $0 = \dot{S} = \dot{s}a^3 + 3\dot{a}a^2 s$ and so $\dot{s} = -3Hs$. It is convenient to rewrite it in terms of the "time variable" $x = m_B/T$, which tracks the evolution of the species B, usually the heaviest involved in the process, from ultra-relativistic to non-relativistic. In this respect, we obtain $s' = -3s/x$, where the $'$ denotes a derivative with respect to x. Then,

$$\begin{aligned}\frac{ds}{dx} = \frac{ds}{dT}\frac{dT}{dx} &= \frac{2\pi^2}{45}\left(T^3\frac{dg_{*s}}{dT} + 3T^2 g_{*s}\right)\left(\frac{d(m_X/T)}{dT}\right)^{-1} = \\ &= \frac{2\pi^2}{45}g_{*s}T^3\frac{3}{T}\left(-\frac{T^2}{m_X}\right)\left(1 + \frac{1}{3}\frac{T}{g_{*s}}\frac{dg_{*s}}{dT}\right) = \\ &= -3\frac{s}{x}\left(1 - \frac{1}{3}\frac{\partial \log g_{*s}}{\partial \log x}\right).\end{aligned}$$

Therefore, from the second line we can derive the following Boltzmann equation for Y_X in terms of the bath temperature

$$\frac{dY_X}{d\log T} = -\left(1 + \frac{1}{3}\frac{\partial \log g_{*S}}{\partial \log T}\right)\frac{\mathcal{C}_\alpha(T)}{H(T)s(T)}, \tag{2.17}$$

where we can account for the variation of g_{*S} during the expansion of the Universe. We will see that its evolution is almost always negligible, except during the epoch of the QCD phase transition around $T \sim 150$ MeV, when it decreases abruptly from ~ 60 to ~ 10 (see also Section A.3.1). Instead, from the last line we obtain

$$\frac{dY_X}{d\log x} = \left(1 - \frac{1}{3}\frac{\partial \log g_{*S}}{\partial \log x}\right) \frac{\mathcal{C}_\alpha(x)}{H(x)s(x)}. \tag{2.18}$$

In Chapter 4 we will use them to provide approximate results to some concrete examples of interesting scattering processes. Actually, Eq. (2.18) will be the starting point of many of our full-numerical solutions, since our aim is to exactly solve for the comoving density, namely the integral

$$\boxed{Y_X(x) = \int_0^x \frac{\mathrm{d}x'}{x'} \left(1 - \frac{1}{3}\frac{\partial \log g_{*S}}{\partial \log x'}\right) \frac{\mathcal{C}_\alpha(x')}{H(x')s(x')}} \tag{2.19}$$

which we label as our **master equation**. Here, we notice a crucial aspect that we will have to keep in mind: the lower integration extreme can be put at 0 only in the cases where particle production is IR dominated, as in all scenarios with a standard cosmology and a renormalizable operator mediating the interaction, both for freeze-out and freeze-in mechanisms [5, 12, 39]. However, a UV-dominated interaction would necessarily be bounded by the highest energy-scale present in the epoch during which particles were produced. This scale might be represented by the reheating temperature T_{RH}, or the maximum temperature T_{MAX} reached during the reheating phase [10, 11, 30]. The precise extremes will be discussed in details in Chapter 4 and Chapter 5.

We emphasize a particular feature of this derivation, as depicted in the footnote on page 120 of Kolb and Turner book [2]: the fact that we have chosen a specific form for the distribution functions of the involved particles, namely the equilibrium densities for bath particles, specifies the particular frame in which we are working, breaking the covariance of the Boltzmann equation (explicit in Eq. (2.7)). Consequently, we must evaluate all the quantities in the chosen frame, which in our case is the *comoving frame*.

2.2.2 A reformulation of the Boltzmann equation

In this thesis, we are essentially interested in 2-body scattering processes. For example, if we were to focus on a $1 + 2 \to 3 + 4$ process, we could look at the evolution of n_1 and rewrite the collision operator on the r.h.s of Eq. (2.14), obtaining

$$\begin{aligned}
\dot{n}_1 + 3Hn_1 = &\int \mathrm{d}\Pi_1\, \mathrm{d}\Pi_2\, \mathrm{d}\Pi_3\, \mathrm{d}\Pi_4\, (2\pi)^4\, \delta^{(4)}(p_1 + p_2 - p_3 - p_4) \\
&\times \left\{ |\mathcal{M}_{3+4\to 1+2}|^2\, f_3 f_4 [1 \pm f_1][1 \pm f_2] - |\mathcal{M}_{1+2\to 3+4}|^2\, f_1 f_2 [1 \pm f_3][1 \pm f_4] \right\} \\
= &\int \mathrm{d}\Pi_1\, \mathrm{d}\Pi_2\, \mathrm{d}\Pi_3\, \mathrm{d}\Pi_4\, (2\pi)^4\, \delta^{(4)}(p_1 + p_2 - p_3 - p_4) \\
&\times |\mathcal{M}|^2 \left\{ f_3 f_4 [1 \pm f_1][1 \pm f_2] - f_1 f_2 [1 \pm f_3][1 \pm f_4] \right\}
\end{aligned} \tag{2.20}$$

where $|\mathcal{M}_{1+2\to3+4}|^2$ is the probability amplitude (matrix element), usually summed over the initial and final polarization states, f_i are the distribution functions of the i^{th} species and the Dirac delta is needed for assuring four-momentum conservation[2]; we have also assumed T (or CP) invariance to put $|\mathcal{M}_{3+4\leftrightarrow1+2}|^2 = |\mathcal{M}_{1+2\to3+4}|^2 \equiv |\mathcal{M}|^2$. The first addend in the parenthesis accounts for the *creation* of species 1 and so it needs to be proportional to f_3 and f_4, whereas the second addend represents the *destruction* of species 1, hence the need for a proportionality to f_1 and f_2. The $-$ $(+)$ indicates the presence of a Pauli blocking (Bose enhancement) effect due to the particular statistics the involved particles obey. In the early Universe, the typical energies are high enough to let us omit these quantum contributions. Moreover, supposing that the system is in kinetic equilibrium, we can safely approximate all the distributions with Maxwell-Boltzmann functions; for instance, in this thesis we will always assume

$$f_i = \frac{1}{e^{(E_i-\mu_i)/T} \pm 1} \approx e^{-(E_i-\mu_i)/T}$$
$$\Downarrow$$
$$1 \pm f_i \approx 1.$$

Hence, we can substitute these approximations into Eq. (2.20) obtaining

$$\begin{aligned}\dot{n}_1 + 3Hn_1 = &\int d\Pi_1\, d\Pi_2\, d\Pi_3\, d\Pi_4\, (2\pi)^4\, \delta^{(4)}(p_1+p_2-p_3-p_4) \\ &\times |\mathcal{M}|^2\, e^{-\frac{E_1+E_2}{T}} \{e^{-\frac{\mu_3+\mu_4}{T}} - e^{-\frac{\mu_1+\mu_2}{T}}\}.\end{aligned}$$

Using Eq. (2.13) and defining an equilibrium number density distribution (with $\mu_i = 0$) as

$$n_i^{eq}(t) = \frac{g_i}{(2\pi)^3} \int d^3\mathbf{p_i}\, e^{-E_i/T} \tag{2.21}$$

we have $f_i = f_i^{eq}\, e^{\mu_i/T} = e^{-E_i/T} n_i/n_i^{eq}$ and so our Boltzmann equation becomes

$$\begin{aligned}\dot{n}_1 + 3Hn_1 = &\int d\Pi_1\, d\Pi_2\, d\Pi_3\, d\Pi_4\, (2\pi)^4\, \delta^{(4)}(p_1+p_2-p_3-p_4) \\ &\times |\mathcal{M}|^2\, e^{-\frac{E_1+E_2}{T}} \left[\frac{n_3 n_4}{n_3^{eq} n_4^{eq}} - \frac{n_1 n_2}{n_1^{eq} n_2^{eq}}\right].\end{aligned} \tag{2.22}$$

We can introduce the *thermally averaged cross section* (times the relative velocity) $\sigma_{\text{th.}}$ as

$$\sigma_{\text{th.}} = \langle\sigma v\rangle = \frac{1}{n_1^{eq}} \frac{1}{n_2^{eq}} \int \mathrm{d}\Pi_1\, \mathrm{d}\Pi_2\, \mathrm{d}\Pi_3\, \mathrm{d}\Pi_4\, (2\pi)^4 \delta^{(4)}(p_1+p_2-p_3-p_4) |\mathcal{M}|^2\, e^{-\frac{E_1+E_2}{T}} \tag{2.23}$$

[2]One may wonder why we are integrating only over three-momenta and not over energies. Technically, we are supposed to have $\int d^3\mathbf{p}\, dE$, but since $E^2 = \mathbf{p}^2 + m^2$, we are forced to insert a Dirac delta, $\int d^3\mathbf{p}\, dE\, \delta(E^2 - \mathbf{p}^2 - m^2)$. Using the property $\delta(f(x)) = \sum_i \delta(x - x_i)/|f'(x_i)|$, with $f(x_i) = 0$, we end up with $\int d^3\mathbf{p} \int_0^\infty dE\, \delta(E - \sqrt{\mathbf{p}^2 - m^2})/2E = \int d^3\mathbf{p}/2E\,|_{E=\sqrt{\mathbf{p}^2+m^2}}$.

namely weighting the average over the equilibrium number densities of species 1 and 2; this result refers to a $1+2 \to 3+4$ process, but clearly if we had other annihilation channels, such as $1+2 \to X+\overline{X}$ and so on, one should sum over all the possible contributions to provide a total annihilation cross section [2].

Finally, substituting Eq. (2.23) into Eq. (2.22) we obtain

$$\boxed{\dot{n}_1 + 3Hn_1 = n_1^{eq} n_2^{eq} \langle \sigma v \rangle \left[\frac{n_3 n_4}{n_3^{eq} n_4^{eq}} - \frac{n_1 n_2}{n_1^{eq} n_2^{eq}} \right]}. \tag{2.24}$$

2.3 Freeze-out and WIMPs

In this section we review the most popular production mechanism and thermal relic: the freeze-out of WIMPs (see also Chapter 1 for a qualitative discussion). In this case, we usually consider annihilation processes like $X + \overline{X} \leftrightarrow \ell + \bar{\ell}$, with X the dark matter and ℓ some light particle. If we assume that these light particles are tightly coupled to the bath plasma, they manage to maintain their equilibrium densities, $n_\ell = n_\ell^{eq}$. Furthermore, we can assume that initially there was a symmetry providing $n_X = n_{\overline{X}}$; hence, from $E_X + E_{\overline{X}} = E_\ell + E_{\bar{\ell}}$, we can put

$$n_\ell n_{\bar{\ell}} = n_X^{eq} n_{\overline{X}}^{eq} = (n_X^{eq})^2,$$

so that Eq. (2.24) becomes

$$\dot{n}_X + 3Hn_X = -\langle \sigma v \rangle \, [n_X^2 - (n_X^{eq})^2]. \tag{2.25}$$

This can be easily manipulated by supposing that our process is adiabatic and by introducing the *comoving number density* $Y_X = n_X/s$ and the "time variable" $x = m_X/T$, obtaining

$$\begin{aligned} \frac{dx}{dt} &= m_X \frac{d(T^{-1})}{dt} = -m_X \frac{\dot{T}}{T^2} = \frac{m_X}{T} \frac{\dot{a}}{a} = m_X \, H(x) \\ \implies \frac{d}{dt} &= xH \frac{d}{dx}, \end{aligned}$$

yielding

$$\begin{aligned} \dot{Y}_X &= \frac{1}{s}\dot{n}_X - \frac{\dot{s}}{s^2} n_X = \frac{1}{s}\left(\dot{n}_X + 3\frac{\dot{a}}{a} n_X \right) = \frac{1}{s}(\dot{n}_X + 3Hn_X) \\ \implies \dot{n}_X + 3Hn_X &= sxH \frac{dY_X}{dx}. \end{aligned}$$

Thus, we end up with

$$\frac{dY_X}{dx} = -\frac{s\langle \sigma v \rangle}{Hx} [Y_X^2 - (Y_X^{eq})^2]. \tag{2.26}$$

which is the Boltzmann equation for the codensity. In deriving this result, we considered $g_* = const.$ and we used the fact that $T \propto a^{-1}$ and that $s \propto T^3 \propto a^{-3}$.

If we imagine to be fully inside the radiation dominated era, from the first Friedmann equation we have

$$H^2 = \frac{\rho}{3M_{Pl}^2} \sim g_* \frac{T^4}{M_{Pl}^2} \implies H \sim g_*^{1/2} \frac{T^2}{M_{Pl}}$$

hence,

$$x^2 H \sim \frac{m^2}{T^2}\frac{T^2}{M_{Pl}} = \frac{m^2}{M_{Pl}^2} \sim H(T=m) \implies x^2 H(x) = H(x=1).$$

Substituting this result and the expression for the entropy density into Eq. (2.26), we obtain

$$\begin{aligned} \frac{dY_X}{dx} &= -\frac{x\langle\sigma v\rangle}{H(x=1)}\frac{2\pi^2 g_{*s} T^3}{45}[Y_X^2 - (Y_X^{eq})^2] \\ &= -\frac{\lambda}{x^2}[N_X^2 - (N_X^{eq})^2] \end{aligned} \tag{2.27}$$

where we have defined

$$\lambda = \frac{2\pi^2}{45} g_{*s} \frac{m_X^3 \langle\sigma v\rangle}{H(x=1)}. \tag{2.28}$$

If we only focus on cold dark matter relics, we can safely state that the cross section should be proportional to the velocity of the particles, $\sigma v \propto \sigma^p$. Also, $\langle v\rangle \sim T^{1/2}$ and so we can parameterize the cross section times the relative velocity as [44]

$$\langle\sigma v\rangle = \sigma_0 (T/m_X)^n = \sigma_0 x^{-n}$$

where m_X has been introduced for dimensional reasons; $n = 0$ represents the case of s-wave cross sections, $n = 1$ for p-wave cross sections, etc. This parameterization is helpful when different partial-wave contributions are involved; for example, if the scattering is made of both an s-wave and a p-wave term, we would have $\sigma_{tot} = \sigma_s + \sigma_p x^{-1}$, as is the case treated in [38].

Let us follow [2] and focus on the simple one-component situation. The Boltzmann equation becomes

$$\frac{dY_X}{dx} = -\frac{\lambda}{x^{n+2}}[Y_X^2 - (Y_X^{eq})^2] \tag{2.29}$$

with $\lambda = \sigma_0 s(x=1)/H(x=1) \simeq 0.2 M_{Pl}\, m_X (g_{*s}/g_*^{1/2})\, \sigma_0$. At very high temperatures before freeze-out ($x \lesssim x_{f.o.}$), the codensity tracks its equilibrium value, $Y_X \simeq Y_X^{eq} \simeq 1$, while at lower temperatures after freeze-out ($x \gtrsim x_{f.o.}$) the equilibrium abundance is exponentially suppressed, $Y_X^{eq} \sim e^{-x}$, and can be neglected. Thus, we can approximate Eq. (2.29) with

$$\frac{dY_X}{dx} \simeq -\frac{\lambda}{x^{n+2}} Y_X^2.$$

Solving this differential equation with a separation of variables yields

$$Y_X^{\infty} \simeq \frac{n+1}{\lambda} x_{f.o.}^{n+1} \simeq \frac{3.79(n+1)x_{f.o.}^{n+1}}{(g_{*S}/g_*^{1/2})M_p m_X \sigma_0}, \tag{2.30}$$

from which we see that the relic density of WIMPs strongly depends on the freeze-out temperature, the mass of the frozen-out particle, the type of non-relativistic scattering and especially the cross section σ_0. Numerical results show that this result is not very sensitive to the precise microphysics involved, namely $x_{f.o} \sim \ln\lambda \sim \ln(M_P m_X \sigma_0)$, and typical values range between $x_{f.o.} \sim 10 - 30$.

Finally, we notice how this result is fully compatible with the one we obtained in Section 1.2, where we used only an heuristic argument and heavy approximations.

2.4 Collision operators for freeze-in scattering processes

In this thesis, we are interested in UV contributions to freeze-in particle production in modified cosmologies. As it is well-known, decays are always IR dominated, hence we will not describe their collision operators (see [5] for the calculation).

Instead, we want to focus on single and pair production of particles via $2 \to 2$ scattering processes, which can be UV dominated under some particular conditions (see Chapter 4 and Chapter 5).

2.4.1 Freeze-in single production

In the following, we will give a complete derivation of the collision operators for the case of single production; the pair production variant will follow automatically.

As depicted in Section 1.3, we know that the peculiarity of the freeze-in mechanism is to make grow an initial very tiny (or negligible) amount of some particle species towards a final relic abundance. Therefore, we can assume that the initial distribution function of the FIMP is $f_\chi \simeq 0$ and we suppose that the full number density of the χ particles will be generated through a process like [39]

$$B_1 + B_2 \to B_3 + \chi,$$

where B_1, B_2 and B_3 are three generic particles in equilibrium with the thermal bath. Thanks to the out-of-equilibrium condition, we can neglect the second addend in the r.h.s of Eq. (2.20) and we remain with the collision operator

$$\begin{aligned} \mathcal{C}^{(a)}_{B_1 B_2 \to B_3 \chi} = \int \mathrm{d}\Pi_{B_1}\, \mathrm{d}\Pi_{B_2}\, \mathrm{d}\Pi_{B_3}\, \mathrm{d}\Pi_\chi\, (2\pi)^4 \delta^{(4)}(p_{B_1} + p_{B_2} - p_{B_3} - p_\chi) \times \\ \times \left|\mathcal{M}_{B_1 B_2 \to B_3 \chi}\right|^2 f^{eq}_{B_1} f^{eq}_{B_2}. \end{aligned} \tag{2.31}$$

Using energy conservation, we can write

$$\begin{aligned} f_{B_1}^{eq} f_{B_2}^{eq} &= \exp[-(E_{B_1} + E_{B_2})/T] \\ &= \exp[-(E_{B_3} + E_\chi)/T] = f_{B_3}^{eq} f_\chi^{eq} \end{aligned}$$

and further assuming CP invariance we have [39]

$$|\mathcal{M}_{B_1 B_2 \to B_3 \chi}|^2 = |\mathcal{M}_{B_3 \chi \to B_1 B_2}|^2. \tag{2.32}$$

The resulting collision operator is the following:

$$\begin{aligned} \mathcal{C}^{(b)}_{B_1 B_2 \to B_3 \chi} = \int \mathrm{d}\Pi_{B_3}\, \mathrm{d}\Pi_\chi\, \mathrm{d}\Pi_{B_1}\, \mathrm{d}\Pi_{B_2}\, (2\pi)^4 \delta^{(4)}(p_{B_3} + p_\chi - p_{B_1} - p_{B_2}) \times \\ \times\, |\mathcal{M}_{B_3 \chi \to B_1 B_2}|^2\, f_{B_3}^{eq} f_\chi^{eq}. \end{aligned} \tag{2.33}$$

The crucial aspect to be noticed here is the fact that these two operators are perfectly equivalent and refer to the *same* scattering process, namely $B_1 + B_2 \to B_3 + \chi$, since we have already said that the inverse one is not affordable in an out-of-equilibrium situation. The presence of f_χ^{eq} in Eq. (2.33) is merely artificial, a consequence of energy conservation. Nevertheless, it is a good idea to keep both expressions in mind, since it is convenient to use the one for the reaction allowed at zero kinetic energy. For example, if $m_{B_1} + m_{B_2} > m_{B_3} + m_\chi$, we use Eq. (2.31), since the reaction $B_1 + B_2 \to B_3 + \chi$ can happen at rest; in the opposite case we use Eq. (2.33).

The Lorentz-invariant cross section (see Appendix B) is given by

$$\begin{aligned} \sigma_{B_1 B_2 \to B_3 \chi}(s) = \frac{1}{g_{B_1} g_{B_2}} \frac{1}{4(p_{B_1} \cdot p_{B_2})\, v_{B_1 B_2}} \times \\ \times \int \mathrm{d}\Pi_{B_3}\, \mathrm{d}\Pi_\chi\, |\mathcal{M}_{B_1 B_2 \to B_3 \chi}|^2\, (2\pi)^4\, \delta^{(4)}(p_{B_1} + p_{B_2} - p_{B_3} - p_\chi), \end{aligned} \tag{B.11}$$

where the squared matrix element is only summed over the initial states (hence the factor $1/g_{B_1} g_{B_2}$).

We can develop the radicand in the numerator of the invariant relative velocity Eq. (B.12) by multiplying and dividing by four:

$$\begin{aligned} &\frac{1}{4}[(p_{B_1}^2 + 2p_{B_1} \cdot p_{B_2} + p_{B_2}^2 - m_{B_1}^2 - m_{B_2}^2)^2 - 4m_{B_1}^2 m_{B_2}^2] = \\ =&\frac{1}{4}\{[(p_{B_1} + p_{B_2})^2 - m_{B_1}^2 - m_{B_2}]^2 - 4m_{B_1}^2 m_{B_2}^2\} = \\ =&\frac{1}{4}[(s - m_{B_1}^2 - m_{B_2}^2)^2 - 4m_{B_1}^2 m_{B_2}^2] = \\ =&\frac{1}{4}[s - (m_{B_1} + m_{B_2})^2][s - (m_{B_1} - m_{B_2})^2] \equiv \lambda(s, m_{B_1}, m_{B_2}). \end{aligned}$$

The collision operator Eq. (2.31) now reads

$$\begin{aligned} \mathcal{C}^{(a)}_{B_1 B_2 \to B_3 \chi} = 2 g_{B1}\, g_{B2} \int \mathrm{d}\Pi_{B_1}\, \mathrm{d}\Pi_{B_2}\, f_{B_1}^{eq} f_{B_2}^{eq} \\ \lambda^{1/2}(s, m_{B_1}, m_{B_2})\, \sigma_{B_1 B_2 \to B_3 \chi}. \end{aligned} \tag{2.34}$$

The hardest task is to carry out the phase space integration, whose LIPS measures can be opened as

$$\begin{aligned} \mathrm{d}\Pi_{B_1}\,\mathrm{d}\Pi_{B_2} &= \frac{|p_{B_1}|^2\,\mathrm{d}|p_{B_1}|\,\mathrm{d}\Omega_{B_1}}{16\pi^3\,E_{B_1}}\frac{|p_{B_2}|^2\,\mathrm{d}|p_{B_2}|\,\mathrm{d}\Omega_{B_2}}{16\pi^3\,E_{B_2}} = \\ &= \frac{|p_{B_1}||P_{B_2}|}{32\pi^4}\mathrm{d}E_{B_1}\mathrm{d}E_{B_2}\mathrm{d}\cos\theta, \end{aligned} \tag{2.35}$$

where θ is the angle between $\mathbf{p}_{B_1}$ and $\mathbf{p}_{B_2}$ and we integrated over the solid angles and used the relativistic dispersion relation to trade $\mathrm{d}p$ with $\mathrm{d}E$. We closely follow the argument shown in [39, 42] and we perform a change of variables,

$$\begin{aligned} E_+ &= E_{B_1} + E_{B_2}, \\ E_- &= E_{B_1} - E_{B_2}, \\ s &= (p_{B_1} + p_{B_2})^2 = m_{B_1}^2 + m_{B_2}^2 + 2\,(E_{B_1}\,E_{B_2} - |p_{B_1}||p_{B_2}|\cos\theta). \end{aligned} \tag{2.36}$$

Tu plug this transformation in our phase space measure, we need its Jacobian

$$J(\{E_+, E_-, s\} \to \{E_{B_1}, E_{B_2}, \cos\theta\}) = \begin{vmatrix} 1 & 1 & 0 \\ 1 & -1 & 0 \\ 2E_{B_1} & 2E_{B_2} & -2|p_{B_1}||p_{B_2}| \end{vmatrix} = 4|p_{B_1}||p_{B_2}|,$$

with which we have

$$\mathrm{d}E_{B_1}\,\mathrm{d}E_{B_2}\,\mathrm{d}\cos\theta = \frac{\mathrm{d}E_+\,\mathrm{d}E_-\,\mathrm{d}s}{4|p_{B_1}||p_{B_2}|} \tag{2.37}$$

and Eq. (2.35) becomes

$$\mathrm{d}\Pi_{B_1}\,\mathrm{d}\Pi_{B_2} = \frac{\mathrm{d}E_+\,\mathrm{d}E_-\,\mathrm{d}s}{128\pi^4}. \tag{2.38}$$

The only thing that remains to be defined is the integration region, which was originally bounded as

$$E_{B_1} \geq m_{B_1}, E_{B_2} \geq m_{B_2}, |\cos\theta| \leq 1.$$

Clearly, the Mandelstam variable s has the bound

$$s \geq (m_{B_1} + m_{B_2})^2 \equiv s_{12}^{min},$$

whereas to find the bounds for E_+ and E_- we need a little bit of algebra [39]. For the first one we have

$$\begin{aligned} E_+^2 &= E_{B_1}^2 + E_{B_2}^2 + 2E_{B_1}E_{B_2} = m_{B_1}^2 + |\mathbf{p_{B_1}}|^2 + m_{B_2}^2 + |\mathbf{p_{B_2}}|^2 + 2E_{B_1}E_{B_2} = \\ &= (m_{B_1}^2 + m_{B_2}^2 + 2E_{B_1}E_{B_2} - 2\mathbf{p_{B_1}}\cdot\mathbf{p_{B_2}}) + (\mathbf{p_{B_1}} + \mathbf{p_{B_2}})^2 = \\ &= s + (\mathbf{p_{B_1}} + \mathbf{p_{B_2}})^2 \end{aligned}$$

$$\implies E_+ \geq \sqrt{s}.$$

Regarding E_-, we impose that $|\cos\theta| \leq 1$ in the last expression of Eq. (2.36) and we find:

$$\frac{|E_- - E_+ \frac{m_{B_1}^2 - m_{B_2}^2}{s}|}{(E_+^2 - s)^{1/2}} \leq \frac{\lambda^{1/2}(s, m_{B_1}, m_{B_2})}{s}.$$

Before performing the integration, let's rewrite Eq. (2.34) with these changes:

$$\mathcal{C}^{(a)}_{B_1B_2\to B_3\chi} = \frac{g_{B_1}g_{B_2}}{64\pi^4}\int_{s_{12}^{min}}^{\infty} \mathrm{d}s \int_{\sqrt{s}}^{\infty} \mathrm{d}E_+ \int_{E_-^{min}}^{E_-^{max}} \mathrm{d}E_- \\ e^{-E_+/T}\lambda^{1/2}(s, m_{B_1}, m_{B_2})\,\sigma_{B_1B_2\to B_3\chi}(s),$$

where we used $f^{eq}_{B_1} f^{eq}_{B_2} = \exp[-(E_{B_1} + E_{B_2})/T] = \exp[-E_+/T]$. It is manifest that this integral does not depend upon E_- and so we can simply carry out the integration over $\mathrm{d}E_-$, remaining with

$$\mathcal{C}^{(a)}_{B_1B_2\to B_3\chi} = \frac{g_{B_1}g_{B_2}}{32\pi^4}\int_{s_{12}^{min}}^{\infty} \mathrm{d}s\, \frac{\lambda(s, m_{B_1}, m_{B_2})}{s}\,\sigma_{B_1B_2\to B_3\chi}(s) \int_{\sqrt{s}}^{\infty} \mathrm{d}E_+\, e^{-E_+/T}\sqrt{E_+^2 - s}.$$

Performing the integration over $\mathrm{d}E_+$ yields

$$\mathcal{C}^{(a)}_{B_1B_2\to B_3\chi} = \frac{g_{B_1}g_{B_2}}{32\pi^4}T\int_{s_{12}^{min}}^{\infty} \mathrm{d}s\, \frac{\lambda(s, m_{B_1}, m_{B_2})}{s}\,\sigma_{B_1B_2\to B_3\chi}(s)\, K_1[\sqrt{s}/T], \tag{2.39}$$

where $K_1[x]$ is the first modified Bessel function of the second kind. This is our final expression for the collision operator, which obviously depend on the specific model we are investigating. In Chapter 4 and Chapter 5, we will always specify the numerical values for the gs, the masses and the cross section.

The very same calculation is valid for Eq. (2.33), yielding

$$\mathcal{C}^{(b)}_{B_3\chi\to B_1B_2} = \frac{g_{B_3}g_{\chi}}{32\pi^4}T\int_{s_{3\chi}^{min}}^{\infty} \mathrm{d}s\, \frac{\lambda(s, m_{B_3}, m_{\chi})}{s}\,\sigma_{B_3\chi\to B_1B_2}(s)\, K_1[\sqrt{s}/T], \tag{2.40}$$

Finally, we notice an interesting property. In fact, comparing Eq. (2.39) and Eq. (2.40) with $\langle\sigma v\rangle$ in Eq. (B.15), we can rewrite the collision operators as

$$\mathcal{C}^{(a)}_{B_1B_2\to B_3\chi} = \langle\sigma_{B_1B_2\to B_3\chi}v\rangle\, n^{eq}_{B_1} n^{eq}_{B_2},$$
$$\mathcal{C}^{(b)}_{B_3\chi\to B_1B_2} = \langle\sigma_{B_3\chi\to B_1B_2}v\rangle\, n^{eq}_{B_3} n^{eq}_{\chi},$$

where n^{eq} is the one in Eq. (B.1). Thus, the physical equivalence of the two collision operators can be also written as

$$\langle\sigma_{B_1B_2\to B_3\chi}v\rangle\, n^{eq}_{B_1} n^{eq}_{B_2} = \langle\sigma_{B_3\chi\to B_1B_2}v\rangle\, n^{eq}_{B_3} n^{eq}_{\chi}.$$

2.4.2 Freeze-in pair production

The computation of the collision operators in the case of a pair production of χ particles, as in the process

$$B_1 + B_2 \to \chi + \chi,$$

goes along with the very same steps we have just carried out for the single production. The result for the collision operators is now

$$\mathcal{C}^{(a)}_{B_1B_2\to\chi\chi} = \frac{g_{B_1}g_{B_2}}{32\pi^4}T\int_{s_{12}^{min}}^{\infty} \mathrm{d}s\, \frac{\lambda(s, m_{B_1}, m_{B_2})}{s}\, \sigma_{B_1B_2\to\chi\chi}(s)\, K_1[\sqrt{s}/T], \tag{2.41}$$

$$\mathcal{C}^{(b)}_{\chi\chi\to B_1B_2} = \frac{g_\chi^2}{32\pi^4}T\int_{s_{\chi\chi}^{min}}^{\infty} \mathrm{d}s\, \frac{\lambda(s, m_\chi, m_\chi)}{s}\, \sigma_{\chi\chi\to B_1B_2}(s)\, K_1[\sqrt{s}/T], \tag{2.42}$$

meaning that

$$\mathcal{C}^{(a)}_{B_1B_2\to\chi\chi} = \langle\sigma_{B_1B_2\to\chi\chi}v\rangle\, n^{eq}_{B_1} n^{eq}_{B_2},$$
$$\mathcal{C}^{(b)}_{\chi\chi\to B_1B_2} = \langle\sigma_{\chi\chi\to B_1B_2}v\rangle\, (n^{eq}_{\chi})^2,$$

with

$$\langle\sigma_{B_1B_2\to\chi\chi}v\rangle\, n^{eq}_{B_1} n^{eq}_{B_2} = \langle\sigma_{\chi\chi\to B_1B_2}v\rangle\, (n^{eq}_{\chi})^2.$$

In Chapter 4 and 5 will have to specify the microphysics of our system in each situation, including mass and spin of the involved particles and their cross section. In particular, we will have to set the interaction lagrangian we want to deal with and the matrix element of the relevant scattering process.

Chapter 3

Cosmological histories

In this chapter, we want to analyze some possible cosmological histories our Universe might have gone through in its earliest age. In fact, up to now, the best probe of the thermal history is the experimental confirmation of the theory of heavy nuclei creation, Big Bang Nucleosynthesis (BBN), which however happened only around one second after the Big Bang, at a temperature of 1 MeV. We still do not have any direct access to the previous epochs, even though the CMB and the study of the large scale structure of the Universe may give us insights for what concerns the formation and evolution of the first perturbations from inflation, which are encoded in peculiar features of the power spectra for scalar and tensor modes.

The standard ΛCDM model of Cosmology assumes that the spacetime fabric of the Universe is ruled on the largest scale by the FLRW metric, whose dynamics is determined by the Friedmann's equations and the equation-of-state $w = P/\rho$ for the matter-energy content (see Appendix A for an overview). Classically, in this model we deal with three types of fluids: *radiation* ($w = 1/3$), *non-relativistic matter* ($w = 0$) and a *cosmological constant* ($w = -1$). The energy density redshifts with the expansion parameter as

$$\rho \propto a^{-3(1+w)}, \tag{A.6}$$

so that the Universe has encountered three main stages in its life: an early radiation-dominated phase, with $\rho_R \propto a^{-4}$, the overcoming of pressureless matter ($\rho_M \propto a^{-3}$) at $T \sim 1$ eV, and the final dominance of dark energy in the form of a cosmological constant ($\rho_\Lambda \propto const$) in the present epoch.

The cosmological expansion can be considered as adiabatic, since there are far more photons in the Universe in thermal equilibrium than baryons. This permits a simple relation between the temperature of the bath T and the scale factor, $T \propto g_{*S}^{-1/3} a^{-1}$ (or $T \propto a^{-1}$ for simplicity), that we will always assume valid, unless we will deal with periods in the primordial evolution during which some particles start to decay, so that the expansion is not adiabatic anymore (it will be crucial in Section 3.1.2).

Hence, the energy densities can be rewritten in terms of T as $\rho_R \propto T^4$ and $\rho_M \propto T^3$. Given that we are interested in particle production in the early Universe, we can focus

on the radiation era, where we can rewrite the Hubble parameter as

$$H = \frac{\sqrt{\rho}}{\sqrt{3}M_P} = \frac{1}{\sqrt{3}M_P}\sqrt{\frac{\pi^2}{30}g_*(T)T^4} = 0.331\frac{g_*^{1/2}(T)}{M_P}T^2, \tag{3.1}$$

where we used the reduced Planck mass $M_P = (8\pi G)^{-1/2} = 2.4 \times 10^{18}$ GeV. This result will serve as a starting point for a comparison with the non-standard cosmological histories we are going to treat in the next sections.

In this regard, it has to be mentioned that Planck data [45] have already confirmed that the spectral index of scalar cosmological perturbations is very close to 0.96 at a 68% C.L. and that the scalar-to-tensor ratio is $\lesssim 0.1$ at 95% C.L., which are strong validations of two crucial predictions of the inflationary model [46, 47]. However, even though inflation is a commonly accepted theory, it still lacks conclusive proofs, such as primordial gravitational waves. This, in addition to having a wide landscape of models for the nature of the inflaton field, allows us to investigate a variety of early scenarios, provided that these do not disrupt cosmological observations, such as CMB, BBN, LSS and relic abundances.

Nevertheless, the general picture of our interest is that, if DM particle production occurred during a non-standard cosmological era, its comoving abundance should have been dramatically affected, leading to important modifications of its properties, such as the interaction cross-section with the thermal bath.

This chapter will discuss two of the most studied alternatives to the standard picture. In Section 3.1, after reviewing the dynamics of inflationary reheating, we will consider the pivotal characteristics of early matter-dominated (MD) epochs. Section 3.2 instead will focus on another very interesting regime: the kination dominated (KD) scenario (when the Universe is ruled by the kinetic energy density of some scalar field). In particular, we will deeply discuss Quintessence, an hypothetical new scalar field which could be responsible of the present missing energy and acceleration of the Universe and could provide a KD period in the early Universe. Finally, in Section 3.3 we will introduce a generic way to modify the standard Hubble parameter, by introducing fluids whose energy density redshifts as $\rho_\phi \propto a^{-(4+n)}$.

3.1 Early matter-domination epoch

The possibility of a primordial epoch in which the energy budget of the Universe was dominated by a non-relativistic fluid are not rare in the literature. For example, when Inflation ends, the inflaton field enters an oscillatory phase, decaying into radiation and, possibly, other particles. As soon as the Hubble friction becomes relevant, it slows down the field, making it transit towards a non-relativistic behavior. This oscillatory aspect can be found in other contexts, such as ultralight scalar bosons, like ultralight axion-like particles (ULAs) or long-lived heavy particles that were once in thermal equilibrium. The consequences of an early MD era have been extensively studied in various works, including [10–12, 44, 48–53].

3.1.1 Reheating dynamics

A way for passing from a period of matter domination to a standard RD scenario is making the dominating field decay, hence producing a reheating period which perturbs the evolution of the Universe.

A standard situation in which this happens is cosmic inflation, where one supposes that the inflaton field ϕ ends the slow-rolling along its potential, approaching the minimum, where it begins to oscillate until it decays into lighter particles, efficiently transferring its huge vacuum energy into the newborn thermal bath.

We can see this fact by considering a scalar field ϕ, minimally coupled to gravity, in a FLRW Universe [2]. The action which describes the dynamics is

$$S = \int \mathrm{d}^4x \, \sqrt{-g} \left[-\frac{1}{2} g^{\mu\nu} \partial_\mu \phi \, \partial_\nu \phi - V(\phi) \right], \tag{3.2}$$

where g is the determinant of the metric tensor, the first addendum is the canonical kinetic term and $V(\phi)$ is the field potential. The equation of motion for a scalar field is the Klein-Gordon equation in a FLRW background metric; assuming a spatially homogeneous field, this equation reads as

$$\ddot{\phi} + 3H\dot{\phi} + V'(\phi) = 0, \tag{3.3}$$

where $V'(\phi)$ is the derivative of the potential with respect to ϕ and the $3H\dot{\phi}$ term accounts for the redshifting of the momentum of ϕ. At $\phi = \omega$, the point of minimum of the potential, we have $V'(\phi) = V''(\omega)\phi + o(\phi^2)$, and if the mass of the field $m^2 \sim V''(\omega)$ is greater than the Hubble friction, then the equation of motion is that of a pure harmonic oscillator, with ϕ interpreted as a condensate of ϕ particles with zero momentum, which oscillate coherently in space.

Actually, we should expect that at this stage the massive field is unstable and decays into lighter, ultrarelativistic particles. Therefore, we must add to Eq. (3.3) an additional damping term $\Gamma_\phi \dot{\phi}$ due to particle creation, where Γ_ϕ is the decay rate of the inflaton. To simplify the expressions thus obtained, we use the definition of the energy-momentum tensor in General Relativity; with this, one can show that, in an homogeneous and isotropic Universe, we have two simple expressions for the energy density and the isotropic pressure of ϕ:

$$\rho_\phi = \frac{\dot{\phi}^2}{2} + V(\phi), \quad P_\phi = \frac{\dot{\phi}^2}{2} - V(\phi). \tag{3.4}$$

Multiplying the equation of motion by $\dot{\phi}$ and using $\dot{\rho}_\phi = \dot{\phi}\ddot{\phi} + V'(\phi)\dot{\phi}$, we obtain

$$\dot{\rho}_\phi + (3H + \Gamma_\phi)\, \dot{\phi}^2 = 0. \tag{3.5}$$

As ϕ is rapidly oscillating around ω, we can take an average over several periods of oscillations and use a standard property of an harmonic oscillator, $\langle E_{kin} \rangle = \langle V \rangle$, from which $\langle \dot{\phi}^2 \rangle = \rho_\phi$. Plugging this into Eq. (3.5), we obtain

$$\dot{\rho}_\phi + 3H\rho_\phi = -\Gamma_\phi \rho_\phi, \tag{3.6}$$

which has the following general solution,

$$\rho_\phi = \rho_\phi^{osc.} \left(\frac{a_{osc.}}{a}\right)^3 e^{-\Gamma_\phi (t - t_{osc.})}, \tag{3.7}$$

where the superscript "osc." stands for "beginning of oscillations". It is reasonable to choose $\rho_\phi^{osc.} = M^4$, with M the vacuum energy of the scalar field at that time. Notice that, in the absence of decays, the field behaves as pure non-relativistic matter, whose pressure vanishes (this could also be understood from the properties of the harmonic oscillator).

Instead, we assume that the decay products behave as relativistic matter, so that we can write the continuity equation for their energy density ρ_R as

$$\dot{\rho}_R + 4H\rho_R = \Gamma_\phi \rho_\phi, \tag{3.8}$$

where the source term has been included. Finally, the gravitational background is governed by the first Friedmann equation,

$$H^2 = \frac{8\pi G}{3}(\rho_\phi + \rho_R). \tag{3.9}$$

In order to solve the system of equations Eq. (3.6), (3.8) and (3.9), we assume that $\rho_\phi \propto a^{-3}$, hence being in a full **matter-dominated** epoch, between the time $t_{osc} \sim H^{-1}$ at which the oscillations start and $t_{dec} \sim \Gamma_\phi^{-1}$, when the field is efficiently decaying. Using $a \propto t^{2/3}$, $H = \frac{2}{3} t^{-1}$ and $\rho_\phi = M^4 (t/t_{osc.})^{-2}$, we can rewrite Eq. (3.8) as

$$\dot{\rho}_R + \frac{8}{3}\rho_R \frac{1}{t} \simeq \Gamma_\phi M^4 \left(\frac{t}{t_{osc.}}\right)^{-2} \simeq \Gamma_\phi \frac{M_P^2}{t^2}, \tag{3.10}$$

where we used the approximation $t_{osc.} \sim H^{-1} \sim M_P/M^2$.

The solution to this differential equation is easily found [2] and reads as

$$\begin{aligned} \rho_R &= \frac{\Gamma_\phi M_P^2}{10\pi}\frac{1}{t}\left[1 - \left(\frac{t}{t_{osc.}}\right)^{-5/3}\right] = \\ &= \frac{(6/\pi)^{1/2}}{10} M_P \Gamma_\phi M^2 \left(\frac{a}{a_{osc}}\right)^{-3/2}\left[1 - \left(\frac{a}{a_{osc}}\right)^{-5/2}\right]. \end{aligned} \tag{3.11}$$

Let us do some comments:

1. We see that for $t < t_{osc.}$ (or $a < a_{osc.}$), ρ_R rapidly grows, but as soon as $a > a_{osc.}$, it decreases as $a^{-3/2}$ and so $T \propto \rho_R^{1/4} \propto a^{-3/8}$. This solution can be found with a more rigorous calculation by employing Eq. (A.29) with the addition of the source term in Eq. (3.8), yielding

$$\frac{1}{T}\frac{\mathrm{d}T}{\mathrm{d}t} = -H\left(1 + \frac{1}{3}\frac{\mathrm{d}\ln g_{*S}(T)}{\mathrm{d}\ln T}\right)^{-1}\left(1 - \frac{\Gamma_\phi \rho_\phi}{3HsT}\right), \tag{3.12}$$

   which can be solved to provide the correct time-temperature relation.

2. ρ_R has a maximum value at a scale factor a_{MAX}, corresponding to the maximum temperature of the radiation bath:

$$T_{MAX} \simeq g_*^{-1/4}(\Gamma_\phi M_P M^2)^{1/4}. \tag{3.13}$$

This value is reached right at the beginning of the evolution of the radiation bath.

3. The entropy of the system $S = sa^3 \propto T^3 a^3$ grows as $a^{15/8}$, due to the huge injection of photons from inflaton decays. Hence, the cosmological expansion is non-adiabatic during reheating.

4. The reheating phase ends when the inflaton field has decayed. This happens at $t \simeq t_{dec} \simeq \Gamma_\phi^{-1}$. Using

$$H_{RH}^2 = \frac{1}{4t^2}\bigg|_{t\simeq\Gamma_\phi^{-1}} \simeq \Gamma_\phi^2 \stackrel{!}{=} \frac{8\pi}{3M_P^2}\frac{\pi^2}{30}g_*(T_{RH})T_{RH}^4,$$

where $T_{RH} = T|_{t=\Gamma_\phi^{-1}}$, we find that

$$T_{RH} \simeq g_*^{-1/4}(T_{RH})(\Gamma_\phi M_P)^{1/2}, \tag{3.14}$$

which is the *reheating temperature* after inflation and also the temperature at the beginning of the radiation-dominated epoch. The remarkable feature of the oscillatory phase is that the evolution is strongly non-adiabatic, due to the continuous injection of entropy from the decaying inflaton. As a consequence, the time-temperature relation is modified and we have $T \propto t^{-1/4} \propto a^{-3/8}$. Hence, the Hubble parameter in MD_{NA} will scale with temperature as $H \propto T^4$, way faster than in the adiabatic MD ($H \propto T^{3/2}$) and in the RD ($H \propto T^2$) epochs. The behavior of the energy densities of the inflaton and of radiation are illustrated in Fig. 3.1, taken from [12].

More precise calculations are derived in [11]:

$$T = \kappa T_{\mathrm{MAX}}\left[(a/a_i)^{-3/2} - (a/a_i)^{-4}\right]^{1/4}, \tag{3.15}$$

where $\kappa = 1.3\,(g_*(T_{\mathrm{MAX}})/g_*(T))^{1/4}$ is almost constant in T.
The maximum temperature reached during reheating can also be written as

$$\begin{aligned} T_{\mathrm{MAX}} &= \frac{3^{2/5}5^{1/8}}{8^{2/5}\pi^{3/8}}\frac{g_*^{1/8}(T_{RH})}{g_*^{1/4}(T_{\mathrm{MAX}})}M_P^{1/4}H_i^{1/4}T_{RH}^{1/2} = \\ &= \left[\frac{g_*(T_{RH})}{10}\right]^{1/8}\left[\frac{10}{g_*(T_{\mathrm{MAX}})}\right]^{1/4}\left(\frac{H_i}{\mathrm{eV}}\right)^{1/4}\left(\frac{T_{RH}}{100\,\mathrm{MeV}}\right)^{1/2}42\,\mathrm{GeV}, \end{aligned} \tag{3.16}$$

where $H_i = H(a_i)$ is the initial value of the Hubble parameter. For $a > a_{\mathrm{MAX}}$, we can approximate Eq. (3.15) with

$$T \simeq \kappa T_{\mathrm{MAX}}(a/a_i)^{-3/8} = \left[\frac{9g_*(T_{RH})}{5\pi^3 g_*^2(T)}\right]^{1/8}(M_P\,H_i\,T_{RH}^2)^{1/4}(a/a_i)^{-3/8}. \tag{3.17}$$

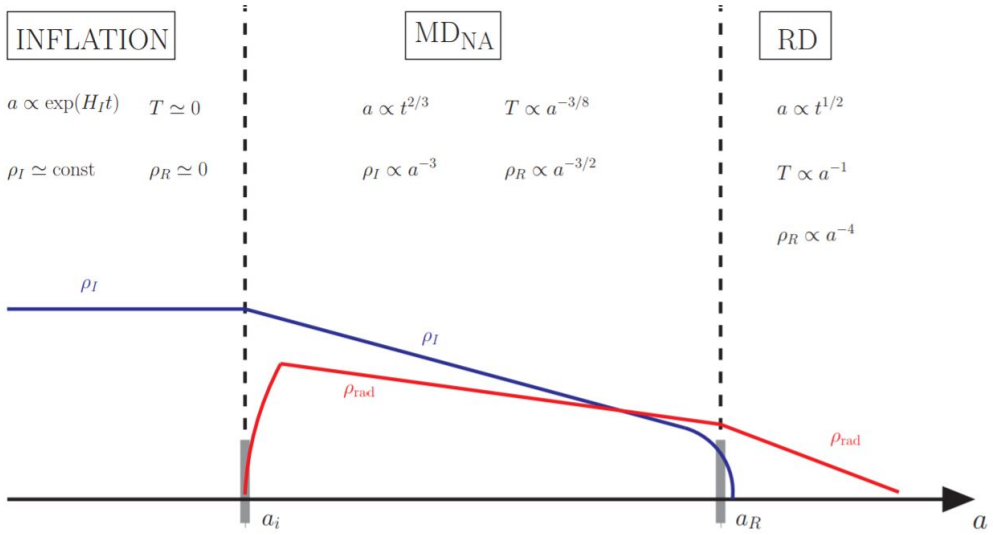

Figure 3.1: The energy densities ρ_I of the inflaton and ρ_R as a function of the scale factor. The Inflation era is dominated by the inflaton only. During the non-adiabatic matter-dominated era, the inflaton behaves as matter, whereas the radiation behaves as in Eq. (3.11). As soon as the inflaton decays, ρ_I is exponentially suppressed and radiation dominates as $\rho_R \propto a^{-4}$. *Source*: Image taken from [12].

We stress once again that a reheating process is not necessarily related to cosmic inflation, but, generically, to an unstable field whose decays produce a considerable injection of radiation and entropy in the Universe. In [11], the authors stress this point, allowing ϕ to be a generic weakly coupled scalar field, unrelated to the inflaton. In the same work, it is deeply analyzed how reheating could actually be a protracted phase, with a low reheating temperature, yielding plentiful implications for a variety of phenomena, especially particle production.

3.1.2 Adiabatic and Non-adiabatic phases

One can also consider a more generic era dominated by a field *behaving like* matter, in which there are both an adiabatic phase MD$_A$ and a non-adiabatic one MD$_{NA}$. If there is a previous RD' stage, the only way to have a subsequent MD era is that the overall evolution is purely adiabatic for a certain amount of time, so that, eventually, $\rho_M \propto T^3$ overwhelms $\rho_R \propto T^4$. If at some point the M particles decay, then the expansion turns to non-adiabatic and evolves as over the course of reheating, with the only difference that there a radiation component is already present from the beginning.

In general, a simple way to discriminate between the adiabatic and non-adiabatic regimes is to specify the origin of the radiation sub-component: if this is is mainly dominated by the redshifted initial radiation, then the MD era is adiabatic; otherwise, if the majority of the radiation contribution is generated from matter decays, the matter evolution is non-adiabatic.

During the MD$_A$ phase, we have entropy conservation and so $g_*^{1/3} aT$ is constant.

Assuming this, we have that the total energy density for a matter-radiation fluid is

$$\rho_A(T) = \frac{\pi^2}{30} g_*(T^4 + T_M T^3),$$

where T_M is the temperature at the onset of MD_A, and the time-temperature relation is $t_A(T) \sim H(T)^{-1} \sim T^{-3/2}$. In the non-adiabatic regime, we obtain the same results discussed in the reheating case,

$$\rho_{NA}(T) = \frac{\pi^2}{30} g_* \left(T^4 + \frac{T^8}{T_{RH}^4} \right),$$

where T_{RH} is the temperature at the beginning of the new RD era. Notice how the non-adiabatic energy density scale, in the high-temperature regime, with the eighth power of T, favouring a faster-than-standard expansion rate, given by $H_{NA}(T) \propto \sqrt{\rho_{NA}(T)} \propto T^4$. Explicitly,

$$H(T) = \frac{1}{\sqrt{3} M_P} \left[\frac{\pi^2}{30} g_*(T) \left(T^4 + \frac{T^8}{T_{RH}^4} \right) \right]^{1/2}, \tag{3.18}$$

where we utilized the reduced Planck mass. A sketch of the admixture of adiabatic and non-adiabatic matter epochs is shown in Fig. 3.2, taken from [12]. The passage from the first one to the second happens at the cosmic time

$$t_{NA} \sim t_M^{2/5} t_R^{3/5},$$

or at a temperature

$$T_{NA} = T_M \left(\frac{t_M}{t_{NA}} \right)^{2/3}.$$

3.2 The kination regime and Quintessence

Another interesting scenario with a modified expansion is the one in which there is a scalar field whose kinetic energy density dominates over its potential energy density, the so-called **kination regime**. From Eq. (3.4), we see that for $\dot{\Phi}^2 \gg V(\Phi)$, one obtains $w = 1$, which also implies

$$\rho_\Phi \propto a^{-6}.$$

In an adiabatic regime, this can be written as $\rho_\Phi \propto T^6$, yielding a faster-than-radiation expansion period with

$$H \propto T^3.$$

It is clear that, if such a field would dominate before inflation, it would be washed away as soon as the constant energy density of the inflaton starts to dominate, and so there is no need for ϕ to be unstable and decay before the beginning of the RD era. In addition to this, if the energy density of the field outnumbers radiation after

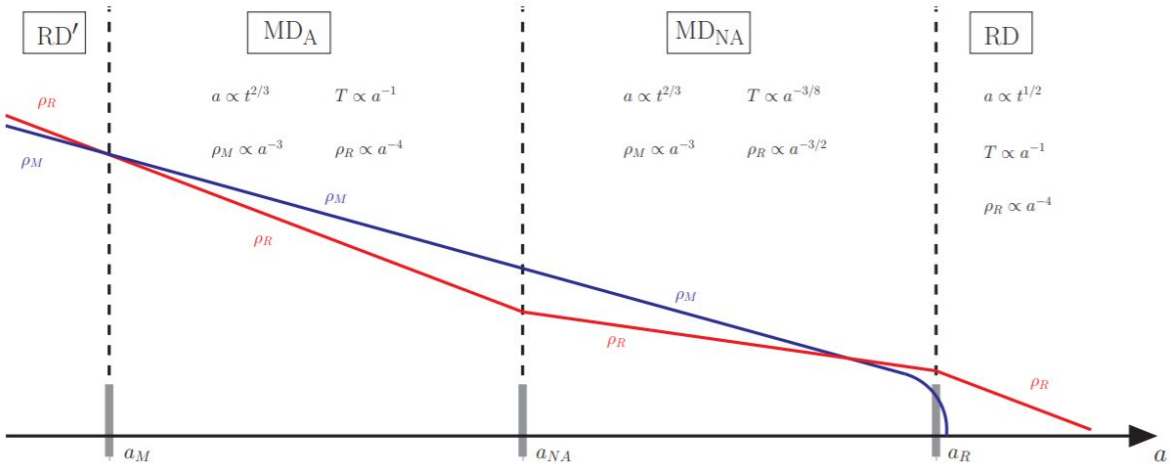

Figure 3.2: Energy densities of matter and radiation in a generic matter-dominated epoch, made of an adiabatic and a non-adiabatic stage, set by the decay of the matter-like particles. *Source*: Image taken from [12].

reheating, the steeper evolution with the scale factor eventually makes it less abundant at a given temperature. On the contrary, if the potential energy dominates, the field behaves just like a cosmological constant term and remains frozen to its initial configuration. In recent years, kination-dominated (KD) scenarios have undergone through an increasing interest by the scientific community, in particular for what regards the phenomenological implications for particle production in the early Universe [54–57]. We will discuss theoretical motivations and the upshots for the freeze-in mechanism in this and in the following chapters.

Finally, another possibility is a kination scenario driven by a decaying field. In this particular case, the kination regime ends when the decay rate Γ_ϕ equals the expansion rate of the Universe; however, the scaling of the energy density with temperature in this case is different because of the non-conservation of entropy. In this thesis we will not explore this eventuality.

One may wonder what could be a physical situation in which a kinetic-dominated field may play a role in the expansion history of the Universe; actually, one of the most intriguing situations is provided by dynamical solutions of the so-called *cosmological constant problem* which we are going to discuss now.

3.2.1 A Quintessential paradigm

The discovery of Dark Energy (DE) [1, 58, 59] and its interpretation as a cosmological constant has posed two problems [60–62]: if it is regarded as the pure vacuum energy density, a natural value would be of order $\rho_\Lambda \sim M_P^4 \sim 10^{76}$ GeV^4. However, the measured value today is $\rho_\Lambda^0 \sim 10^{-47}$ GeV^4 $\sim (1.8 \times 10^{-12}$ GeV$)^4$, almost equal to the critical density ρ_c^0, and so there is a monstrous discrepancy of at least 120 orders of magnitudes from theoretical naturalness and experiments; also, any theoretically

fundamental particle physics scale lies very far away. This is the so-called *"fine-tuning problem"*.

Another struggle is the *"cosmic coincidence* (or *initial conditions*) *problem"*: if DE is a cosmological constant, we would need another enormous fine tuning between the vacuum and radiation energy densities at initial times (e.g. the Planck time):

$$\frac{\rho_\Lambda^i}{\rho_R^i} \sim \frac{\rho_\Lambda^0}{\rho_R^0}\left(\frac{T_0}{M_P}\right)^4 \sim 10^{-125}.$$

Although the order of fine-tuning required is the same, the two problems are profoundly different. The first one is related to an experimental input and a theoretical speculation, the second one is intrinsically inherent in the nature of the cosmological constant and the dynamical models used to explain it.

In fact, the latter issue can be solved by assuming that dark energy is a consequence of the existence of a fifth component other than baryons, photons, neutrinos and dark matter: **Quintessence**, a neutral, stable, spatially homogeneous scalar field Φ, which rolls down its potential $V(\Phi)$, according to the Klein-Gordon equation

$$\ddot{\Phi} + 3H\dot{\Phi} + V'(\Phi) = 0. \tag{3.19}$$

Introducing a dynamical energy component is at least as well motivated by fundamental physics as introducing a cosmological constant. In fact, along with the fine-tuning problem, dynamical fields abound in quantum gravity, supergravity and superstring models (e.g., hidden sector fields, moduli, pseudo-Nambu-Goldstone bosons), and it may even be possible to utilize the interaction of these fields with matter to find a natural explanation why the Φ component and matter have comparable energy densities today. The consequences of a rolling scalar field of this type on cosmology and on a time-variable cosmological constant were first investigated by Ratra and Peebles [63, 64] and then developed in the 90s as the tension between inflationary predictions and observations on the critical density, the age of the Universe and the formation of structures started to become serious (e.g. the work by Wetterich [65], which also addresses the two cosmological constant problems). What makes interesting a model of this kind is that the potential energy density does not get diluted by the expansion of the Universe, so that, eventually, it survives until the present era as a cosmological constant.

The "initial condition problem" can be avoided if one is able to provide an equation-of-state for Φ which is an attractor-like solution, whereby no matter what the initial conditions on Φ and $\dot{\Phi}$ are, since they will always swiftly converge toward a common cosmic evolution, similar to the wipeout caused by inflation. This insensitivity to initial conditions suggests a direct relationship between w_Φ and Ω_Φ, which only depends on the functional form of $V(\Phi)$ and its parameters.

3.2.2 Tracking solutions

Perhaps, one the most famous workaround along this line was achieved by Steinhardt, Wang and Zlatev with *tracking solutions* [66, 67]. In their model, the energy density of

Φ is comparable to the radiation density at the end of inflation (or at most few orders of magnitude lower) and it evolves by tracking the background density for most of the history of the universe until the very recent epoch, when it overwhelms the background energy density. Therefore, one requires that the time-varying equation-of-state w_Φ is maintained always lower or similar to the background w_B during the RD ($w_B = 1/3$) and MD ($w_B = 0$) epochs and, eventually, at some point, ρ_Φ exceeds ρ_M and becomes the dominant component, driving the universe into an accelerating expansion, with $\Omega_\Phi \to 1$ and $w_\Phi \to -1$. Moreover, these solutions are extremely insensitive to initial conditions of ρ_Φ and depend only on a single, free parameter, which, for any class of potentials, defines a whole (infinite) family of possibilities; this parameter turns out to be fixed simply by the measured value of Ω_M today.

An important point that is stressed in the articles is that tracker solutions are not fixed points of the system of differential equations (i.e. Eq. (3.19) and Eq. (A.2) with $k = 0$), as opposed to other results in the literature (see e.g. [68, 69] and the discussion in Section 3.2.3), but instead are time-dependent and the Φ energy density and equation-of-state could maintain a certain amount of difference with respect to the background (hence not necessarily tracking it in a tight way), which allows Φ to ultimately dominate the late fate of the Universe and its accelerating expansion. This proves to be true for certain classes of potentials which are able to provide an evolution for the density parameter Ω_Φ growing as a positive power of cosmic time. In the end, w_Φ and Ω_Φ are intimately related once the tracking is obtained, since for a chosen type of $V(\Phi)$ and for a given measurement of Ω_Φ, the equation-of-state follows automatically.

In the next box, we give a quick outline of the argument proposed in [66, 67]. Here, we just want to furnish the very essential properties for tracking solutions to occur. First of all, the equation-of-state parameter for Quintessence should be nearly constant and should lie between -1 and w_B. From the Klein-Gordon equation of motion one is able to obtain the following relation between the potential, the field derivative w.r.t. time and the Hubble rate (we use dimensionless units as the authors did, with $M_P = 1$):

$$\frac{V'}{V} \approx \frac{1}{\sqrt{\Omega_\Phi}} \approx \frac{H}{\dot{\Phi}}, \tag{3.20}$$

named *tracker condition*. The other fundamental quantity is the *tracker equation*, which reads as follows

$$\Gamma \coloneqq \frac{V''V}{(V')^2} = 1 + \frac{w_B - w_\Phi}{2(1 + w_\Phi)} + (\text{derivatives of } w_\Phi \text{ w.r.t. the scale factor}) \tag{3.21}$$

The pivotal claim is that tracking takes place when $w_\Phi < w_B$ and $\Gamma > 1$ and nearly constant, or when $w_B < w_\Phi < (1/2)(1 + w_B)$ and $1 - (1 - w_B)/(6 + 2w_B) < \Gamma < 1$ and nearly constant, this last one not producing a realistic cosmology today, though. As stressed in [67], the condition $\Gamma > 1$ is equivalent to requiring a potential with $|V'/V|$ decreasing as V declines; in other words, a potential whose derivative falls off more rapidly than the potential itself. This can be understood by staring at Eq. (3.20)

and realizing that, as the field rolls all the way down, its density parameter grows if $w_\Phi < w_B$, making $|V'/V|$ decrease. Potentials with $\Gamma < 1$ would have $|V'/V|$ rising along this evolution. If one neglects the terms with derivatives of w_Φ in Eq. (3.21), a simple relation is easily obtained,

$$w_\Phi \approx \frac{w_B - 2(\Gamma - 1)}{1 + 2(\Gamma - 1)}, \tag{3.22}$$

which shows that $w_\Phi < w_B$ for $\Gamma > 1$.

This outcome demonstrates how the scalar field behaves as a fluid with constant equation-of-state, whose value depends on both the functional form of V and the background, which acts through the Hubble friction in Eq. (3.19). As the Universe moves from RD to MD, w_B switches from 1/3 to 0, and so the scalar field feels a different feedback and, as a consequence, it changes its downhill rolling. In this passage, from Eq. (3.22) it is clear that, along the tracking solution, w_Φ certainly becomes negative when matters dominate (it could be negative already during RD for some potentials). Having a slower redshifting behavior, the energy density of Φ will eventually overtake the background and will come to dominate at some point. Then, the equation-of-state w_Φ will move towards -1 and the Universe will be driven into a period of accelerated expansion, with the field freezing to a constant value Φ_f. As shown in [67], the evolution is actually more complicated and the field goes through several periods of convergence, with the equation-of-state parameter approaching the -1 value in an oscillatory way.

Important developments were carried out by Salati [55], where he noticed that a power-law potential, although perfectly compatible with tracking solutions, has the inconvenient necessity of having $\rho_\Phi^i \ll \rho_B^i$; in fact, if the field were strongly dominating at initial times, its density parameter, determined by the kinetic energy density as the field quickly rolls downhill, would be too large. When the Hubble friction overcomes, the field would freeze at values way higher than the Planck mass, overshooting the tracking solution and failing to provide the correct ρ_Λ^0. On the contrary, a infinite series of inverse power law terms, such as $\exp(M_P/\Phi)$ is reconcilable with all the requirements only with an early kination period. This was the main point of [55] and the consequences drawn on cold dark matter (in particular neutralinos) are remarkable, leading to strong enhancements in the freeze-out comoving density.

A crucial caveat of tracking solutions is that, unless very awkward and artificial potential forms are employed, for $\Omega_M \geq 0.2$ (hence $\Omega_\Phi \leq 0.8$), the equation-of-state parameter is bounded by $w_\Phi > -0.8$ [67], while the most recent measurements indicate that $w_0 < -0.95$ within a 95% of confidence level (w_0 being the present day acceleration of the Universe, regardless of its nature). At the time this solution was published, cosmological observations were unable to provide the stringent bounds we have now, so that the possibility of having w_0 significantly different from -1 was seen as a promising way of determining if the nature of dark energy could depart from a mere cosmological constant and, in particular, if these models of Quintessence could be successful.

Tracking solutions: We want to quickly motivate some results described in the main body, which are displayed in [66, 67]. First, we notice that the evolution of the Quintessential field is purely adiabatic, $\rho_\Phi \propto a^{-3(1+w_\Phi)}$, as a consequence of the conservation of its energy-momentum tensor; secondly, the Hubble parameter gets a further contribution

$$H^2 = \kappa(\rho_B + \rho_\Phi),$$

where $\kappa = 8\pi/3$ ($G = 1$) and $\rho_B = \rho_R + \rho_M$. Therefore, $\Omega_\Phi = \rho_\Phi/\rho_c = \rho_\Phi\,\kappa/H^2$ and so we have $H = \sqrt{\kappa\rho_\Phi/\Omega_\Phi}$.
Since we are considering Φ as a spatially homogeneous scalar field, we can use the equation-of-state defined via Eq. (3.4),

$$w_\Phi = \frac{P_\Phi}{\rho_\Phi} = \frac{\frac{1}{2}\dot\Phi^2 - V}{\frac{1}{2}\dot\Phi^2 + V}. \tag{3.23}$$

By rearranging this expression into

$$1 + w_\Phi = \frac{\dot\Phi^2}{\frac{1}{2}\dot\Phi^2 + V} = \frac{P_\Phi + \rho_\Phi}{\rho_\Phi},$$
$$1 - w_\Phi = \frac{2V}{\frac{1}{2}\dot\Phi^2 + V} = \frac{P_\Phi - \rho_\Phi}{\rho_\Phi},$$

we define the variable

$$x \coloneqq \frac{1 + w_\Phi}{1 - w_\Phi} = \frac{P_\Phi + \rho_\Phi}{P_\Phi - \rho_\Phi} = \frac{\dot\Phi^2/2}{V}, \tag{3.24}$$

which measures the ratio of kinetic to potential energy densities.
We want to obtain an expression for a suitable potential; in order to do so, we derive this last expression with respect to the number of e-folds $N = \ln a$:

$$\begin{aligned}
\frac{dx}{dN} &= \frac{1}{2}\frac{d(\dot\Phi^2)}{dN}\frac{1}{V} - \frac{dV}{dN}\frac{1}{V^2}\frac{\dot\Phi^2}{2} = \\
&= \frac{1}{2}\frac{d(\dot\Phi^2)}{dt}\left(\frac{dN}{dt}\right)^{-1}\frac{1}{V} - \frac{dV}{dQ}\frac{dQ}{dt}\left(\frac{dN}{dt}\right)^{-1}\frac{\dot\Phi^2}{2V^2} = \\
&= \frac{\dot\Phi\ddot\Phi}{HV} - \frac{V'\dot\Phi}{VH}\frac{\dot\Phi^2}{2V} = \frac{\dot\Phi^2/2}{V}\left(\frac{2\ddot\Phi}{H\dot\Phi} - \frac{V'\dot\Phi}{HV}\right) = \\
&= x\left[\frac{2}{H\dot\Phi}(-3H\dot\Phi - V') - \frac{V'\dot\Phi}{HV}\right] = \\
&= x\left[-6 - \frac{2V'}{VH}\left(\frac{2V + \dot\Phi^2}{2\dot\Phi}\right)\right].
\end{aligned}$$

Using the previous relations and $\dot{\Phi} = \sqrt{P_\Phi + \rho_\phi} = \sqrt{\rho_\Phi}\sqrt{1+w_\Phi}$, we obtain:

$$\frac{d\ln x}{d\ln a} = -6 - \frac{2V'}{VH}\left(\frac{2V+\dot{\Phi}^2}{2\dot{\Phi}}\right).$$

Also, taking $\dot{\Phi}^2 = 2V(1+w_\Phi)/(1-w_\Phi)$, we get $(2V+\dot{\Phi}^2) = 4V/(1-w_\Phi)$ and so

$$\frac{d\ln x}{d\ln a} = -6 - \frac{V'}{VH}\frac{2\sqrt{\rho_\Phi}}{\sqrt{\rho_\Phi}\sqrt{1+w_\Phi}} = -6 - 2\frac{V'}{V}\sqrt{\frac{\Omega_\Phi}{\kappa}}\frac{1}{\sqrt{1+w_\Phi}} = \\ = 6\left(-1 - \frac{1}{3}\frac{V'}{V}\sqrt{\frac{\Omega_\Phi}{\kappa}}\frac{1}{\sqrt{1+w_\Phi}}\right).$$

Inverting this relation, we obtain the following "equation of motion"

$$\left|\frac{V'}{V}\right| = 3\sqrt{\frac{\kappa}{\Omega_\Phi}}\sqrt{1+w_\Phi}\left(1+\frac{1}{6}\frac{d\ln x}{d\ln a}\right), \tag{3.25}$$

which takes the place of Eq. (3.19). The tracking solution of Eq. (3.25) is the one for which $-1 < w_\Phi < w_B$ during the RD and MD epochs, meaning that we can assume $1+w_\Phi \sim \mathcal{O}(1)$ and $\Omega_\Phi H^2 = \kappa\rho_\Phi \simeq \kappa\dot{\Phi}^2$, which also implies the "tracker condition" of Eq. (3.20). This ensures that, as the fields rolls down its potential, making its density parameter increase, $|V'/V|$ jointly decreases with V, a condition that can be encoded in the following requirement:

$$\frac{\mathrm{d}|V'/V|}{\mathrm{d}V} < 0 \implies \Gamma \coloneqq \frac{V''V}{(V')^2} > 1. \tag{3.26}$$

Taking the derivative of Eq. (3.25), after some calculations we obtain

$$\Gamma = 1 + \frac{w_B - w_\Phi}{2(1+w_\Phi)} - \frac{1+w_B-2w_\Phi}{2(1+w_\Phi)}\frac{\dot{x}}{6+\dot{x}} - \frac{2}{1+w_\Phi}\frac{\ddot{x}}{(6+\dot{x})^2},$$

where $\dot{x} = \mathrm{d}\ln x/\mathrm{d}\ln a$ and $\ddot{x} = \mathrm{d}^2\ln x/\mathrm{d}\ln a^2$, as we anticipated in the main body of the section; in the limit with $\Gamma \approx const.$ (or $x \approx const.$), Eq. (3.22) follows. From this, we can infer some conditions on Γ in order to provide the desired tracking solutions. In fact, by requiring that $w_\Phi < w_B$, the tracking solution is trivially obtained for $\Gamma > 1$ (and nearly constant). Moreover, all the solutions of this equation differing by the tracking one w_0 of a small amount δ, have that, at first order, $\delta \propto a^\gamma$, with γ a complex number with negative real part for $-1 \le w_0 \le (1/2)(1+w_B)$, meaning that δ plummets down to zero very soon. To obtain a constant Γ, one can test if

$$\left|\frac{1}{\Gamma}\frac{\mathrm{d}(\Gamma-1)}{H\mathrm{d}t}\right| \approx \left|\frac{\Gamma'/\Gamma}{V'/V}\right| \ll 1,$$

where in the second equality we have inserted the tracker condition.
The two main functional forms for the potential analyzed in [67] and satisfying the $\Gamma > 1$ constraint were the inverse power-law potential $V(\Phi) = M^{4+\alpha}/\Phi^{\alpha}$ with $\alpha > 0$ and the exponential potential of the form $V(\Phi) = M^4 \exp(1/\Phi)$, which is nothing but a series of infinite inverse power-law potentials with growing α. From these, it is easy to obtain $w_\Phi \approx 1 + \alpha^{-1}$ and $w_\Phi \approx 1 + 2Q$ (with $Q \ll 1$).

3.2.3 Exponential potential: fixed-point solutions

One of the first (and most simple) attempts to describe a cosmology with a relevant scalar field component, evolving throughout the history of the Universe and possibly dominating at late times, is the one carried out in [65, 70, 71] and then by Ferreira and Joyce [69] and Copeland, Liddle and Wands [68], shortly before the tracking solution study just described.

The potential employed in these models has an exponential form

$$V(\Phi) = V_0 \exp\left(-\lambda \frac{\Phi}{M_P}\right) \tag{3.27}$$

and the Universe is filled with the energy density of Quintessence ρ_Φ plus the relevant background component ρ_B ($B = R$ during the radiation era and $B = M$ during the matter era) with a barotropic equation-of-state. The choice of this potential arose from previous studies regarding solutions to cosmic Inflation (e.g. the famous power-law inflationary model [72]) and because it was well-known that exponential forms are pretty common in various areas of theoretical physics.

In fact, exponential potentials are natural in theories with extra compact dimensions, such as Kaluza-Klein superstring models [70, 73], M-theory [74], supergravity [75–78] and very commonly with non-perturbative effects.

The interesting fact is that, as the field rolls down the potential, its kinetic energy increases, but at the same time it gets damped by the Hubble friction, which depends also on the background content. This balance is translated into the scaling of the energy density $\rho_\Phi \propto a^{-3(1+w_\Phi)}$, with w_Φ spanning from $+1$ (a pure kinetic regime) to -1 (a cosmological constant). The λ parameter is solely responsible for the steepness of the potential, hence it triggers different scaling and late-time attractor solutions.

As shown in [68], the equations defining the physical system (i.e. Eq. (3.19) and Eq. (A.2) with $k = 0$), exhibit up to five fixed points, depending on the values of λ and w_B. Two of these are when the field is completely dominated by its kinetic energy and $w_\phi = 1$; these solutions are unstable and play a role only at the very early time. A third fixed point is the one in which the background rules and $\Omega_\Phi = 0$. Also this solution is unstable for any $w_B > -1$, so that there is always a residue of Ω_Φ.

The last two alternatives are the *late-time attractor solutions*, by which one finds $\lambda^2 = 3(1 + w_\Phi)$. From this last identity follows that $\rho_\Phi \propto a^{-\lambda^2}$ and $a \propto t^{2/\lambda^2}$. The two attractors are stable, depend on the value of λ and w_B and have the peculiarity

of making the density parameter and the equation-of-state of the scalar field converge toward a fixed-point value $\Omega_\Phi^\star$ and $w_\Phi^\star$. They are divided into

- Global attractor for $\lambda > \sqrt{3(1+w_B)}$. Here, the energy density of the scalar component scales faster than the background and one may wonder if it gets completely damped in the end. Actually, this damping makes the kinetic energy of Φ reduce its power and the fluid turns back to scale slower and mimic ρ_B. At the end, the fixed point is reached and one finds $w_\Phi^\star = w_B$ and $\Omega_\Phi^\star = 3(1+w_B)/\lambda^2$. This is the famous "self-tuning solution" (described in full details in [68, 69]), where the scalar field closely mimics the scaling of the dominating background, with the density parameter of Φ which keeps on being a fixed fraction of the background component. Oddly, w_Φ spontaneously changes from 1/3 to 0 at the time of matter-radiation equality.

- Late-time attractor for $\lambda < \sqrt{3(1+w_B)}$ with $w_\Phi^\star = \lambda^2/3 - 1$ and $\Omega_\Phi^\star = 1$, hence a complete Φ domination in the future. For different values of λ one may obtain a variety of late-time scenarios: if $\lambda = \sqrt{2}$, $w_\Phi^\star = -1/3$, meaning that the Universe will be asymptotically expanding at constant velocity; for $\lambda < \sqrt{2}$, $w_\Phi^\star < -1/3$, hence eternal acceleration cannot be avoided. The Universe will eventually start to decelerate only if $\lambda > \sqrt{2}$ (and $\lambda < \sqrt{3}$) with $w_\Phi^\star > -1/3$ (and $w_\phi^\star < 0$).

The exponential potential is not a tracking one, since it provides $\Gamma = 1$. A problem with this model, already noted in [67] and then in [79], is that the self-tuning solution makes the quintessence field energy density contribute either too much in the early Universe or too little now, jeopardising in one case the success of BBN and current observations in the other. More dramatically, one obtains $w_\Phi^\star = w_B = 0$, which totally disagrees with all observations.

The difficulties arising from exponential models made this class of models a bit unfamiliar and overlooked, unless one slightly modifies the functional form by adding some complications (e.g. more fields, polynomial prefactors or exponentiating a field with power-law dependence). However, as noted in [79–81], the late-time attractor solution might not have already reached the fixed-point today and there is room for the parameters to provide a viable cosmology. Certainly, this could pose some serious fine-tuning problems, but this issue was not even resolved with the more natural tracking solution of [67] and still remains as one of the most important dilemmas in modern physics.

In [79], the focus is on $\lambda^2 < 3$, when Quintessence has not reached the fixed point yet. Its density parameter starts from a small fraction towards unity along the late-time attractor. Initially, the field has a negligible value, while it is completely ruled by its kinetic energy density, which scales as a^{-6}. The parameter space they find is quite large for different set of initial conditions and start to be very narrow only if one requires a complete KD quintessential fluid over radiation at the beginning. This restriction follows from the fact that the energy density of Quintessence would be too much abundant by the time of BBN.

Finally, in [82], the authors consider a Quintessential scenario with exponential potential and an early predominant KD regime during which a CDM particle candidate decouples and yields the DM we observe today. We will refer to this work when we will discuss (see Section 5.2.2) the freeze-in production of FIMP dark matter within a KD cosmology and we will dedicate ample space to the discussion of the allowed parameter space.

3.3 A generic modification of the standard scenario

In this section we want to briefly review some results derived in [38, 39] and appreciate how a generic, non-standard expansion history affects the Hubble rate and, consequently, particle production. Therefore, let us consider a cosmology with a new scalar species ϕ dominating at high-energies, whose energy-density redshifts as $\rho_\phi \propto a^{-(4+n)}$, with n a generic number, that might go from -4 (cosmological constant) to some positive number. For $n = 0$ we have that this species redshifts exactly as radiation. The total energy density will be given by

$$\rho_{\rm TOT}(T) = \rho_R(T) + \rho_\phi(T), \tag{3.28}$$

with

$$\rho_R(T) = \frac{\pi^2}{30} g_*(T) T^4.$$

By defining the temperature T_r as the one at which the equality with the radiation epoch occurs ($\rho_\phi(T_r) = \rho_R(T_r)$) and using the red-shift behavior of ρ_ϕ, we can write

$$\rho_\phi(T) = \rho_\phi(T_r) \left(\frac{a(T_r)}{a(T)}\right)^{4+n} = \rho_\phi(T_r) \left(\frac{g_{*S}(T)}{g_{*S}(T_r)}\right)^{(4+n)/3} \left(\frac{T}{T_r}\right)^{4+n}, \tag{3.29}$$

where in the second passage we assumed the validity of entropy conservation, using $a(T) \propto g_{*S}^{-1/3}\, T^{-1}$. Inserting this relation into Eq. (3.28), we obtain

$$\begin{aligned}
\rho_{\rm TOT}(T) &= \rho_R(T) \left[1 + \frac{\rho_\phi(T)}{\rho_R(T)}\right] = \\
&= \rho_R(T) \left[1 + \frac{1}{\rho_R(T_r) \left(\frac{T}{T_r}\right)^4 \frac{g_*(T)}{g_*(T_r)}} \rho_\phi(T_r) \left(\frac{g_{*S}(T)}{g_{*S}(T_r)}\right)^{(4+n)/3} \left(\frac{T}{T_r}\right)^{4+n}\right] = \\
&= \rho_R(T) \left[1 + \left(\frac{g_*(T_r)}{g_*(T)}\right) \left(\frac{g_{*S}(T)}{g_{*S}(T_r)}\right)^{(4+n)/3} \left(\frac{T}{T_r}\right)^{n}\right].
\end{aligned} \tag{3.30}$$

The Hubble parameter is thus given by

$$H = \frac{\sqrt{\rho_{\rm TOT}}}{\sqrt{3}M_P} = \\ = H_R \left[1 + \left(\frac{g_*(T_r)}{g_*(T)}\right)\left(\frac{g_{*s}(T)}{g_{*s}(T_r)}\right)^{(4+n)/3}\left(\frac{T}{T_r}\right)^n\right]^{1/2}, \tag{3.31}$$

where $H_R = \sqrt{\rho_R}/\sqrt{3}M_P$.

Clearly, in the limit $T \gg T_r$, we can always simplify the expressions above, also assuming $g_*(T) = g_{*S}(T) = const. \equiv \overline{g}_* \approx 10^2$. Making this approximation, we find

$$H \simeq \frac{\rho_R^{1/2}}{\sqrt{3}M_P}\left(\frac{T}{T_r}\right)^{\frac{n}{2}} \simeq \frac{\pi}{3\sqrt{10}}\overline{g}_*^{1/2}\frac{T^2}{M_P}\left(\frac{T}{T_r}\right)^{\frac{n}{2}}. \tag{3.32}$$

Within this limit, it is evident that in a modified cosmological scenario with $n > 0$, the Hubble rate is always greater than in the standard one, with $H \propto T^{2+n/2}$.

When dealing with the freeze-out mechanism, we stressed that this competition is crucial in determining the temperature at which the produced particles leave the equilibrium condition and remain as a thermal relic with constant comoving number density. Needless to say, if we improve the rate of the cosmic background expansion, particles tend to separate each other and their interactions become rarer. The direct consequence is that their number density gets frozen at earlier times, while tracking their Boltzmann distribution; due to the exponential tail, it suffices to slightly anticipate the freezing time that an improved comoving abundance can be produced. With the aim of reconciling the theoretical prediction and the observed abundance, one may try to enhance the interaction rate, a task which practically boils down to boost the interaction cross-section between the freezing particle and the equilibrium bath.

Another novel phenomenon was identified in [38], where, for $n \geq 2$ and after freeze-out, particles tend to keep annihilating with themselves, since the interaction rates are now proportional to T^3 (T^4) for s-wave (p-wave) annihilations. The higher the values of n, the steeper the scaling of H as the Universe cools down, leaving room for a residual s-wave (p-wave) annihilation rate that redshifts slower than H when $n \geq 2$ ($n \geq 4$). This occurrence was dubbed *relentless annihilation*.

Regarding the freeze-in mechanism, we encounter the same outcome, but for the opposite motivations: a faster-than-radiation expansion reduces the interaction probability and the non-thermal production of FIMPs is dumped, favouring a lower final yield. Again, the cross-section needs to be increased and the right relic density can be obtained with improved couplings. In this scenario, however, there is no relentless trend, since the frozen-in particles had never attained thermodynamical equilibrium.

Nevertheless, the general picture outlined in [39] for freeze-in decay, single production and pair production of dark matter particles is that one may need coupling enhancements of 4 or 5 orders of magnitude to adjust reductions of the relic density that might reach 10^{10} in the extreme case with $n = 4$ and a scalar-radiation equality temperature T_r of order the BBN scale.

One may wonder how far back in time this non-standard cosmological scenario is active. In [39], the authors give as a rule of thumb that the energy density ρ_ϕ must not overcome Planckian values, namely that when $\rho_\phi \sim M_P^4$ this treatment breaks down. Consequently, they find a bound on the reheating temperature after inflation simply by imposing that

$$H \propto \frac{T_{RH}^2}{M_P}\frac{T_{RH}^{n/2}}{T_r^{n/2}} \propto \frac{\sqrt{\rho_\phi(T_{RH})}}{M_P} \lesssim M_P,$$

giving the bound

$$T_{RH} \lesssim M_P \left(\frac{T_r}{M_P}\right)^{n/(n+4)}. \tag{3.33}$$

At the same time, the presence of a new species from the earliest epochs should not be able to spoil the successful predictions of BBN, meaning that the faster-expansion period cannot last for too long. To quantify how low could possibly be T_r, we use the bounds on the effective number of relativistic species described in Section 1.4. Using Eq. (1.27), we can substitute Δg_*^ϕ with the second addendum in Eq. (3.31) (multiplied by $g_*(T)$), leading to

$$\Delta N_{eff} = \frac{4}{7} g_*(T_r) \left(\frac{g_{*s}(T)}{g_{*s}(T_r)}\right)^{(4+n)/3} \left(\frac{T}{T_r}\right)^n. \tag{3.34}$$

Considering the worst scenario, with T_r close to BBN temperatures (around the MeV), we can put $g_*(T) \simeq g_*(T_r) \simeq g_{*S}(T_r) \simeq 10.75$, yielding

$$\Delta N_{eff} \simeq 6.14 \left(\frac{T}{T_r}\right)^n$$

and by imposing the bound $\Delta N_{eff} \lesssim 1.1$ described in Section 1.4 (see [36, 38]), one finds

$$T_r \gtrsim (15.4)^{1/n} \text{ MeV}. \tag{3.35}$$

These bounds are shown in the (T_r, n) plane of Fig. 3.3, taken from [39].

So far, we have not commented any kind of theoretically-motivated cosmological scenarios with $n > 2$. In fact, theories in which these could be accommodated are quite controversial and there is no general consensus on their origin and feasibility. To give an idea, as highlighted in [38], a scalar field with negative potential providing $w_\phi > 1$ is of the exponential form and a scenario in which faster-than-kination cosmologies may arise is the attraction between visible and hidden branes in the context of ekpyrotic cyclic inflation in multibrane cosmology [83]. We will not delve into these possibilities.

As a last remark, we stress two important points one has to keep in mind when constructing a non-standard cosmological background. Firstly, in the scenarios with $n > 0$ the dominating field drives the the Universe in a faster expansion phase and redshifts away to a negligible level soon, so that we recover the standard history without jeopardizing experimental observations. For the same purpose, if $n < 0$, we are forced to assume that the dominating field promptly decays at some point, otherwise it would

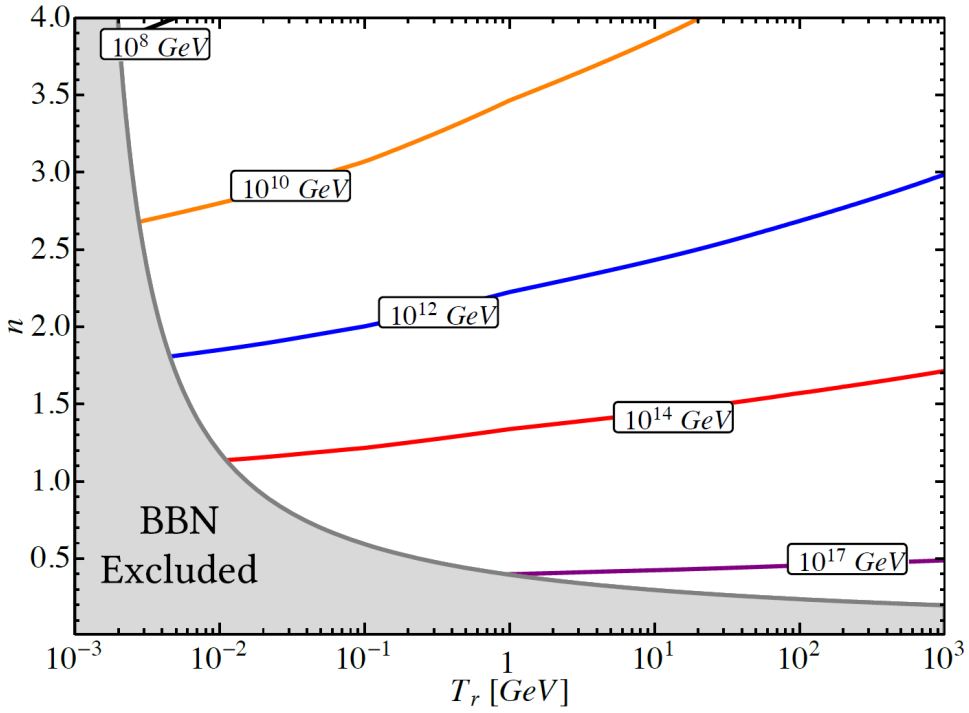

Figure 3.3: Contour curves of the maximum allowed reheating temperatures after inflation as a function of T_r and n. The faster the cosmology, the sooner ρ_ϕ reaches Planckian values, so that a lower reheating temperature is required. *Source*: Image taken from [39].

remain as a stable relic for too long. One usually wants the field to disappear before temperatures around some MeV, in order not to screw up the successes of BBN. Lastly, a decaying field with $n > 0$ is another viable possibility, but is not mandatory in the sense highlighted above.

Chapter 4

Higgs portal in early non-adiabatic MD epochs

One of the most attractive features of the freeze-in mechanism, as proposed in the original paper [5], is that the final relic abundance of the produced FIMP particles is strongly *IR-dominated* for renormalizable couplings, as a result of the exponential suppression in the number density of the parent particles at temperatures around their mass. This property allows to get rid of the unknown UV physics and the uncertain cosmological history of the Universe, relying only on very few parameters, such as masses and couplings which, in principle, could be measured in laboratories. On the other hand, differently from freeze-out, the final yield does not depend on the FIMP mass, opening up an immense window of mass parameters for DM candidates.

We have already seen how a modification of the thermal history at early times dramatically affects the interaction among particles, especially when their number density is depleted by a faster-than-standard Hubble expansion rate. If the portal interaction is renormalizable, the main feature one notices is that in a faster Universe one needs to enhance the couplings between the visible and the dark sector to obtain the observed relic abundance [39].

What happens if, instead, one assumes that the portal interaction connecting the sectors is *non-renormalizable* (sometimes named *irrelevant*), or an admixture of the two? By definition, one should expect some UV-contribution to the number density, which might struggle with unknown high-energy physics and early-time cosmology, because one is forced to find out what was the precise cosmological evolution *before* the radiation era. This is another crucial difference with respect to freeze-out, where the early-stage thermal equilibrium state wipes out all the information about initial conditions. Even though this could be seen as a negative aspect, one may find general predictions that could still be tested with experiments, such as the reheating temperature, the interaction mass scale, the velocity distribution of halos and many others, depending on the particular model one is assuming.

Nevertheless, one of the advantages of non-renormalizable interactions is that the generation of very suppressed couplings between FIMPs and visible sector becomes

more natural, because resulting solely from the existence of the UV scale, a feature very well-known in other popular contexts, like those regarding neutrino masses and the hierarchy problems. For references on DM genesis through portal interactions, especially for what concerns UV production and the freeze-in mechanism, we refer, for example, to the works of [16, 30, 31, 84–88].

In this chapter, we will first explore how a generic irrelevant operator affects particle generation in a non-standard cosmological background (Section 4.1) and we will focus on the fermionic Higgs portal operator (FHPO) of mass dimension 5, deriving the collisional term to be inserted into the Boltzmann equation for the freeze-in mechanism (Section 4.2). We will then analyze this process within an early, non-adiabatic matter-dominated phase and put some constraints on the reheating temperature and the interaction energy scale (Section 4.3).

4.1 Non-renormalizable operators and modified cosmologies

In this section we want to highlight how a freeze-in portal operator of mass dimension $d > 0$ generically relates to an adiabatic non-standard cosmological background driven by $\rho_\phi \propto a^{-(4+n)}$, having in mind that this analysis will find its full utility in the next chapter. However, it is useful to address this topic at this point in order to capture some important features when reading the rest of the discussion in this chapter. Basically, the operator affects the temperature dependence of the interaction rate, whereas the new fluid, as seen in Eq. (3.31), produces a modification of the Hubble-temperature relation. What is the condition on d and n to provide IR or UV-dominated production?

In order to answer this question, we need a rule of thumb for deriving the comoving number density of FIMP particles, which can be approximated with (see also Eq. (1.13))

$$Y(T) \simeq \frac{\gamma(T)}{H(T)},$$

with $\gamma(T)$ the rate of the interactions occurring between visible and dark sectors and $H(T)$ the Hubble rate.

As a first example, we discuss decays, $B_1 \to B_2\psi$, from visible sector particles B_i to a generic FIMP ψ. Correcting for the Lorentz time-dilatation factor, the decay width is lowered by a factor of m_{B_1}/T: $\gamma_{B_1\to B_2\psi}(T) = \Gamma_{B_1\to B_2\psi}\, m_{B_1}/T$. In the high-energy limit approximation, we use Eq. (3.32) for the Hubble rate and we obtain

$$Y_\psi(T)_{decay} \simeq \Gamma_{B_1\to B_2\psi} \frac{m_{B_1} M_P T_r^{n/2}}{T^{3+n/2}}, \tag{4.1}$$

which shows how decays are always IR-dominated.

For a $2 \to 2$ scattering process, the interaction rate is given by Eq. (1.1), namely $\gamma(T) \simeq n(T)\sigma(T)$. We can give a rough estimate of the cross section for a generic

d-dimensional interaction lagrangian

$$\mathcal{L}_d \sim \frac{\mathcal{O}_d}{\Lambda^{d-4}},$$

where $\mathcal{O}_d$ is the portal operator with mass dimension d and Λ is the interaction energy scale, at which one should expect that new degrees of freedom (integrated out in the low-energy limit) emerge from the UV-complete theory. The matrix element of a generic $2 \to 2$ process is dimensionless in a 4-dimensional space and, since there are no relevant energy scales other than Λ, the only form it can take is

$$\mathcal{M}_{2\to2} \sim \left(\frac{E}{\Lambda}\right)^{d-4},$$

with E the center-of-mass energy. Accordingly, the cross section is simply given by

$$\sigma \sim \frac{1}{E^2}\left(\frac{E}{\Lambda}\right)^{2d-8} = \frac{E^{2d-10}}{\Lambda^{2d-8}}.$$

Assuming $E \simeq T$ and using $n_\psi \propto T^3$, the interaction rate scales as $\gamma_{2\to2}(T) \simeq T^{2d-7}/\Lambda^{2d-8}$. Finally, the yield for a scattering process producing a FIMP (single or pair production) is given by

$$Y_\psi(T)_{scattering} \propto \frac{T^{2d-7}}{\Lambda^{2d-8}}\frac{M_P T_r^{n/2}}{T^{2+n/2}} = \frac{T^{2d-9-n/2}}{\Lambda^{2d-8}} M_P\, T_r^{n/2}. \tag{4.2}$$

Thus, it is clear that freeze-in particle production via scatterings is IR-dominated only if the condition

$$d < 4.5 + n/4 \tag{4.3}$$

is fulfilled. Some values for this mass dimension threshold are shown in Table 4.1, where is also indicated the dimension an operator should have to provide an IR or UV domination in the various cosmological scenarios.

As relevant case studies, we notice that for a standard history ($n = 0$), the relic abundance will be IR-dominated only for renormalizable interactions ($d \leq 4$), whereas for $n > 2$ one might have most of the contribution at low temperatures even for non-renormalizable operators. This last situation might occur if the portal operator has mass dimension 5 and the background cosmology is driven by an Hubble rate scaling as $H \propto T^4$. Alternatively, with such an operator and assuming a period of ϕ domination with $n = 2$ (kination regime), the ratio between the $\gamma(T)$ and $H(T)$ is nearly constant, with loss of information about the relevant scale at which the relic abundance freezes-in.

4.2 Scattering with a Fermionic Higgs Portal

The main interaction we are interested in this thesis is a five-dimensional portal operator, which we assume to be the only connection between the visible and the dark

Cosmology	n	$d_{\rm th} = 4.5 + n/4$	$d_{\rm IR}$	$d_{\rm UV}$
Cosmological constant	-4	3.5	3	4
$w = -1/3$	-2	4	3	5
Pressureless matter	-1	4.25	4	5
Radiation	0	4.5	4	5
Kination	2	5	4	6
Ultra-stiff	3	5.25	5	6

Table 4.1: Values for n and for the mass dimension threshold $d_{\rm th}$ to provide an IR (UV) sensitivity, obtained if $d \leq d_{\rm IR}$ ($d \geq d_{\rm UV}$).

sectors, that is to say we do not consider DM particles directly produced by other processes, such as inflaton decays. Using the Higgs as a portal between the two sectors is a well-known minimal choice; the simplest connection one may think is with a new scalar ϕ, whose interaction is ruled by $\lambda_s|\phi|^2 H^\dagger H$. If DM has a vectorial nature, its interaction lagrangian with the Higgs is not renormalizable, because in the massless limit it would not preserve gauge-invariance; hence one finds $\frac{m^2}{M_P^2}\lambda_V V_\mu V^\mu H^\dagger H$.

A very simple irrelevant operator can be obtained by introducing a new fermion ψ, with the interaction given by $\overline{\psi}\psi H^\dagger H$, whose mass-dimension is precisely five. This operator is of interest for different reasons. First, it is the lowest-dimensional, non-renormalizable operator, which is compatible with SM-gauge and Lorentz invariance, hence, among the possible effective operators, it could potentially provide the most important interaction term connecting visible and dark sectors. The Higgs field is also the main responsible for electroweak symmetry breaking (EWSB), leading to important consequences on the couplings and the masses in both the visible and dark sectors [85].

We want to work within an effective field theory (EFT) description of the portal interaction [5, 30, 84, 85, 88], assuming that the mediator fields of the UV-complete theory are heavy enough (at least heavier than the most relevant scale between the reheating temperature and the mass of the FIMP candidate) to have already been integrated out. The total lagrangian density is thus given by

$$\mathcal{L} = \mathcal{L}_{\rm SM} + \mathcal{L}_{\rm d} + \mathcal{L}_{\rm int}, \tag{4.4}$$

with

$$\mathcal{L}_{\rm d} = \overline{\psi}\left(i\partial\!\!\!/ - m_\psi\right)\psi, \tag{4.5}$$

$$\mathcal{L}_{\rm int} = \frac{1}{\Lambda} H^\dagger H \overline{\psi}\psi, \tag{4.6}$$

where H is the SM Higgs doublet, ψ is a SM gauge singlet Dirac fermion (for Majorana fermions it is substantially equivalent) of the dark sector, stabilized by some internal symmetry[1], and Λ is a UV energy scale, suppressing the interaction. We are not interested in the particular UV completion of our EFT, but we demand this scale to be as high as possible, since we want to maintain the production mechanism out of the equilibrium. To be more precise, we assume that all particle production takes place at temperatures high enough to work with electroweak-unbroken fields (also in low reheating temperature scenarios, where we keep this approximation, although not precise), but low enough to avoid stumbling in the unknown UV completion. Moreover, we make the identification between (inverse) coupling and the energy scale of interaction, assuming that, if any, the couplings connecting the dark and visible sectors are $\mathcal{O}(1)$. This premise is not generally true, because one should always make a distinction between the energy scale at which the theory becomes strongly coupled and the one at which new dynamics arises, usually given by the product of a certain scale and a coupling. Examples of this are the Fermi Theory (the scale where the EW theory breaks down is the Higgs v.e.v $v \sim 246$ GeV, but new degrees of freedom appear already at $M_W \sim 80$ GeV), the mass of right-handed neutrinos with the scale of the Weinberg operator and the Planck scale versus the string mass for the graviton coupling [91].

The amplitude of the pair production process $h+h \to \overline{\psi}+\psi$ in the ultra-relativistic limit is roughly given by

$$|\mathcal{M}|^2 \sim \frac{s}{\Lambda^2}, \tag{4.7}$$

where $s \simeq E_{cm}^2$ is the square of the center-of-mass energy, supposed much higher than the scale of EWSB, so that the Higgs field can be treated as a massless $SU(2)_L$ scalar doublet

$$H = \begin{pmatrix} H^+ \\ \\ H^0 \end{pmatrix}.$$

We will have to consider both the two identical contributions to the final abundance, given by the charged components of the Higgs doublet, $H^+H^-\overline{\psi}\psi$, and by the neutral components, $H^{0\dagger}H^0\overline{\psi}\psi$, hence the final collision operator in the Boltzmann equation will be multiplied by a factor of two.

An order of magnitude estimate of the cross-section of the process is given by

$$\sigma \sim \frac{1}{s}|\mathcal{M}|^2 \sim \frac{1}{\Lambda^2}, \tag{4.8}$$

[1] An example might be a $\mathbb{Z}_2$ stabilizing symmetry, namely a ψ-parity, for which the lagrangian density is invariant under a $\psi \to -\psi$ transformation, or else, if DM is the lightest supersymmetric particle, a $\mathbb{Z}_2$ R-parity symmetry. The Higgs sector would be automatically unaffected by these changes. For further discussions on DM and stabilizing symmetries, see for example [89, 90].

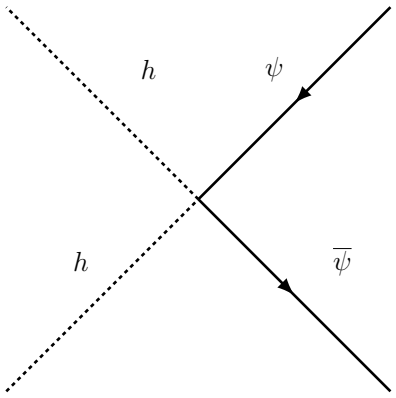

Figure 4.1: Feynman diagram of the $hh \to \overline{\psi}\psi$ contact interaction when the heavy degrees of freedom are integrated out.

which shows how the interaction probability does not depend on the energy of the particles at first glance (actually it has a small dependence as we will demonstrate later).

4.2.1 Collision operator $\mathcal{C}_{h_1h_2\to\overline{\psi}\psi}$

In order to write down the Boltzmann equation for n_ψ, the number density of the ψ particles, we need to derive the collision operator for the $h_1h_2 \to \overline{\psi}\psi$ process. This is given by the $\mathcal{C}^{(b)}$ formula, written in Section 2.4,

$$\mathcal{C}^{(b)}_{h_1h_2\to\overline{\psi}\psi} = \int \frac{\mathrm{d}\Pi_{\overline{\psi}}\mathrm{d}\Pi_\psi\,\mathrm{d}\Pi_{h_1}\,\mathrm{d}\Pi_{h_2}\, f^{eq}_\psi f^{eq}_{\overline{\psi}}\,|\mathcal{M}_{\psi\overline{\psi}\to h_1h_2}|^2\times}{(2\pi)^4\delta^{(4)}(p_{\overline{\psi}}+p_\psi-p_{h_1}-p_{h_2})}, \tag{4.9}$$

because the condition on the masses is now $m_\psi + m_{\overline{\psi}} = 2m_\psi > m_{h_1} + m_{h_2} = 0$. There, we turned the operator into the following form (omitting the (b) superscript)

$$\mathcal{C}_{h_1h_2\to\overline{\psi}\psi} = 2\,g^2_\psi \int \mathrm{d}\Pi_\psi\,\mathrm{d}\Pi_{\overline{\psi}}\, f^{eq}_\psi f^{eq}_{\overline{\psi}} \lambda^{1/2}(s,m_\psi,m_\psi)\,\sigma_{\psi\overline{\psi}\to h_1h_2}(s), \tag{4.10}$$

also applying Eq. (B.12) and (B.11), but in the pair production context. The cross-section in Eq. (B.11) is now given by

$$\boxed{\begin{aligned}\sigma_{\overline{\psi}\psi\to h_1h_2}(s) = &\frac{1}{g^2_\psi}\frac{1}{4\,(p_{\overline{\psi}}\cdot p_\psi)\,v_{\overline{\psi}\psi}}\times \\ &\times\int \mathrm{d}\Pi_{h_1}\,\mathrm{d}\Pi_{h_2}\,|\mathcal{M}_{\overline{\psi}\psi\to h_1h_2}|^2\,(2\pi)^4\,\delta^{(4)}(p_{\overline{\psi}}+p_\psi-p_{h_1}-p_{h_2}),\end{aligned}} \tag{4.11}$$

where our initial relative velocity is

$$v_{\overline{\psi}\psi} = \frac{\lambda^{1/2}(s,m_\psi,m_\psi)}{2\,p_{\overline{\psi}}\cdot p_\psi}.$$

The integration over momenta provides the result already depicted in Eq. (2.41),

$$\boxed{\mathcal{C}_{h_1h_2\to\psi\psi} = \frac{g_\psi^2}{32\pi^4}T\int_{s_{\psi\psi}^{min}}^{\infty}\mathrm{d}s\,\frac{\lambda(s,m_\psi,m_\psi)}{s^{1/2}}\,\sigma_{\overline{\psi}\psi\to h_1h_2}(s)\,K_1[\sqrt{s}/T],} \tag{4.12}$$

with $s_{\psi\psi}^{min} = (m_\psi + m_\psi)^2 = 4m_\psi^2$.

The derivation of the cross section for the annihilation process of each the complex scalars in the Higgs doublet $h + h \to \overline{\psi}\psi$ can be found in Section B.2.3; the result is given by

$$\boxed{\sigma_{\overline{\psi}\psi\to h_1h_2}(s) = \frac{1}{8\pi g_\psi^2}\frac{1}{\Lambda^2}\frac{\sqrt{s-4m_\psi^2}}{\sqrt{s}},} \tag{B.22}$$

where we notice the mild dependence on the CoM energy, asymptotically vanishing when $s \to \infty$.

We are now ready to insert this expression into Eq. (4.12) and obtain

$$\begin{aligned}\mathcal{C}_{h_1h_2\to\overline{\psi}\psi} &= \frac{g_\psi^2}{32\pi^4}T\int_{4m_\psi^2}^{+\infty}\mathrm{d}s\,\frac{s(s-4m_\psi^2)}{\sqrt{s}}K_1[\sqrt{s}/T]\frac{1}{8\pi g_\psi^2}\frac{1}{\Lambda^2}\frac{\sqrt{s-4m_\psi^2}}{\sqrt{s}}\\ &= \frac{T}{256\pi^5}\frac{1}{\Lambda^2}\int_{4m_\psi^2}^{+\infty}\mathrm{d}s\,(s-4m_\psi^2)^{3/2}K_1[\sqrt{s}/T] =\\ &= \frac{T}{256\pi^5}\frac{1}{\Lambda^2}12\sqrt{\pi}\,m_\psi^5\,G_{1,3}^{3,0}\big(\,{}^{0}_{-5/2,-1/2,1/2}\,\big|\,m_\psi^2/T^2\big),\end{aligned} \tag{4.13}$$

where in the last passage we used the definition of Meijer G-function [92], which can be translated in a more comfortable fashion, using the following relation [112]:

$$G_{1,3}^{3,0}\big(\,{}^{0}_{5/2,-1/2,1/2}\,\big|\,x^2\big) = \frac{2}{3}\frac{K_2^2[x]-K_1^2[x]}{\sqrt{\pi}\,x}.$$

Thus, the collision operator for each complex scalar, as a function of the thermal bath temperature, becomes

$$\boxed{\mathcal{C}_{h_1h_2\to\overline{\psi}\psi}(T) = \frac{T^2}{32\pi^5}\frac{1}{\Lambda^2}m_\psi^4\,\left(K_2^2[m_\psi/T]-K_1^2[m_\psi/T]\right),} \tag{4.14}$$

instead, using the "time variable" $x = m_\psi/T$, we obtain

$$\boxed{\mathcal{C}_{h_1h_2\to\overline{\psi}\psi}(x) = \frac{m_\psi^6}{32\pi^5}\frac{1}{\Lambda^2}\frac{K_2^2[x]-K_1^2[x]}{x^2}.} \tag{4.15}$$

From these expressions it is evident how the collision operator for our process will be dramatically determined by the highest temperatures (conversely, the smallest x values), hence the UV-domination we were expecting to find for operators with $d > 4$.

We can show this fact more explicitly by applying the asymptotic behaviors of the modified Bessel functions of the second kind,

$$K_1[x] \sim \begin{cases} x^{-1} & x \ll 1 \\ \sqrt{\frac{x}{2\pi}} e^{-x} & x \gg 1 \end{cases}, \quad K_2[x] \sim \begin{cases} 2x^{-2} & x \ll 1 \\ \sqrt{\frac{x}{2\pi}} e^{-x} & x \gg 1 \end{cases}, \tag{4.16}$$

from which we see that, at $x \gg 1$ (low temperatures), the collision operator is exponentially suppressed by the Boltzmann distribution, whereas in the opposite limit $x \ll 1$ (high temperatures), the dominant behavior is the one of $K_2^2[x] \sim x^{-4}$, which is translated into the asymptotic form $\mathcal{C}_{h_1 h_2 \to \bar{\psi}\psi}(x) \sim m_\psi^6 \, x^{-6} = T^6$, which makes the strong UV-dominance more evident.

We can reshape the collision operator in Eq. (4.12) in the ultrarelativistic limit, when the amplitude is given by Eq. (4.7) [5, 39, 42]. The cross-section for each complex scalar now is constant and reads as

$$\sigma^{UR}_{\bar{\psi}\psi \to h_1 h_2}(s) \sim \frac{1}{8\pi g_\psi^2 \Lambda^2}, \tag{4.17}$$

yielding

$$\mathcal{C}_{h_1 h_2 \to \bar{\psi}\psi} = \frac{T}{256\pi^5} \frac{12}{\Lambda^2} \int_{4m_\psi^2}^{\infty} \mathrm{d}s \, \sqrt{s} \, (s - 4m_\psi^2) \, K_1[\sqrt{s}/T]. \tag{4.18}$$

In this limit we can substantially treat the ψ particles as massless, obtaining

$$\begin{aligned} \mathcal{C}_{h_1 h_2 \to \bar{\psi}\psi} &\simeq \frac{T}{256\pi^5 \Lambda^2} \int_0^{\infty} \mathrm{d}s \, s^{3/2} \, K_1[\sqrt{s}/T] = \\ &= \frac{T^6}{8\pi^5 \Lambda^2}. \end{aligned} \tag{4.19}$$

This is the result also derived in [5, 30] for a single production process driven by a 5-dimensional operator and it perfectly agrees with the estimation for $x \ll 1$ derived in the previous section.

4.3 UV sensitivity during an early MD_{NA} phase

In this section, we analyze the UV sensitivity of the FHPO during a reheating phase, when a massive field, not necessarily the inflaton, decays and the Universe turns to be dominated by an early non-adiabatic matter era. The cosmological background we need is much alike the one proposed in Section 3.1.

We assume that, at early times, the Universe was dominated by an unstable field ϕ, behaving like matter while decaying into radiation R. The Boltzmann equations for the energy densities $\rho_R(T)$ and $\rho_\phi(T)$ read as follows [10, 11]

$$\frac{\mathrm{d}\rho_\phi}{\mathrm{d}t} + 3H\rho_\phi = -\Gamma_\phi \rho_\phi, \tag{4.20}$$

$$\frac{\mathrm{d}\rho_R}{\mathrm{d}t} + 4H\rho_R = \Gamma_\phi \rho_\phi - 2\langle E_\psi \rangle \, \mathcal{C}^{\mathrm{FHPO}}_{h_1 h_2 \to \overline{\psi}\psi}, \tag{4.21}$$

with Γ_ϕ the decay width of the unstable field, which can be expressed in terms of the reheating temperature T_{RH} as (see also Eq. (3.14) for a rough estimate)

$$\Gamma_\phi = \frac{\pi}{30}\sqrt{g_*(T_{RH})}\frac{T_{RH}^2}{M_P}. \tag{4.22}$$

The second term on the r.h.s of Eq. (4.21) accounts for FIMP particle production from the bath, hence the term $2\langle E_\psi \rangle$, which represents the average energy brought away by annihilation processes. It is clear that, in our scheme, this term gives a completely negligible contribution to the radiation energy density evolution and we will not consider it anymore in the following.

The system is closed by the Friedmann equation for the cosmological expansion,

$$H^2 = \frac{1}{3M_P^2}(\rho_R + \rho_\phi), \tag{4.23}$$

neglecting the contribution of the ψ particles, as we said. We demand, as initial conditions for solving the system of equations, that $\rho_{R_i} = 0$ and $\rho_{\phi_i} \gg T_{RH}^4 \simeq (M_P \Gamma_\phi)^2$, but we know that these choices do not affect our results, since what really matters is the reheating temperature after inflation, which is a free parameter of the theory and will be set by hand.

The behavior of the energy densities ρ_ϕ, ρ_R, the Hubble parameter H and the total entropy S (see Eq. (A.26)) during and after the coherent oscillations and decay of the pressureless field ϕ are shown in Fig. 4.2 as a function of the logarithm of the scale factor. The last two have obviously distinct mass dimensions, so that the various graphs have been superimposed. We stress that the radiation energy density actually starts from very low values, even though the figure seems to show a different initial condition. This because the rise from zero to T_{MAX} is extremely steep. The field decays in correspondence of $t = \Gamma_\phi^{-1}$ (or when $H = \Gamma_\phi$), which, for the reference value of $T_{RH} = 1$ TeV chosen for this plot (other values do not affect the general picture), amounts to $\Gamma_\phi \sim 10^{-13}$. After the decay, the evolution is adiabatic and the total entropy is conserved along the expansion of the scale factor.

In addition, we have the Boltzmann equation for the number density of ψ particles,

$$\frac{\mathrm{d}n_\psi}{\mathrm{d}t} + 3Hn_\psi = 2\,\mathcal{C}^{\mathrm{FHPO}}_{h_1 h_2 \to \overline{\psi}\psi}, \tag{4.24}$$

where the factor of 2 in the r.h.s accounts for the equal contribution of the two Higgs complex scalars during the electroweak unbroken phase.

We rewrite Eq. (4.24) by defining the ψ comoving number density as $\mathcal{X} = n_\psi a^3$, which is better suited than $Y = n_\psi/s$ in situations in which entropy is not conserved. Hence, we obtain a new master's equation written in terms of the scale factor a (see Eq. (2.17) for the equivalent with Y)

$$\frac{d\mathcal{X}}{d\log a} = 2\,\frac{a^3}{H(a)}\,\mathcal{C}(a). \tag{4.25}$$

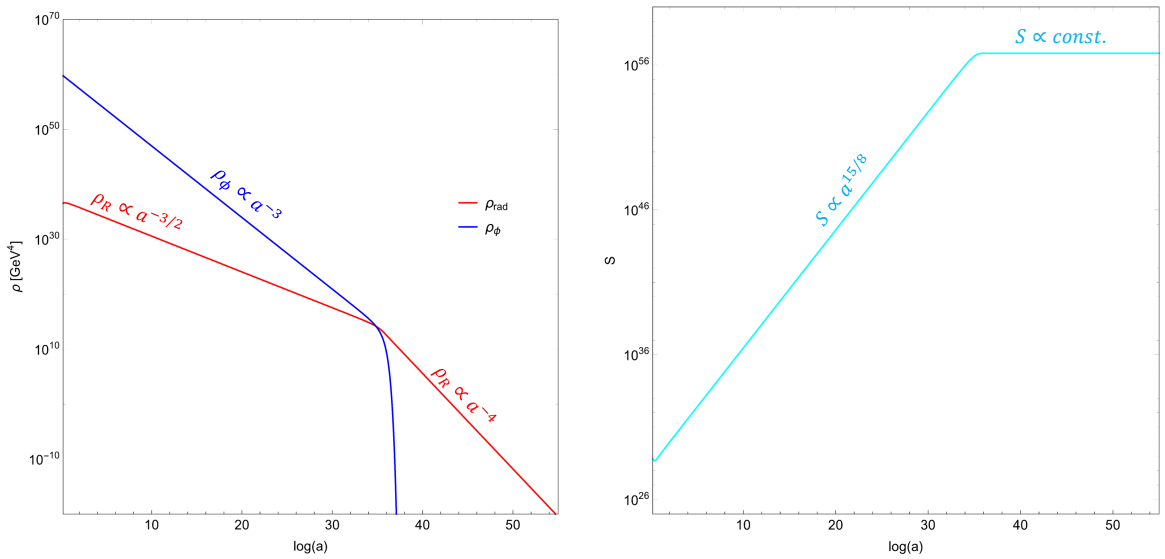

Figure 4.2: Plots of the three main cosmological quantities during an early MD_{NA} era: the energy densities of radiation (red line) and the decaying non-relativistic field ϕ (blue line) in units of GeV^4; the total entropy (cyan line) in dimensionless units. The reheating temperature is $T_{RH} = 1\mathrm{TeV}$. Notice that $\rho_{R_i} \simeq 0$, but its rise is so steep that the graph shows it when already set at T_{MAX}.

The link with the usual comoving abundance is easily obtained with

$$Y(T) = \frac{\mathcal{X}(T)}{S(T)},$$

where $S(T)$ is the total entropy of the Universe. We further define

$$\xi_\psi = \frac{\rho_\psi}{s} = \Omega_\psi \frac{\rho_c}{s} = 0.44\,\mathrm{eV}, \tag{4.26}$$

and using $\rho_\psi = m_\psi n_\psi$ we recognize the relation

$$m_\psi Y_\psi = 0.44\,\mathrm{eV}; \tag{4.27}$$

hence, with a dark matter candidate at the TeV scale, we should expect a yield of the order of $Y_\psi \sim 4.4 \times 10^{-13}$.

If we assume a complete non-adiabatic MD background, the Hubble rate scale as $H \propto \rho_\phi^{1/2} \propto T^4$, faster than in the common RD scenario, as we saw in Section 3.1. As an example, if we take decays and renormalizable scattering processes, the collision operator in the high-T limit goes as as T^2 and T^4, respectively. Hence, the yield $\mathcal{X}$ will be approximately given by

$$\mathcal{X} \propto \frac{T^{-8}}{T^4} \begin{pmatrix} T^2 \\ T^4 \end{pmatrix} = \begin{pmatrix} T^{-10} \\ T^{-8} \end{pmatrix},$$

where the first entry refers to decays and the second to renormalizable scattering processes. With a $d = 5$ operator the collision operator scale as T^6 in the UV limit, hence the yield is expected to exhibit a T^{-6} behavior. In general, the production will be always IR-dominated for interactions mediated by operators with mass dimension less than 8.

These approximations are valid only if $T_{RH} < m_\psi$. In fact, we should consider both the scenarios:

- $T_{RH} < m_\psi$, particle production happens entirely within the MD_{NA} epoch.
- $T_{RH} > m_\psi$, particle production ends in the RD era.

The first possibility is of particular interest, because, when the abundance freezes-in, there is still a consistent injection of entropy from the reheating process that lowers the yield by a *dilution factor* D, which can be estimated as the ratio between the values of the entropy at a temperature $T > T_{RH}$ and at T_{RH},

$$D(T) \simeq \frac{S(T_{RH})}{S(T > T_{RH})} \simeq \frac{(T_{RH} a_{RH})^3}{(Ta)^3} \simeq \frac{T^5}{T_{RH}^5}. \tag{4.28}$$

For this reason, if $T_{RH} < m_\psi$, the DM yield today is not merely $Y_{prod.}(T) \sim \Gamma(T)/H(T)$, but is given by

$$Y(T) \sim \frac{Y_{prod.}(T)}{D(T)} \sim Y_{prod.}(T) \frac{T_{RH}^5}{T^5}. \tag{4.29}$$

We can give an estimation for $Y_{prod.}(T)$ for the five-dimensional operator of our interest based on the Hubble rate $H(T) \simeq T^4/(M_P T_{RH}^2)$ (see Eq. (3.18)) and the interaction rate $\Gamma(T) \simeq T^3/\Lambda^2$, yielding

$$Y_{prod.}(T) \sim \frac{M_P}{\Lambda^2} \frac{T_{RH}^2}{T} \tag{4.30}$$

and finally

$$Y(T) \sim \frac{M_P}{\Lambda^2} \frac{T_{RH}^7}{T^6},$$

which definitively freezes at $T = T_{RH}$ if $T_{RH} < m_\psi$ or at $T = m_\psi$ in the opposite case:

$$Y_0 \sim \begin{cases} \dfrac{M_P T_{RH}}{\Lambda^2} & \text{if } T_{RH} > m_\psi \\ \dfrac{M_P T_{RH}^7}{\Lambda^2 m_\psi^6} & \text{if } T_{RH} < m_\psi \end{cases}. \tag{4.31}$$

One needs to be careful in setting up the system and the Boltzmann equation for the ψ abundance, because if we allow the cross section (hence the coupling strength) to be too high, then we can reach the equilibrium condition and the freeze-in mechanism is no longer applicable and needs to be substituted by conventional freeze-out.

In [12], with only decays to DM from the lightest visible sector particle B carrying the stabilizing symmetry, the authors find that couplings greater than 10^{-7} might endanger the freeze-in production. It is shown that, for the given masses, an increase of the couplings values entails a lowering of T_{RH}, so as to provide the observed relic abundance. The reason is that one needs to prolong the reheating phase in order to supply a powerful dilution from entropy injection, which can oppose the overshooting of ψ production. In our numerical calculations we should always control that the peak of the comoving density does not exceed the equilibrium abundance, namely $Y_{peak} \lesssim Y_{eq}$.

4.3.1 A more quantitative analysis

Before turning to our numerical results, we want to give an estimate of what to expect from our analysis. To do so, we exploit the discussion just done, simplifying the Boltzmann equation by using the ultrarelativistic approximation. We divide the whole particle production into two separated phases, the RD and the MD_{NA}, solving the Boltzmann equations within these different regimes and imposing that the abundances match at $T = T_{RH}$ (if produced after reheating) or at $T = m_\psi$ (if produced during reheating) [31].

$\boldsymbol{T_{RH} > m_\psi}$ **:** Let us first esteem the final frozen-in yield Y_ψ in the standard context with $T_{RH} > m_\psi$, which is not very different from a standard RD era which starts at T_{RH}. Inserting the collision operator of Eq. (4.19) in Eq. (2.17) with constant g_{*S} and accounting for the equal contribution of charged and neutral higgses, we obtain

$$\frac{\mathrm{d}Y_\psi}{\mathrm{d}\log T} \simeq 2\,\frac{T^6}{8\pi^5\Lambda^2}\frac{1}{H(T)s(T)}. \tag{4.32}$$

The usual expressions for the Hubble parameter and the entropy density are given by Eq. (3.1) and Eq. (A.28); inserting these into the Boltzmann equation, we obtain

$$\frac{\mathrm{d}Y_\psi}{\mathrm{d}\log T} = \frac{T^6}{4\pi^5\Lambda^2}\frac{M_P}{0.331 g_*^{1/2}(T)T^2}\frac{45}{2\pi^2 g_{*S}(T)T^3} \simeq \frac{1}{0.06\pi^7 g_*^{3/2}}\frac{M_P T}{\Lambda^2},$$

where we considered $g_*(T) = g_{*S}(T) \equiv g_* = 106.75$. Integrating this differential equation from $T < T_{RH}$ to T_{RH} yields

$$Y_\psi(T) \simeq Y_\psi\big|_{T=T_{RH}} + \frac{1}{0.06\pi^7 g_*^{3/2}}\frac{M_P}{\Lambda^2}(T_{RH} - T),$$

but since we are considering $T < T_{RH}$, it becomes

$$Y_\psi(T) \simeq Y_\psi\big|_{T=T_{RH}} + \frac{1}{0.06\pi^7 g_*^{3/2}}\frac{M_P T_{RH}}{\Lambda^2} = \text{const.}, \tag{4.33}$$

because the total number of ψ particles is preserved by the expansion of the Universe if the reactions have stopped. We notice that the yield is constant after T_{RH} since all

the reaction is UV-dominated; for the same reason, the final abundance will depend on T_{RH}, not only on the mass and the coupling of DM particles.

In the $T > T_{RH}$ regime, instead, we simplify the time-temperature relation and we use $a \propto T^{-8/3}$ and $H \simeq \beta_{RH}^{-4} T^4/(M_P T_{RH}^2)$, with $\beta_{RH} = (9/5\pi^3 g_*(T_{RH}))^{1/8}$ (see Eq. (3.17) and [11]). Thus, Eq. (4.25) gets the following form (remember that $\mathcal{X} = n_\psi a^3$)

$$\begin{aligned}\frac{\mathrm{d}}{\mathrm{d}T}\left(\frac{n_\psi}{T^8}\right) &\simeq -2\frac{8}{3H(T)T^9}\frac{T^6}{8\pi^5\Lambda^2} \\ &= -\frac{2}{3\pi^5}\beta_{RH}^4\frac{M_P T_{RH}^2}{\Lambda^2}\frac{1}{T^7},\end{aligned}$$

which, after integrating between an initial T_i and T_{RH}, becomes

$$\begin{aligned}\left.\frac{n_\psi(T)}{T^8}\right|_{T=T_{RH}} &\simeq \left.\frac{n_\psi}{T^8}\right|_{T=T_i} + \frac{2\beta_{RH}^4 M_P T_{RH}^2}{18\pi^5\Lambda^2}\left(\frac{1}{T_{RH}^6} - \frac{1}{T_i^6}\right) \\ &\simeq \frac{\beta_{RH}^4}{9\pi^5}\frac{M_P}{\Lambda^2 T_{RH}^4},\end{aligned}$$

where in the last passage we supposed that $T_i \gg T_{RH}$ and that $(n_\psi/T^8)_{T=T_i} \ll 1$, namely that $N_{\psi_i} = n_{\psi_i} a_i^3 \ll 1$, which is a reasonable assumption. At $T = T_{RH}$ we obtain

$$n_\psi(T_{RH}) = \frac{\beta_{RH}^4}{9\pi^5}\frac{M_P T_{RH}^4}{\Lambda^2} \tag{4.34}$$

or

$$Y_\psi(T_{RH}) = \frac{5\beta_{RH}^4}{2\pi^7 g_*}\frac{M_P T_{RH}}{\Lambda^2} = \frac{1}{1.6\,\pi^7 g_*^{3/2}}\frac{M_P T_{RH}}{\Lambda^2}. \tag{4.35}$$

Therefore, Eq. (4.33) becomes

$$Y_\psi(T) \simeq \alpha\frac{M_P T_{RH}}{\Lambda^2}, \tag{4.36}$$

where

$$\alpha = \left(\frac{1}{0.06} + \frac{1}{1.6}\right)\frac{1}{\pi^7 g_*^{3/2}} \simeq 5.2 \times 10^{-6}.$$

The relic density follows from the equal contribution of ψ and anti-ψ particles to the total number density, hence

$$\Omega_\psi = \frac{2m_\psi Y_{\psi_0} s_0}{\rho_{c0}} \simeq 0.258\left(\frac{m_\psi}{\mathrm{TeV}}\right)\left(\frac{Y_{\psi_0}}{4.4\times10^{-13}}\right),$$

which shows the well-known general outcome for a TeV-scale-DM freeze-in production. This can be translated into a constraint on the reheating temperature and the interaction scale given by, for example,

$$Y_{\psi_0} \simeq 4.4\times10^{-13}\left(\frac{T_{RH}}{10^8\,\mathrm{GeV}}\right)\left(\frac{5\times10^{16}\,\mathrm{GeV}}{\Lambda}\right)^2. \tag{4.37}$$

$\boldsymbol{T_{RH} < m_\psi}$ **:** Let us see what are the typical values for the interaction scale and the reheating temperature we would obtain in the scenario with $T_{RH} < m_\psi$, where the freeze-in mechanism ends before the matter field has completely decayed and codensities are diluted by entropy injection. We utilize Eq. (4.35) and we integrate between $T = T_i$ and $T = m_\psi$, obtaining

$$Y_\psi(m_\psi) \simeq \frac{5\beta_{RH}^4}{2\pi^7 g_*} \frac{M_P T_{RH}^2}{m_\psi \Lambda^2}. \tag{4.38}$$

After the temperature has dropped below m_ψ, the total number of ψ particles is conserved, but its density is reduced,

$$n_\psi(T_{RH}) = n_\psi(m_\psi) \frac{a^3(m_\psi)}{a^3(T_{RH})} = n_\psi(m_\psi) \frac{T_{RH}^8}{m_\psi^8}, \tag{4.39}$$

so that the comoving abundance at T_{RH} is given by

$$Y_\psi(T_{RH}) = \frac{n_\psi(T_{RH})}{s(T_{RH})} = Y_\psi(m_\psi) \frac{s(m_\psi)}{s(T_{RH})} \frac{T_{RH}^8}{m_\psi^8} \simeq \frac{5\beta_{RH}^4}{2\pi^7 g_*} \frac{M_P T_{RH}^7}{\Lambda^2 m_\psi^6}. \tag{4.40}$$

This last result has been obtained with the implicit assumption that the production mechanism suddenly terminates when the temperature is equal to the DM mass. Actually, the strong IR-dependence on the exponential tail of the Boltzmann distribution of the ψ particles during the non-adiabatic regime enhances the production of ψ particles by a factor of 10^4 before the matter field has completely decayed.

Accounting for this correction, we have the following estimation for the comoving abundance today (approximately equal to the one at T_{RH}) when the production happens entirely during the non-adiabatic regime:

$$Y_{\psi_0} \simeq 4.4 \times 10^{-13} \left(\frac{\text{TeV}}{m_\psi}\right)^6 \left(\frac{T_{RH}}{10\,\text{GeV}}\right)^7 \left(\frac{3 \times 10^8\,\text{GeV}}{\Lambda}\right)^2. \tag{4.41}$$

We notice a significant reduction in the energy scale of the non-renormalizable interaction, with the natural consequence that the coupling between DM and the Higgs complex scalars is boosted by many orders of magnitude. The reason for this is that we need to provide a stronger production mechanism to deal with entropy dilution before the reheating process is completed.

4.3.2 Numerical results

All numerical results have been obtained by means of a complete solution of the system of Boltzmann equations described at the beginning of this section. In Fig. 4.3 it is depicted how Λ and T_{RH} are related once we numerically solve the system of Boltzmann equations and impose that the final relic abundance is equal to the observed one, using a TeV-scale DM candidate. The behaviors

$$\Lambda^2 \propto T_{RH},$$

for $T_{RH} < m_\psi$, and

$$\Lambda^2 \propto T_{RH}^7$$

for $T_{RH} < m_\psi$ are clearly evident.

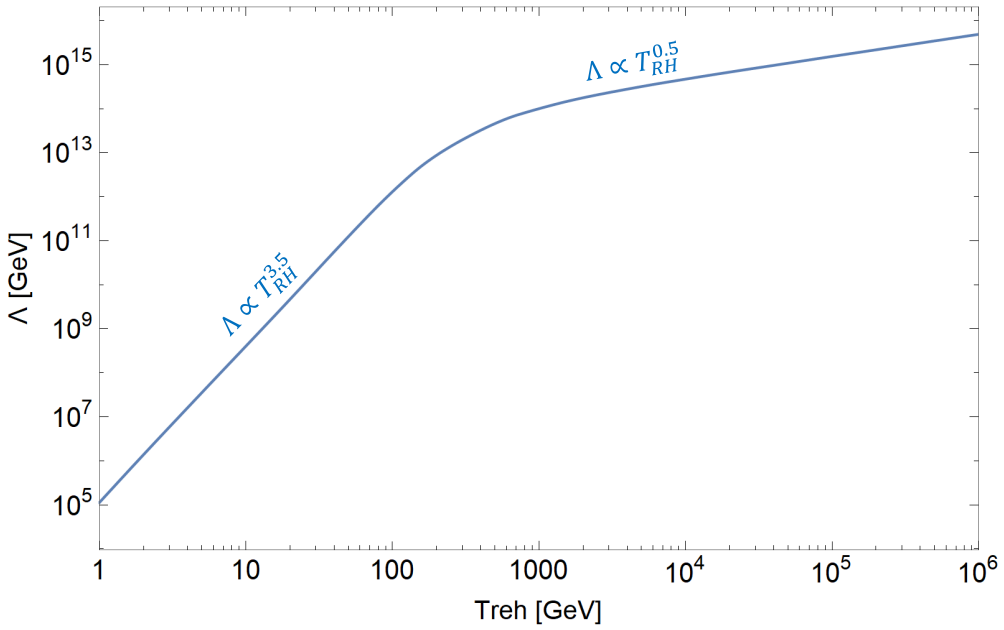

Figure 4.3: The relationship between the UV interaction scale Λ and the reheating temperature T_{RH} for $m_\psi = 1$ TeV, once the final relic density is fixed to the observed one. It can be appreciated the $\Lambda \propto (T_{RH})^{3.5}$ behavior at low reheating temperatures, while, for $T_{RH} > m_\psi$, we have $\Lambda \propto (T_{RH})^{0.5}$.

In Fig. 4.4 we show how the freeze-in yield varies with the reheating temperature (from 10^6 GeV to 100 MeV), once the interaction scale is fixed at a reference value of $\Lambda = 10^{16}$ GeV, needed to reproduce the observed yield in the highest T_{RH} scenario. Lowering T_{RH} has the dramatic consequence of reducing the production power of the Higgs-annihilation reaction down to few orders of magnitude when $T_{RH} > m_\psi$ and up to a huge interval when the dilution effect of entropy injection becomes predominant in very low reheating temperatures scenarios.

Instead, in Fig. 4.5 we adjust Λ in order to reproduce the observed comoving abundance for different T_{RH}. The general feature we observe is that if the reheating phase ends before the bath temperature reaches m_ψ, the production is UV-dominated at T_{RH}. Lowering T_{RH} has the consequence of increasing the coupling strength between DM and the Higgs bath. For the same reason, if the reaction happens well inside the reheating process, we need to require a decrease of the interaction scale Λ because the dilution factor is fixed by $(T_{RH}/m_\psi)^5$, hence we can still have underabundance of DM.

In the panels, we have also plotted the equilibrium abundance for comparison; it can be noticed that around $T_{RH} \sim 1$ GeV our framework begins to be unsuccessful,

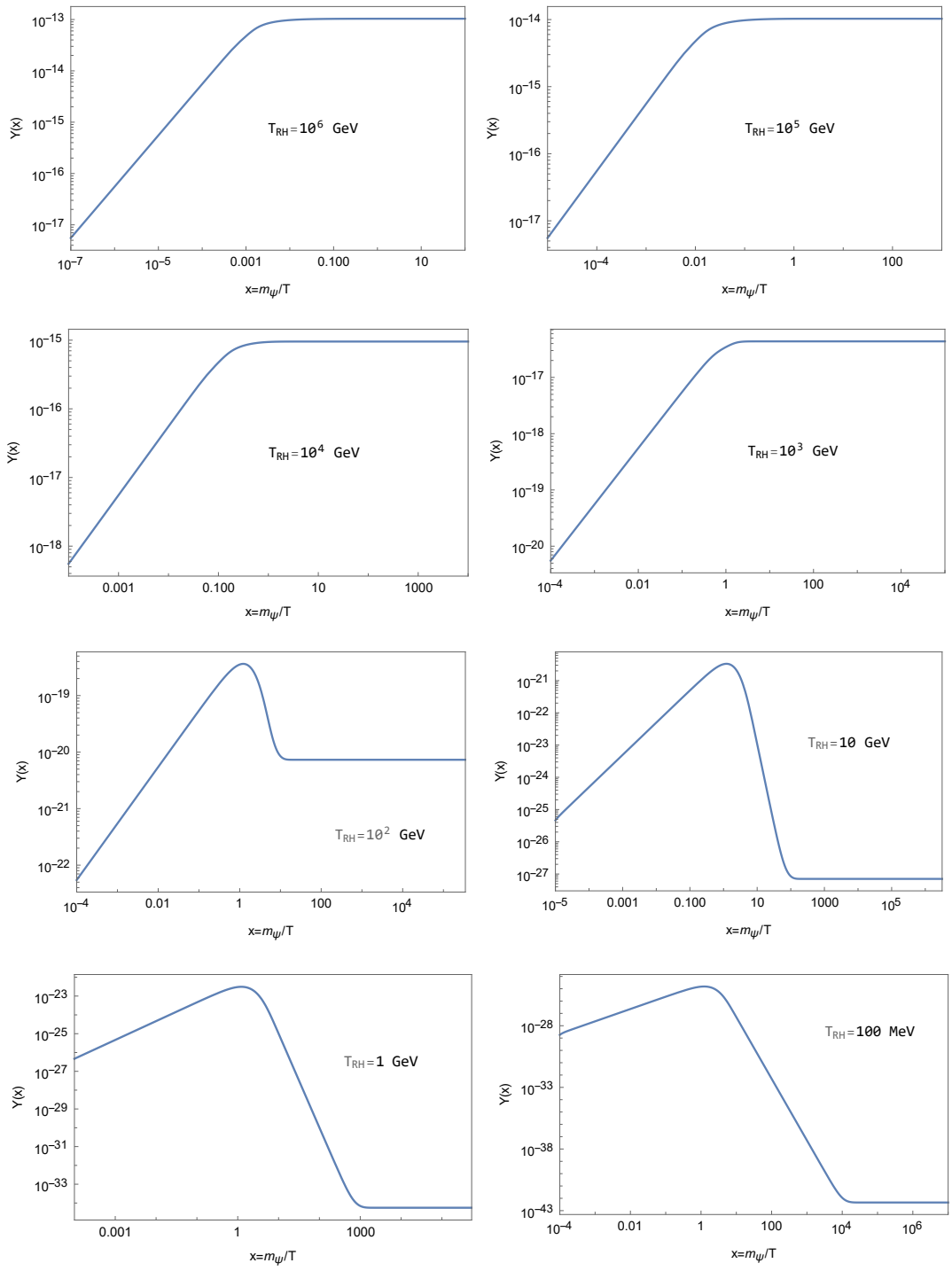

Figure 4.4: Yield $Y_\psi(x)$ for freeze-in of a TeV-scale fermionic DM candidate, mediated by a Λ_{GUT}-scale Higgs portal operator in the MD_{NA} era at different reheating temperatures, from 10^6 GeV (up-left panel) to 100 MeV (bottom-right panel). When $T_{RH} < m_\psi$, entropy suppression greatly reduces the final codensity.

because the ψ particles start to populate the thermal bath with inverse reactions and we cannot use the freeze-in mechanism anymore.

This analysis clearly shows that very low reheating temperatures scenarios require a serious boost of the couplings between the DM candidates and the Higgses. The yield we have found and the constraints on the parameter space $(T_{RH}, \Lambda, m_\psi)$ are consistent to what previously shown in the semi-analytical analysis of Section 4.3.1.

Another interesting observation is that, commonly, when the DM candidate mass is quite larger than the reheating temperature and its production is able to attain the non-equilibrium condition, we are in a situation very similar to that of thermal production of WIMPzillas [33], although the masses and temperatures utilized in that framework are usually much higher. However, possible connections to superheavy DM could be studied.

We have to stress that the results obtained for reheating temperatures below the electroweak scale, namely around 10^2 GeV, must be corrected by including the effects of EWSB, which were not considered. In particular the Higgs fields acquire a vev, which splits the FHPO interaction in a renormalizable effect (an additional mass term for DM) and a non-renormalizable interaction between the Higgs boson and the DM fermions. These effects should not dramatically modify the overall output, but need to be incorporated.

We observe that the reheating temperatures we have chosen are perfectly consistent with observational data, since there are no stringent bounds other than BBN successes, which give a constraint $T_{RH} > 20$ MeV. For what regards the upper bounds, we do not know what is the UV physics dominating those energies, so that we have a certain amount of freedom in setting the limit. However, on the one side, a plausible conservative upper limit is given by the scale of Inflation, $T_{RH} < \Lambda_{inf} \sim 10^{16}$ GeV, but on the other hand, there are many reasons to consider a much lower value, among all the gravitino problem, which forces $T_{RH} < 10^{10}$ GeV [93].

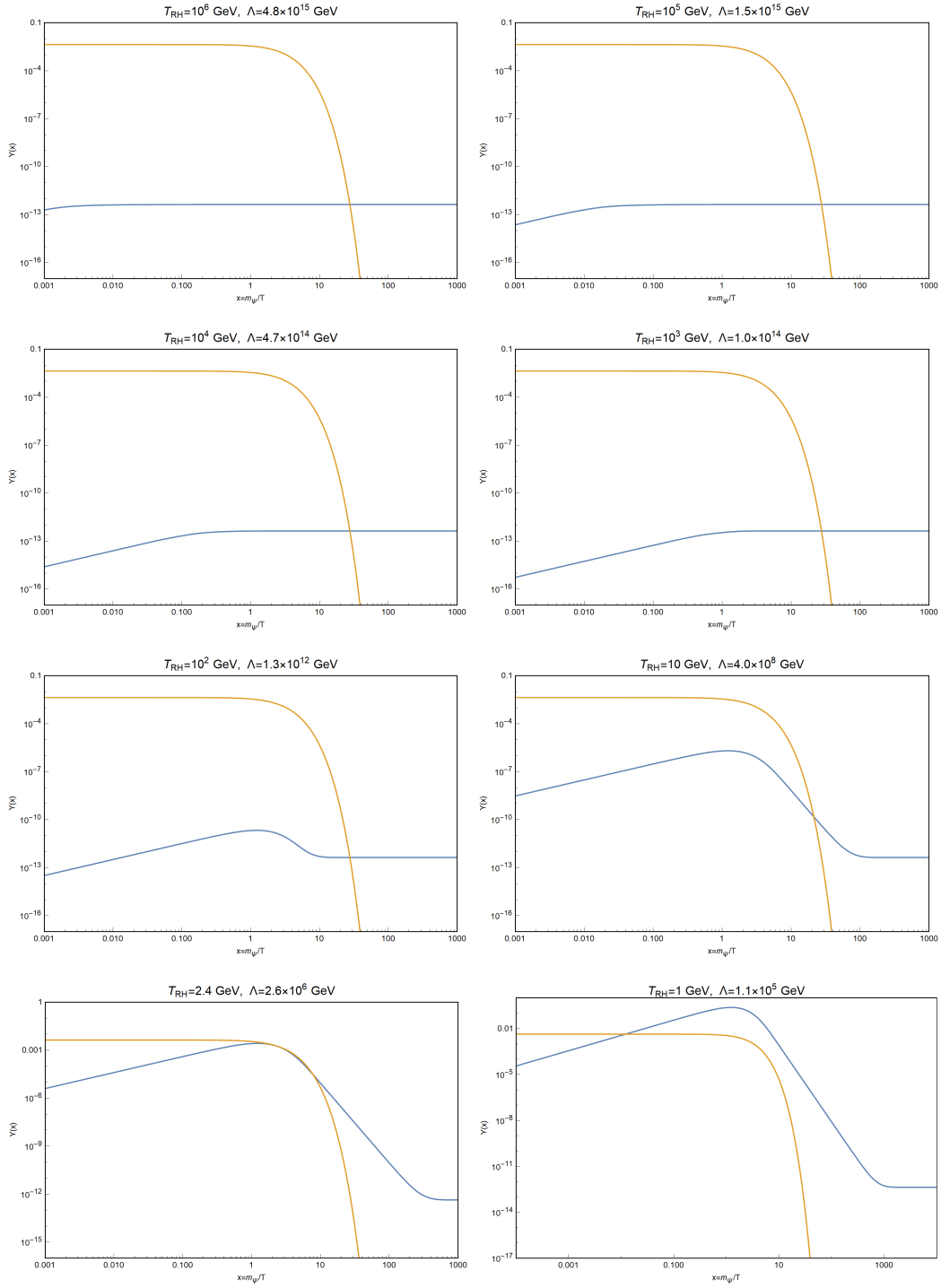

Figure 4.5: Yield $Y_\psi(x)$ (the blue curves) for freeze-in mediated by a fermionic Higgs portal operator in the MD_{NA} era at different (low) reheating temperatures. The coupling strength has been tuned in order to reproduce the observed comoving abundance at late times. The yellow curve represents the equilibrium abundance, reached at around $T_{RH} = 2.4$ GeV, so that the freeze-in mechanism stops to be valid.

Chapter 5

UV sensitivities in Fast-Expanding Cosmologies

In this chapter, we want to explore the extent of the UV sensitivity of the Higgs portal for freeze-in production of a fermionic DM particle candidate. In the previous chapters, we developed the formal background for both the cosmology and the field theory involved, with a particular digression on an early MD_{NA} epoch, where we studied how the energy scale Λ of the non-renormalizable interaction is affected by a modification of the reheating temperature when the matter field has completely decayed.

Here, we want to concentrate on cosmologies characterized by an adiabatic, faster-than-radiation evolution, driven by a generic scalar field ϕ with equation of state $w_\phi > 1/3$, as we likewise discussed in Section 3.3 and Section 4.1. For renormalizable interactions, if we let the primordial Universe to have a phase before the BBN, during which the Hubble rate is higher than the standard scenario, the frozen-in yield is automatically reduced by a factor $\mathcal{F}$ of some orders of magnitude, which could reach $10^9 - 10^{11}$ for exotic scenarios with $w_\phi > 1$ [39]. Consequently, the couplings between DM and the thermal bath needs to be increased by roughly $\sqrt{\mathcal{F}}$ (couplings appear squared in the relic density), hence potentially up to 10^5 times those commonly assumed in a standard RD freeze-in scenario after inflation (usually of order 10^{-12}). The evident output is that for small T_r (long-lasting fast-expansions) the Hubble rate had had enough time to tear apart the number density of DM particles and the effect is more evident for higher n. In Fig. 5.1 from [39], it is shown the contour plot of the relic density suppression in the case of renormalizable pair production as a function of T_r (the temperature of ϕ-radiation equivalence) and $n = 3w_\phi - 1$.

Our intent here is to extend this analysis by using the Fermionic Higgs Portal, a non-renormalizable interaction, whose IR/UV sensitivity was shown in Eq. (4.3). Therefore, for operators with $d = 5$, we expect an IR domination for $n < 2$, while an UV domination for $n > 2$. The intermediate case (a kination epoch) is expected to give a logarithmic dependence on the temperature extremes of integration.

This chapter is subdivided into two parts: in the first one (Section 5.1), we update the analysis of [39] to non-renormalizable interactions and we analyze the DM pair

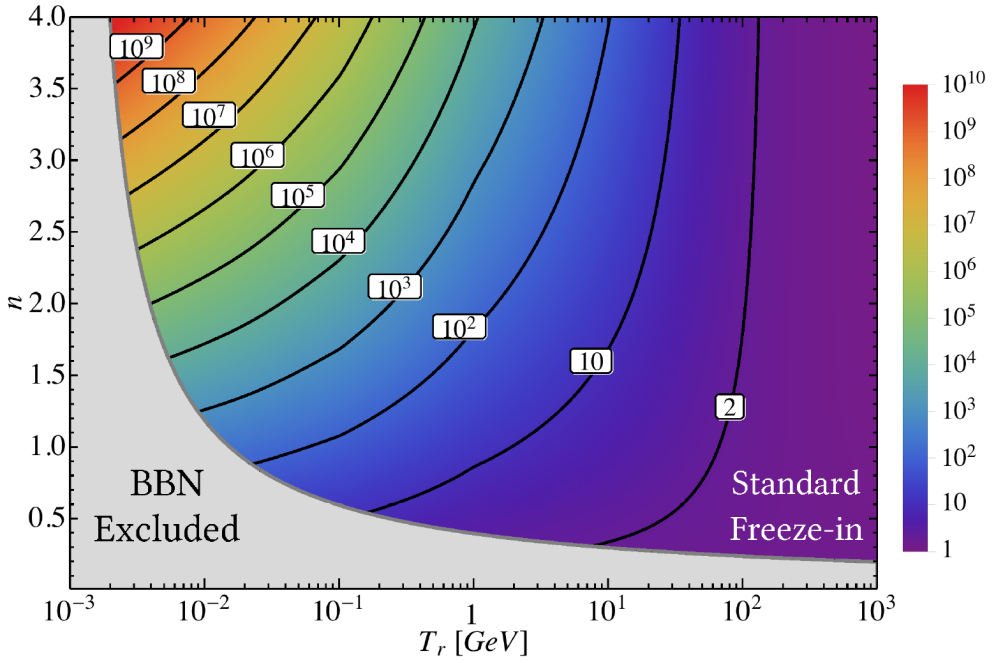

Figure 5.1: Frozen-in relic density suppression for modified cosmologies with respect to the standard scenario in a renormalizable pair production annihilation process. The BBN bound is extracted by using Eq. (3.35). *Source*: Image from [39].

production with a generic scalar field redshifting as $\rho_\phi \propto a^{-(4+n)}$. We calculate the relic abundance and we make considerations about the parameters involved: Λ, n, T_r and T_{RH}. In the second part (Section 5.2), we address the same problem within a more physically concrete scenario: Quintessential cosmology (see also Section 3.2 for a deeper discussion).

5.1 Steady-state scalar field

We assume that the cosmological background is driven primarily by a stable, massless scalar field ϕ, redshifting as $\rho_\phi \propto a^{-(4+n)}$, with the Hubble parameter given by Eq. (3.31),

$$H = \frac{\sqrt{\rho_R + \rho_\phi}}{\sqrt{3}M_P} = \frac{\sqrt{\rho_R}}{\sqrt{3}M_P}\left[1 + \left(\frac{g_*(T_r)}{g_*(T)}\right)\left(\frac{g_{*s}(T)}{g_{*s}(T_r)}\right)^{(4+n)/3}\left(\frac{T}{T_r}\right)^n\right]^{1/2}, \qquad (3.31)$$

where the only configuration in which the radiation energy density is predominant is when $n = 0$, namely the scalar field behaves as an additional radiation degree of freedom.

To give an idea of the expected results, we set ourselves in the high-energy limit,

where the expression for the Hubble parameter is given by Eq. (3.32),

$$H \simeq \frac{\pi g_*^{1/2}}{3\sqrt{10}} \frac{T^2}{M_P} \left(\frac{T}{T_r}\right)^{n/2} . \tag{3.32}$$

In the following, we will keep this approximation for the Hubble parameter. Numerical calculations will employ the full expression.

5.1.1 Generic non-renormalizable operators

To start with a generic case, we analyze in a deeper way the yield we have obtained in Eq. (4.2), where we have considered a generic operator with mass dimension $d > 4$ and a Hubble rate evolving with $T^{2+n/2}$. The production turns out to be IR dominated only if $d < d_{\rm th} = 4.5 + n/4$ (see Eq. (4.3)) and the integration procedure needs to be split in two cases: when d is equal to this threshold value and when not.

Hence, the Boltzmann equation reads as

$$\begin{aligned} \frac{\mathrm{d}Y_\psi}{\mathrm{d}\log T} &\simeq 2\frac{T^{2d-4}}{\Lambda^{2d-8}} \frac{3\sqrt{10}}{\pi g_*^{1/2}} \frac{M_P T_r^{n/2}}{T^{2+n/2}} \frac{45}{2\pi^2 g_* T^3} = \\ &= \frac{135\sqrt{10}}{\pi^3 g_*^{3/2}} \frac{M_P T_r^{n/2}}{\Lambda^{2d-8}} T^{2d-n/2-9}, \end{aligned}$$

which can be solved by choosing the reheating temperature after inflation T_{RH} and the DM mass m_ψ as the upper and lower extreme of integration, respectively. Inside this assumption, we are implicitly supposing that the inflaton field decays almost instantaneously, so that we are not interested in low-reheating temperature scenarios and that $T_{RH} > m_\psi > T_r$.

$$Y_{\psi_0} \simeq \frac{135\sqrt{10}}{\pi^3 g_*^{3/2}} \frac{M_P T_r^{n/2}}{\Lambda^{2d-8}} \times \begin{cases} \dfrac{1}{2d - n/2 - 9} T_{RH}^{2d-n/2-9} & \text{if } d > 4.5 + n/4 \\ \log\left(\dfrac{T_{RH}}{m_\psi}\right) & \text{if } d = 4.5 + n/4 \\ \dfrac{1}{n/2 + 9 - 2d} m_\psi^{2d-n/2-9} & \text{if } d < 4.5 + n/4 \end{cases} \tag{5.1}$$

where the expressions have been simplified to retain only the significant terms (T_{RH} when UV-dominated, m_ψ when IR dominated). The most interesting fact is that, when $d = 4.5 + n/4$, the yield has a logarithmic behavior. Since d is a positive integer, the only situations in which the equality is verified are those for which $n = -2, 2, 6, ...$, but, concretely, only the first two are of interest in cosmology, namely when $w = -1/3$ (zero acceleration) and $w = 1$ (kination); then the mass dimension threshold for the interaction operator is 4 and 5, respectively.

5.1.2 Fermionic Higgs Portal

Following the same path, we can write the Boltzmann equation for the freeze-in pair production process through the annihilations $hh \to \overline{\psi}\psi$ of the two massless Higgs complex scalars:

$$\frac{\mathrm{d}Y_\psi}{\mathrm{d}\log T} \simeq 2\frac{T^6}{8\pi^5\Lambda^2}\frac{3\sqrt{10}}{\pi g_*^{1/2}}\frac{M_P T_r^{n/2}}{T^{2+n/2}}\frac{45}{2\pi^2 g_* T^3} = \\ = \frac{135\sqrt{10}}{8\pi^8 g_*^{3/2}}\frac{M_P T_r^{n/2}}{\Lambda^2}T^{1-n/2},$$

or

$$\mathrm{d}Y_\psi = \frac{135\sqrt{10}}{8\pi^8 g_*^{3/2}}\frac{M_P T_r^{n/2}}{\Lambda^2}\frac{\mathrm{d}T}{T^{n/2}}. \tag{5.2}$$

As we have done in the general case, to integrate this equation we have to distinguish between the cases with $n > 2$, $n < 2$ and $n = 2$.

From Eq. (5.1), the final yield (with instantaneous reheating, as we said) reads as follows,

$$Y_{\psi_0} \simeq \frac{135\sqrt{10}}{8\pi^8 g_*^{3/2}}\frac{M_P}{\Lambda^2} \times \begin{cases} \dfrac{2}{2-n}T_{RH}\left(\dfrac{T_r}{T_{RH}}\right)^{n/2} & \text{if } n < 2 \\ T_r \log\left(\dfrac{T_{RH}}{m_\psi}\right) & \text{if } n = 2\,. \\ \dfrac{2}{n-2}m_\psi\left(\dfrac{T_r}{m_\psi}\right)^{n/2} & \text{if } n > 2 \end{cases} \tag{5.3}$$

We notice the features we were expecting: for $n < 2$ the UV sensitivity of the Fermionic Higgs Portal has a preponderant effect, with the yield dominated by T_{RH}. For $n = 2$ the abundance is basically set up by T_r and Λ^2, with only a logarithmic dependence on the initial and final temperatures. Finally, despite the non-renormalizable interaction, exotic scenarios with $n > 2$ show again an IR-domination, with the yield determined by the lowest temperature, in this case m_ψ, after which the reaction is no longer effective. Notice that the role of T_r becomes increasingly crucial in setting the final yield as n grows; the cooler the $\phi-$radiation equivalence temperature, the later radiation will overcome on the fast-expanding regime, leading to suppressed codensities. Again, we stress that the main differences with the standard radiation epoch are determined by n, T_{RH} and T_r, while the interaction scale does not play any role, simply because related only on the type of particle physics interaction (in other words, it always appears squared at the denominator).

The relic abundance today is easily computed in the following way:

$$\Omega_\psi = \frac{\rho_\psi}{\rho_{c0}} = \frac{2 m_\psi s_0 Y_{\psi_0}}{\rho_{c0}} = \\ \simeq 6.7 \times 10^{21}\ \text{GeV}\, \frac{m_\psi}{\Lambda^2} Y_{\psi_0}, \tag{5.4}$$

which we can analyze for the relevant cases of $n \in [0, 4]$:

$$\Omega_\psi^{n=0} \simeq 0.258 \left(\frac{m_\psi}{\text{TeV}}\right) \left(\frac{T_{RH}}{10^8\,\text{GeV}}\right) \left(\frac{5 \times 10^{16}\,\text{GeV}}{\Lambda}\right)^2 \tag{5.5}$$

$$\Omega_\psi^{n=1} \simeq 0.258 \left(\frac{m_\psi}{\text{TeV}}\right) \left(\frac{T_{RH}}{10^8\,\text{GeV}}\right)^{1/2} \left(\frac{T_r}{20\,\text{MeV}}\right)^{1/2} \left(\frac{1.4 \times 10^{14}\,\text{GeV}}{\Lambda}\right)^2 \tag{5.6}$$

$$\Omega_\psi^{n=2} \simeq 0.258 \left(\frac{m_\psi}{\text{TeV}}\right) \left(\frac{T_r}{20\,\text{MeV}}\right) \left(\frac{2.4 \times 10^{12}\,\text{GeV}}{\Lambda}\right)^2 \log\left(\frac{T_{RH}}{10^8\,\text{GeV}} \frac{\text{TeV}}{m_\psi}\right) \tag{5.7}$$

$$\Omega_\psi^{n=3} \simeq 0.258 \left(\frac{m_\psi}{\text{TeV}}\right)^{1/2} \left(\frac{T_r}{20\,\text{MeV}}\right)^{3/2} \left(\frac{7 \times 10^{10}\,\text{GeV}}{\Lambda}\right)^2 \tag{5.8}$$

$$\Omega_\psi^{n=4} \simeq 0.258 \left(\frac{T_r}{20\,\text{MeV}}\right)^2 \left(\frac{3.2 \times 10^{9}\,\text{GeV}}{\Lambda}\right)^2 . \tag{5.9}$$

The reference DM relic abundance is taken from [9], whereas we normalized the various quantities by means of a reheating temperature of 10^8 GeV, which is compatible with all the cosmological histories here considered; this limit is shown in Fig. 3.3, with the bounds taken from

$$T_{RH} \lesssim M_P \left(\frac{T_r}{M_P}\right)^{n/(n+4)}, \tag{3.33}$$

In Table 5.1 we show some upper bounds for T_{RH}. We notice that, in principle, the reheating phase could last up to temperatures of order 10^8 GeV, much lower than the Planck scale. As a last remark, we stress that in all the semi-analytical estimations,

n	0	1	2	3	4
T_{RH}^{max} [GeV]	M_P	2.3×10^{14}	5×10^{11}	6×10^9	2.2×10^8

Table 5.1: Upper bound on the reheating temperature after inflation, for some values of n and $T_r = 20$ MeV, obtained by imposing that the scalar field does not overcome Planckian values.

we have always considered the $\phi-$radiation equivalence temperature in the most conservative way, choosing $T_r = 20$ MeV, compatible with BBN experimental data [39]. If the equivalence occurs well before BBN, the field could have begun to dominate at higher temperatures and the bounds on T_{RH} relax.

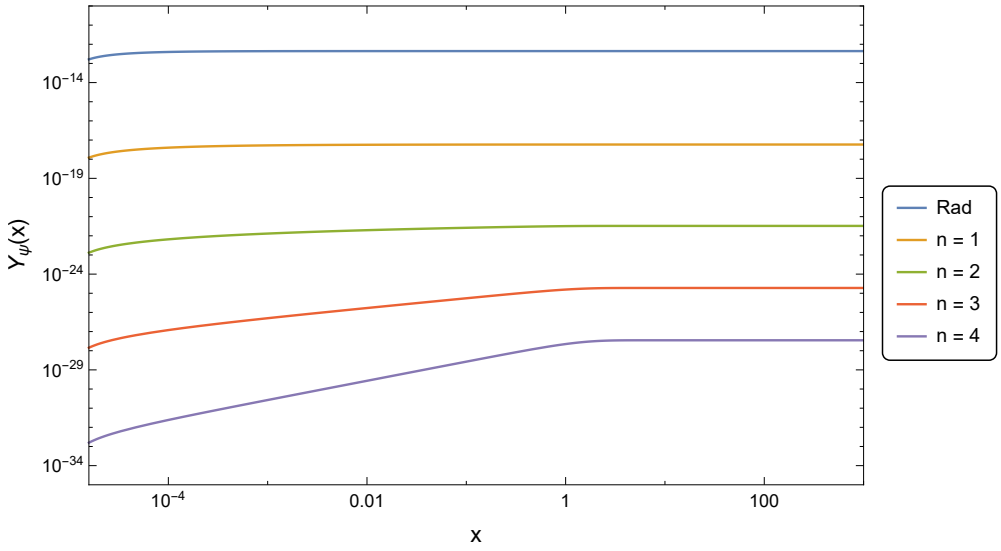

Figure 5.2: Numerical solutions for the comoving number density Y_ψ with $m_\psi = 1$ TeV and the Higgs scalars considered as massless. We choose $T_{RH} = 10^8$ GeV, $T_r = 20$ MeV and $\Lambda = 5 \times 10^{16}$ GeV to reproduce the observed yield for RD.

Our numerical results are obtained by integrating the Boltzmann equation, using Eq. (2.19), where we take the reheating temperature as the superior extreme of integration, an approximation valid in the limit of instantaneous reheating, as we said previously. Clearly, with a five-dimensional operator, the choice of T_{RH} is crucial for determining the yield in the slower expansion scenarios, but it has a minor role during kination and is completely inert for the fastest cosmologies.

This fact can be seen in Fig. 5.2, where we set $T_{RH} = 10^8$ GeV and $\Lambda = 5 \times 10^{16}$ GeV; the lines show a comoving density already frozen at small x for $n \leq 2$, while the same grows from zero to the final value at $x \sim 1$ for $n > 2$. The final comoving density (hence the final relic abundance) in the next-to-RD scenarios is $5 - 10$ orders of magnitude lower, whereas for $n = 4$ the suppression is around 10^{15}.

Keeping the reheating temperature at 10^8 GeV, we adjust the interaction scale in order to reproduce the observed relic density. The results, depicted in Fig. 5.3, are in good agreement with the estimations done in Equations (5.5)–(5.9). We observe that, as n increases, the effective field theory we rely upon has a more limited range of applicability, because the heavier degrees of freedoms of the unknown UV-complete theory could possibly become relevant in the fastest scenarios, where the interaction scale could be of order the reheating temperature. For example, in the setup here considered, with a long-lasting $n = 4$ expansion, we might have $T_{RH}^{n=4} \lesssim 10^8$ GeV and $\Lambda \sim 10^9$ GeV.

Actually, cosmologies with $n > 2$ are of little interest in our context, because UV-insensitive to the non-renormalizable interaction of the FHPO. If we concentrate on $n \leq 2$ we can make some further considerations. First, once the final relic abundance is fixed, the interaction scale is related to T_{RH} with different powers: $\Lambda \propto T_{RH}^{1/2}$ during

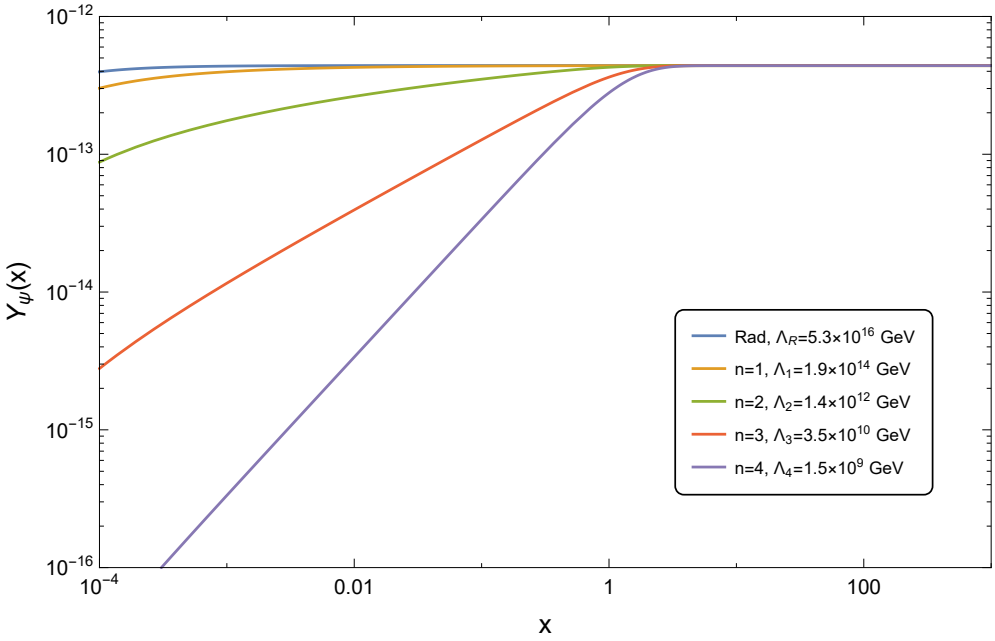

Figure 5.3: Numerical solutions for the comoving number density Y_ψ with $m_\psi = 1$ TeV and the Higgs complex scalars considered as massless. We choose $T_{RH} = 10^8$ GeV and $T_r = 20$ MeV, but Λ is changed in order to reproduce the observed relic abundance $Y_\psi^0 \simeq 4.4 \times 10^{-13}$ ($\Lambda_1 = 1.9 \times 10^{14}$ GeV, $\Lambda_2 = 1.4 \times 10^{12}$ GeV, $\Lambda_3 = 3.5 \times 10^{10}$ GeV, $\Lambda_4 = 1.5 \times 10^9$ GeV).

RD (or a scalar field redshifting with $n = 0$) and $\Lambda \propto T_{RH}^{1/4}$ for $n = 1$. During kination, we have $\Lambda^2 \propto \log T_{RH}$, with the number density practically determined by Λ and T_r.

If we let T_{RH} take the maximum values as in Table 5.1, we should correct for Λ in this way: for $n = 0$ and $T_{RH} = M_P$ we have $\Lambda_0 \gg M_P$, with $n = 1$ and $T_{RH} = 2.3 \times 10^{14}$ GeV we obtain $\Lambda_1 \sim 5.4 \times 10^{17}$ GeV and for $n = 2$ with $T_{RH} = 4.8 \times 10^{11}$ GeV we get $\Lambda_2 \sim 1.2 \times 10^{13}$ GeV. Cosmologies with $n > 2$ do not give use insights on the reheating temperature if interactions have mass dimensions less or equal to 5.

For what regards the two exotic UV-sensitive scenarios ($n = 1$ and $n = 2$), the evolution of the freezing-in yield during a cosmology driven by an energy density that redshifts as $\rho_\phi \propto a^{-5}$ is shown in Fig. 5.4, where we set $\Lambda = \Lambda_1 = 1.9 \times 10^{14}$ GeV and we used four different values of T_{RH}: 10^8 GeV, 10^{10} GeV, 10^{12} GeV and 2.3×10^{14} GeV. The comoving number density is almost totally frozen to a constant value right at the onset of the non-standard era, i.e. at the reheating temperature, hence the UV-sensitivity is extreme. We did the same within a kination regime, using $\Lambda = \Lambda_2 = 1.4 \times 10^{12}$ GeV and three different values of T_{RH}: 10^8 GeV, 10^{10} GeV and 4.8×10^{11} GeV. The results, depicted in Fig. 5.5, show the sudden rise of the comoving number density as the initial conditions are set, while it evolves logarithmically as the Universe cools down, freezing-in at $T = m_\psi$. The values for the reheating temperature are bounded by the maximum of $T_{RH}^{n=2} \simeq 4.8 \times 10^{11}$ GeV.

In the $\Lambda - n$ plane of Fig. 5.6 we show how the interaction scale changes in order to reproduce the observed DM abundance for $m_{DM} = 1$ TeV and four reheating temper-

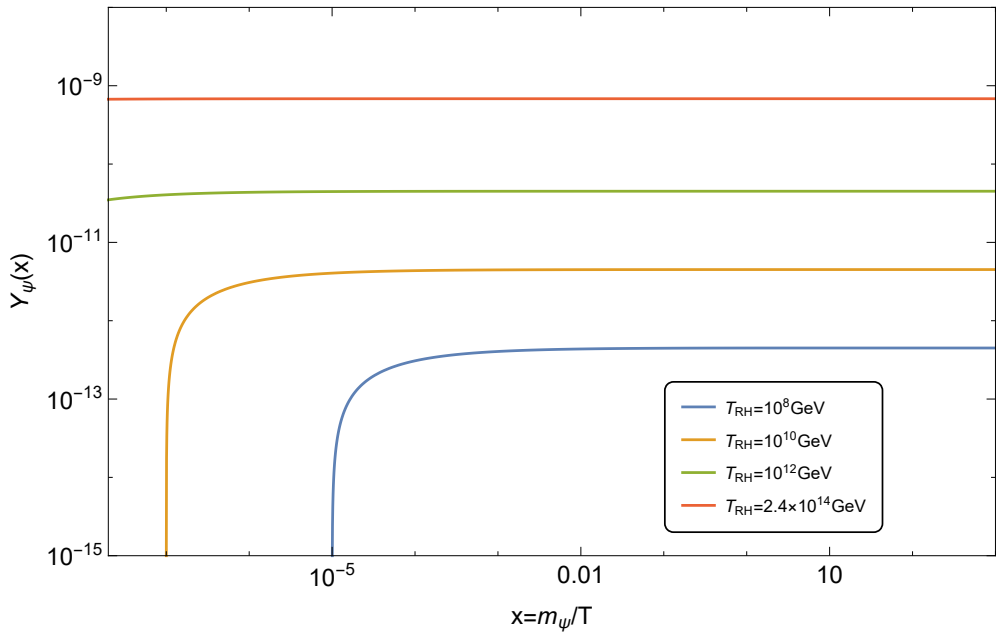

Figure 5.4: Numerical solutions for the comoving number density Y_ψ with $m_\psi = 1$ TeV during a $n = 1$ cosmology for different values of T_{RH}. We put $\Lambda = 1.9 \times 10^{14}$ GeV, which reproduces the observed relic abundance if $T_{RH} = 10^8$ GeV. We always have $T_r = 20$ MeV.

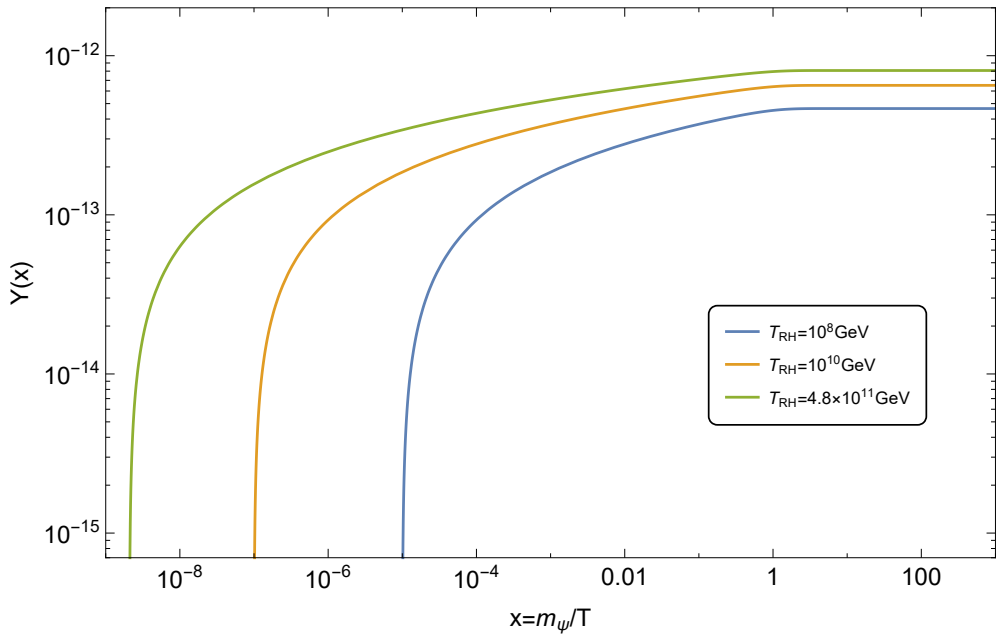

Figure 5.5: Numerical solutions for the comoving number density Y_ψ with $m_\psi = 1$ TeV during a $n = 2$ cosmology for different values of T_{RH}. We put $\Lambda = 1.4 \times 10^{12}$ GeV, which reproduces the observed relic abundance if $T_{RH} = 10^8$ GeV. We always have $T_r = 20$ MeV.

atures of reference: $T_{RH} = 10^4$ GeV, $T_{RH} = 10^6$ GeV, $T_{RH} = 10^8$ GeV and $T_{RH} = 10^{10}$ GeV. The separation between IR and UV domination is highlighted in correspondence of $n = 2$, after which the two lines join into a single one, meaning that the information about T_{RH} is lost. The values we obtain for Λ span a very wide spectrum; in particular, for $n \in [0, 4]$, one obtains enhancement factors which can go from few units to ten orders of magnitude.

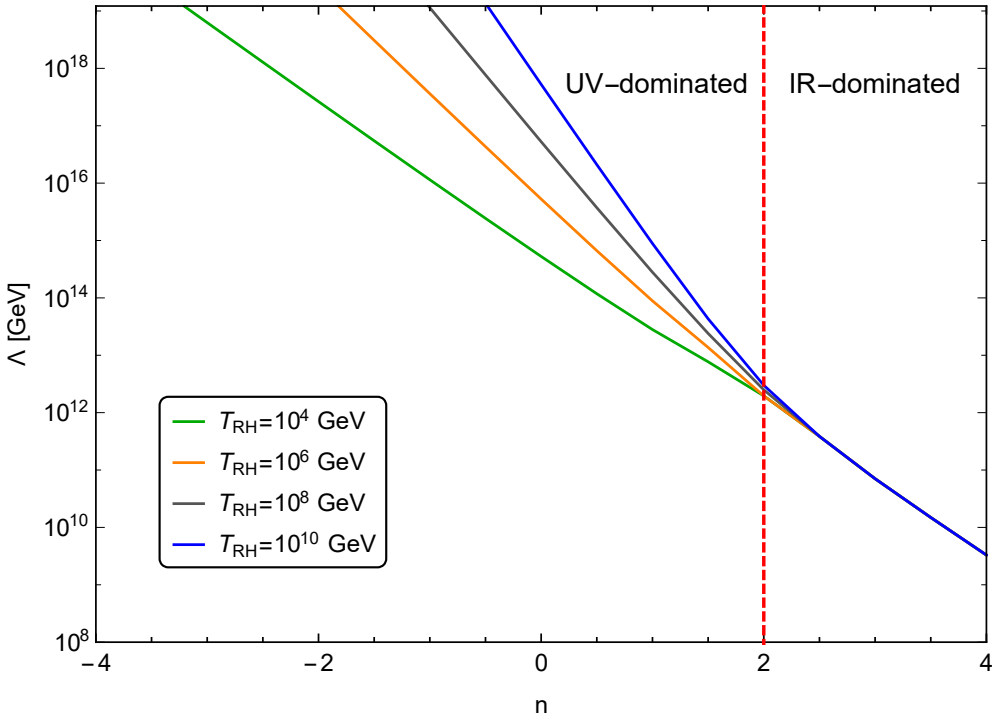

Figure 5.6: Contours for the interaction scale Λ that reproduces the observed relic abundance of DM in cosmologies with $n \in [-4, 4]$, when $m_\psi = 1$ TeV and $T_r = 20$ MeV. In green, orange, gray and blue are indicated the values when $T_{RH} = 10^4$ GeV, $T_{RH} = 10^6$ GeV, 10^8 GeV and $T_{RH} = 10^{10}$ GeV, respectively. The red dashed line at $n = 2$ (kination) marks the edge between IR and UV domination, the plot has been cut at $M_P = 1.22 \times 10^{19}$ GeV.

5.1.3 Relic density suppression

The relic density, which gets more and more suppressed with the increase n, as a result of the fast expanding background Universe, has a novel feature when the operator responsible for the freeze-in production has a dimension greater than four. In fact, in the simpler case of renormalizable interactions, the ratio between the relic abundance for RD and the one for $n > 0$ goes like

$$\mathcal{F}(T_r, n) \coloneqq \frac{Y_\psi^\infty\big|_n}{Y_\psi^\infty\big|_{\rm rad}} \sim (m_\psi/T_r)^{-n/2}, \tag{5.10}$$

but when we deal with higher-dimensional operators, the production mechanism is UV-dominated in the standard RD era by a certain T_{UV} and we use to take $T_{UV} = T_{RH}$. Hence, the differences between UV and IR domination during a modified cosmology have the consequence of adding small changes in the first case and very large alterations in the latter. This can be understood by explicitly deriving the ratio for each n in the case of a five-dimensional operator like the FHPO (we write the inverse ratio for convenience and we neglect numerical factors):

$$\mathcal{F}(T_r, n)^{-1} = \frac{Y_\psi^\infty\big|_{\rm rad}}{Y_\psi^\infty\big|_n} \sim \begin{cases} \left(\dfrac{T_{RH}}{T_r}\right)^{1/2} & \text{if } n = 1 \\ \dfrac{T_{RH}}{T_r \log(T_{RH}/m_\psi)} & \text{if } n = 2 \\ \dfrac{T_{RH}\, m_\psi^{1/2}}{T_r^{3/2}} & \text{if } n = 3 \\ \dfrac{T_{RH}\, m_\psi}{T_r^2} & \text{if } n = 4 \end{cases} . \tag{5.11}$$

The firs two cases show that the ratio has the same dependence on $(T_{\rm f.i.}/T_r)^{-n/2}$ as in the standard situation, but now the temperature of particle production is $T_{\rm f.i.} = T_{RH}$ and not m_ψ. The kination scenario has also the usual logarithmic factor. If we evaluate them at $T_{RH} = 10^8$ GeV and $T_r = 1$ MeV, we obtain a suppression around 10^5 and 10^{10}, respectively, pretty much alike the same found with renormalizable interactions in [39]. Clearly, an anticipation of the end of Inflation would provide larger factors.

The last two possibilities involve both the high-temperature contribution of $Y_\psi^\infty\big|_{\rm rad}$ and the DM mass from $Y_\psi^\infty\big|_n$. For $T_{RH} = 10^8$ GeV and $T_r = 20$ MeV we have that, for a TeV-scale DM candidate, the reduction in the relic density amounts to 10^{12} and 10^{14}, much larger than before.

The possible values attained by the inverse ratio $\mathcal{F}^{-1}$ are shown in the $T_r - n$ planes of Figures 5.7–5.8. The different choices for the initial temperature, i.e. T_{RH}, entail a miscellaneous set of suppression factors, which however is limited by a reduction in the parameter space after 10^8 GeV due to Eq. (3.33) (when the energy density of the scalar field reaches super-Planckian values). The BBN bound is taken from Eq. (3.35). The best enhancement one can achieve is always when the faster scenario lasts for the longest possible time, namely until the radiation temperature cools to few MeV. In that case, the suppression can be a factor 10^{16} smaller than in a standard cosmology. Increasing the reheating temperature to higher values, such as 10^{10} GeV could provide, in principle, much higher reductions, but the bounds of Eq. (3.33) force the parameter space to shrink considerably. We remind the reader that the computations have been carried out within the instantaneous reheating approximation.

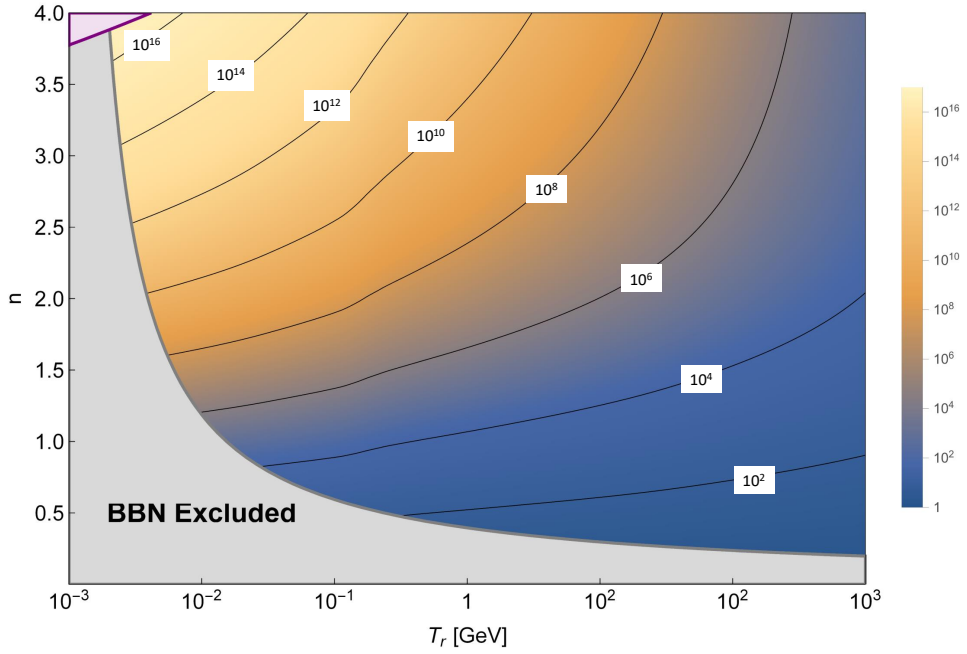

Figure 5.7: Contour plot in the $T_r - n$ plane of the relic density reduction/enhancement with $T_{RH} = 10^8$ GeV. The bound Eq. (3.33) on T_{RH} (the small lilac top-left corner) is not relevant in this case.

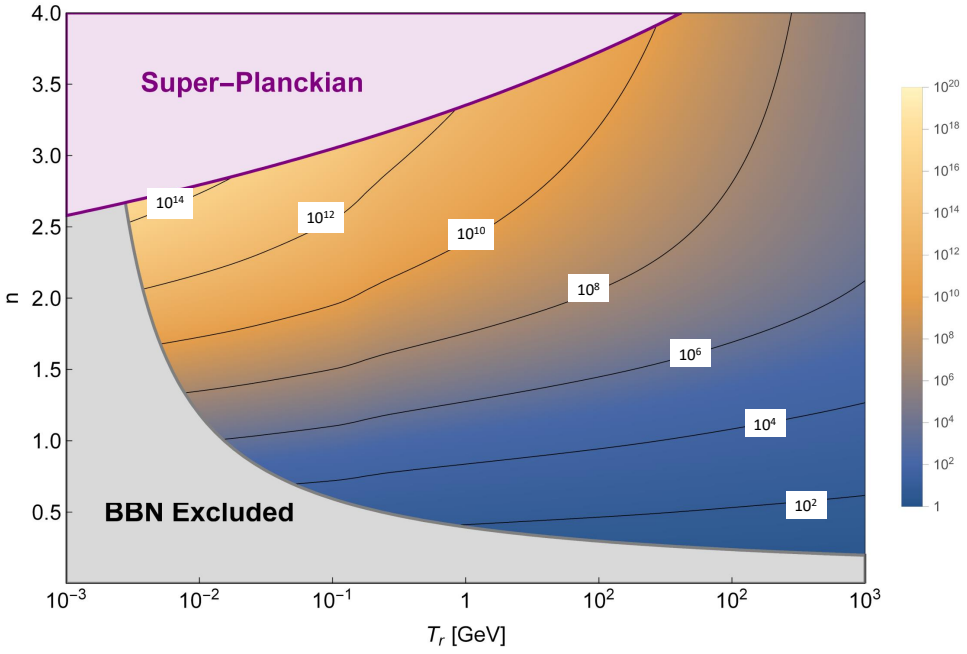

Figure 5.8: Contour plot in the $T_r - n$ plane of the relic density reduction/enhancement with $T_{RH} = 10^{10}$ GeV. The bound Eq. (3.33) on T_{RH} (the lilac region) excludes the region where the parameters would give a super-Planckian scalar field energy density.

5.2 Quintessential Kination

In this last section, we focus on freeze-in production of FIMP dark matter in a cosmology populated with Quintessence [63, 64, 94] (see also Section 3.2.1), an additional stable, rolling scalar field ϕ characterized by a potential with exponential form, which makes its energy density evolve from a pure kinetic-energy-domination towards a pure potential-energy-domination, changing its barotropic equation of state from $w = 1$ to $w = -1$. Thus, we suppose that the early Universe was kination dominated (KD) and that the same field is responsible for the missing energy in the Universe today, namely that its vacuum energy density corresponds to the observed DE component and leads to the present accelerated expansion. Therefore, we aim at studying how the results we have obtained in the context of a generic KD cosmology with $\rho_\phi \propto a^{-6}$ relates to a more fundamental framework, where we identify the generic fluid with Quintessence. In other words, we want to solve the equations of motion for ϕ and see how the new energy density modifies the Hubble rate and particle production, taking care of the most up-to-date constraints on fundamental cosmological parameters.

The equation of motion (EoM) for the spatially homogeneous scalar field ϕ is given by the Klein-Gordon equation in a FLRW background,

$$\ddot{\phi} + 3H\dot{\phi} = -\frac{\mathrm{d}V(\phi)}{\mathrm{d}\phi}, \tag{3.19}$$

where we assume a potential with exponential form as [55, 56, 63, 64, 68, 69, 79, 82, 94–96]

$$V(\phi) = V_0 \exp\left[-\lambda \frac{\phi}{M_P}\right]. \tag{5.12}$$

The Hubble parameter reads as

$$H^2 = \frac{\rho_\phi + \rho_R + \rho_M}{3M_P^2}, \quad \text{with} \quad \rho_\phi = \frac{\dot{\phi}^2}{2} + V(\phi). \tag{5.13}$$

The field is rolling down its potential, whose scaling is strictly dependent on what type of matter-energy content the Universe has, since the Hubble rate, acting as a frictional term, plays a crucial role in balancing the damping of the kinetic energy of the field, compared to the relative intensification with respect to the potential energy. It is clear that we will have to require a certain amount of steepness for the potential to provide a solution which eventually reproduces the observed Universe with good agreement.

Following a standard procedure [63, 64, 68, 79, 81, 82, 95], we convert time derivatives into derivatives with respect to the logarithmic time

$$\tau = \ln(a/a_0) = -\ln(1+z), \tag{5.14}$$

with z the redshift, which implies $\dot{\tau} = H$ and $\mathrm{d}t = H^{-1}\mathrm{d}\tau$. As is the custom, we take $a_0 = 1$. The other relevant quantities we need to express as functions of τ are the

temperature, for which we have the differential equation

$$\frac{1}{T}\frac{\mathrm{d}T}{\mathrm{d}\tau} = -\left(1+\frac{1}{3}\frac{\mathrm{d}\ln g_{*S}}{\mathrm{d}\ln T}\right)^{-1}, \tag{A.30}$$

whereas the entropy density, and the energy density for radiation and pressureless matter can be cast as

$$s = s_0\, e^{-3\tau}, \quad \rho_R = \rho_R^0 \frac{g_*}{g_*^0}\left(\frac{g_{*S}^0}{g_{*S}}\right)^{4/3} e^{-4\tau}, \quad \rho_M = \rho_M^0\, e^{-3\tau}, \tag{5.15}$$

with $s_0 \simeq 2.2\times10^{-38}$ GeV^3, $\rho_{R0} \simeq 3.4\times10^{-51}$ GeV^4 and $\rho_{m0} \simeq 1.2\times10^{-47}$ GeV^4 [1].

We carry out this change of variables in Eq. (3.19) and we recast the second-order differential equation into a pair of first-order equations as follows

$$\begin{cases} \Phi = H\phi' \\ H\Phi' + 3H\Phi = -\dfrac{\mathrm{d}V}{\mathrm{d}\phi} \end{cases}, \tag{5.16}$$

where the prime denotes derivative w.r.t τ. This strategy leads to an easily computing problem if we perform the following normalization of our variables [79, 81, 82, 95],

$$\rho_i \to \hat{\rho}_i = \frac{\rho_i}{\rho_c^0}, \quad V_0 \to \hat{V}_0 = \frac{V_0}{\rho_c^0}, \quad \hat{\phi} = \frac{\phi}{\sqrt{3}M_P}, \tag{5.17}$$

from which

$$H \to \hat{H} = \frac{H}{H_0} = \sqrt{\hat{\rho}_\phi + \hat{\rho}_R + \hat{\rho}_M}, \quad \varphi \to \hat{H}\hat{\varphi} = \frac{\varphi}{\sqrt{\rho_c^0}}, \tag{5.18}$$

$$V \to \hat{V} = \hat{V}_0 \exp\left[-\sqrt{3}\lambda\hat{\Phi}\right], \tag{5.19}$$

leading to the equivalent adimensional problem

$$\begin{cases} \hat{\Phi} = \hat{H}\hat{\phi}' \\ \hat{H}\hat{\Phi}' + 3\hat{H}\hat{\Phi} = -\dfrac{\mathrm{d}\hat{V}}{\mathrm{d}\hat{\phi}} \end{cases}. \tag{5.20}$$

We employ the following reference values: $\rho_c^0 = 1.053\times10^{-5}\,h^2$ GeV cm^{-3}, $T_0 = 2.7255$ K, $\Omega_M = 0.315$, $\Omega_R = 2.473\times10^{-5}h^{-2}$ and $h = 0.678$ [1, 9], with the relic abundances calculated from

$$\Omega_i = \frac{\rho_i}{\rho_{\mathrm{TOT}}}. \tag{5.21}$$

[1] We are using the most recent data from Planck 2018 [1], where $s_0 = 2891$ cm^{-3} $= 2.2\times10^{-38}$ GeV^3, $\rho_{m0} = \Omega_m\rho_{c0} = 0.315\cdot3.8\times10^{-47}$ GeV^4 and $\rho_{R0} = \pi^2/30\, g_*^0 T_0^4$, with $T_0 = 2.3\times10^{-13}$ GeV.

In particular, Quintessence has an energy density given by

$$\hat{\rho}_\phi = \frac{\hat{\Phi}^2}{2} + \rho_c^0 \hat{V}_0 e^{-\sqrt{3}\lambda\hat{\phi}}. \tag{5.22}$$

and the barotropic equation of state for the scalar field evolves according to

$$w_\phi = \frac{P_\phi}{\rho_\phi} = \frac{\hat{\Phi}^2/2 - \hat{V}}{\hat{\Phi}^2/2 + \hat{V}} = 1 - \frac{2\hat{V}}{\hat{\rho}_\phi}. \tag{5.23}$$

In order to solve Eq. (5.20), we need to set the proper initial conditions, which could be $\phi_I = \phi(\tau_I)$ and $\phi_I' = \phi'(\tau_I)$. Again, we follow the analysis carried out in [82] and we decide to put $\phi(\tau_I) = 0$, because, from Eq. (5.19), choosing $\phi(\tau_I) \neq 0$ is equivalent to a re-scaling of $\hat{V}_0$ into $\hat{V}_0 \exp\left[-\sqrt{3}\lambda\hat{\phi}_I\right]$. Since in our model the Universe is evolving within a KD scenario in its earliest stage, we demand that, initially, the Hubble rate is determined by the kinetic-energy density of the scalar field, $\hat{\rho}_{K_I} = \hat{\Phi}^2_{\tau_i}/2 \simeq \hat{\rho}_{\phi_I} \simeq \hat{H}_I^2$. Therefore, the free parameters of the model are λ, H_I and τ_I. The last two can be traded with other parameters and in particular we can swap τ_I with the initial temperature T_I, by solving Eq. (A.29). For what regards H_I, we leave the discussion to Section 5.2.2

The choice of V_0 is already constrained by requiring the tuning of the present energy density of the scalar field to the observed dark energy component $\Omega_{\phi 0}$ (see Eq. (5.24)). This is true for every choice of H_I, since the field reaches an attractor solution at late times when $\lambda < \sqrt{3(1+w_B)}$, with w_B the equation-of-state of the dominant background energy density ($\lambda < \sqrt{3}$ at the end of the matter era). hence the initial expansion rate is not relevant [65, 68, 69]. In the model here presented, the scalar field is still evolving at present time toward the attractor solution, which could be eventually reached in the future.

We refer the reader back to Chapter 3 for a review of the solutions described by Quintessential Cosmology and the description of the parameters.

5.2.1 Updated constraints on the model

The model we are describing is characterized by several parameters, whose allowed regions of values are constrained by experimental observations. Since we want the freeze-in mechanism to be active during a KD phase, the most naive constraint is that, initially, we have $\Omega_\phi(\tau_I) \equiv \Omega^I \sim 1$. In general, one can safely enlarge the possibilities to the less restrictive $\Omega_\phi^I > 0.5$. Updating the analysis in [40, 82] to present experimental data, we identify the following restrictions: present acceleration constraint, coincidence problem constraint, BBN constraints, inflationary constraints.

Coincidence problem constraint

As we recall in Section 3.2.1, one of the problems of the cosmological constant paradigm is to explain why the missing energy is so close to the closure parameter (and to the

matter component). This means that every good Quintessential model must be able to reproduce

$$\Omega_{\phi 0} = \Omega_\Lambda = 0.685 \pm 0.012 \quad \begin{matrix} 68\% \text{ C.L. } \textit{Planck} \text{ TT,TE,EE} \\ +\text{lowE}+\text{lensing} \end{matrix} \tag{5.24}$$

and this can be achieved by tuning V_0, which in fact is not a free parameter, as we said.

Acceleration constraint

The Universe today is accelerating, driven by a fluid with equation-of-state [1]

$$-1 \leq w_0 < -0.95 \quad \begin{matrix} 95\% \text{ C.L. } \textit{Planck} \text{ TT,TE,EE} \\ +\text{lowE}+\text{lensing}+\text{SNe}+\text{BAO} \end{matrix} \quad , \tag{5.25}$$

where we are requiring to stay out of the phantom regime ($w < -1$). This result is consistent with a cosmological constant. Accordingly, the "steepness" parameter λ is constrained by the requirement that $w_\phi(0) = w_0$, which implies

$$0 < \lambda \lesssim 0.6. \tag{5.26}$$

This limit is more restrictive than those utilized in the literature [40, 79, 82, 95], the reason relying upon the much more tight experimental constraints by the latest observations (Planck 2018 among all), with respect to those used previously (based on WMAP and Supernovae projects data).

BBN constraints

Demanding the existence of a new scalar species from the beginning of the Universe needs to preserve the successes of BBN, which acts at $T_{\rm BBN} \sim 1$ MeV, or at the logarithmic time $\tau_{\rm BBN} = -23.9$, accounting for the correct temperature function Eq. (A.30)[2]. We transfer the limits on the effective number of new neutrino species N_{eff} to an upper bound for $\Omega_\phi(T_{\rm BBN}) = \Omega_\phi^{\rm BBN}$ with [69, 97]

$$\Omega_\phi^{\rm BBN} = \frac{\rho_\phi}{\rho_\phi + \rho_R} = \frac{7\Delta N_{eff}/4}{10.75 + 7\Delta N_{eff}/4}, \tag{5.27}$$

where $\Delta N_{eff} = N_{eff} - 3.045$ (see Section 1.4). Using the 2σ conservative bound found in [36] of $\Delta N_{eff} \lesssim 1.1$, we require

$$\Omega_\phi^{\rm BBN} \leq 0.15 \quad 95\% \text{ C.L.} \tag{5.28}$$

[2] In [82] the author utilizes the adiabatic approximation throughout the cosmic evolution and finds $\tau_{\rm BBN} = -22.5$.

Inflationary constraint

Planck 2018 data [1, 45] show a remarkable accordance with slow-roll, single-field Inflation, predicting a spectral index n_s which is 8σ away from scale-invariance. Moreover, measurements of the tensor-to-scalar ratio r entail an upper bound on the Hubble parameter during Inflation, which we assume as an upper bound on the initial value H_I for our model. In particular, data show that at the pivot scale $k_{002} = 0.002$ Mpc^{-1} the tensor-to-scalar ratio is $r_{002} < 0.056$ at 95% C.L., assuming the validity of the consistency relation $n_t = -r/8$, yielding an Hubble rate at the pivot scale (which we assume to be our initial value) [45]

$$\frac{H_I}{M_P} < 2.5 \times 10^{-5} \implies H_I \lesssim 3 \times 10^{14}\,\text{GeV} \quad 95\%\ \text{C.L.}. \tag{5.29}$$

This implies that our normalized initial Hubble parameter is bounded by $\hat{H}_I \lesssim 2\times 10^{56}$, having taken $H_0 = 0.678$ km s^{-1} Mpc^{-1}.

5.2.2 Relevant stages of the Quintessential evolution

The initial requirement of having a Universe in a KD phase implies that $w_\phi \simeq 1$ and that the energy density scales as $\rho_\phi \propto a^{-6}$ and so

$$\rho_\phi = \rho_{\phi_p} \frac{g_*(T)}{g_*(T_p)} \left(\frac{T}{T_p}\right)^6, \tag{5.30}$$

with p a reference point. Afterwards, the Universe enters the standard RD epoch at a temperature T_r, which we have estimated to be $T \gtrsim 3.9$ MeV with Eq. (3.35), using the BBN constraints on $\Delta N_{eff} < 1.1$ of Section 1.4. Here, for the sake of clarity and consistency with BBN constraints, we want to trade T_r with Ω_ϕ^{BBN} [40]. Thus, we can compare the energy densities of radiation and Quintessence at T_r, taking as a reference point $T_p = T_{\text{BBN}}$, finding

$$\rho_\phi(T_r) = \rho_R(T_r) \implies T_r = T_{\text{BBN}} \left(\frac{1-\Omega_\phi^{\text{BBN}}}{\Omega_\phi^{\text{BBN}}}\right)^{1/2} \left(\frac{g_*(T_{\text{BBN}})}{g_*(T_r)}\right)^{1/2}, \tag{5.31}$$

where we assumed that $\Omega_R^{\text{BBN}} = 1 - \Omega_\phi^{\text{BBN}}$ and we approximated $g_{*S} = g_*$. Inserting this expression into Eq. (3.31) we find

$$H = \frac{\sqrt{\rho_R}}{\sqrt{3}M_P} \left[1 + \frac{1-\Omega_\phi^{\text{BBN}}}{\Omega_\phi^{\text{BBN}}} \frac{g_*}{g_*^{\text{BBN}}} \left(\frac{T}{T_{\text{BBN}}}\right)^2\right]^{1/2}, \tag{5.32}$$

for any temperature $T > T_r$ and $\Omega_R^I \neq 0$. Therefore, for any given initial temperature T_I, we automatically find H_I as a function of Ω_ϕ^{BBN}, which can be regarded as the new

free parameter, instead of H_I. For instance, $T_{\rm BBN} = 1$ MeV and $g_{*r} = g_*^{\rm BBN} = 10.75$, the conservative upper bound of Eq. (5.28) can be translated to the lower bound

$$T_r \gtrsim 2.4 \text{ MeV}, \tag{5.33}$$

compatible with the previous value of 3.9 MeV. Notice that, in the case the upper bounds in Eq. (5.28) and Eq. (5.29) are saturated, the maximum initial temperature we can attain is $T_I \sim 5 \times 10^9$ GeV, whereas larger values can be obtained if ϕ is much more underabundant at the time of BBN. For instance, taking an extreme case with $T_I \sim 10^{16}$ GeV, entails $\Omega_\phi^{\rm BBN} \lesssim 10^{-40}$ (and consequently $T_r \sim T_I$, which means that the scalar field has no role in the early Universe).

Evaluating Eq. (5.32) at the initial temperature and inverting the formula, we can solve for T_I, obtaining

$$T_I = T_{\rm BBN} \sqrt{\frac{g_*^{\rm BBN}}{g_*^I} \frac{1-\Omega_\phi^{\rm BBN}}{\Omega_\phi^{\rm BBN}} \frac{\Omega_\phi^I}{1-\Omega_\phi^I}}, \tag{5.34}$$

where we used the fact that $\hat{H}_I^2/\hat{\rho}_R^I - 1 = \Omega_\phi^I/(1-\Omega_\phi^I)$. Taking the logarithm on both sides yields

$$\log \Omega_\phi^{\rm BBN} - \log\big(1-\Omega_\phi^{\rm BBN}\big) = -2\log T_I + C, \tag{5.35}$$

with $C = 2\log T_{\rm BBN} + \log\big(g_*^{\rm BBN}/g_*^I\big) - \log\big(1/\Omega_\phi^I - 1\big)$, which does not significantly vary with Ω_ϕ^I. Since the density parameter of quintessence at the time of BBN must be small we can neglect the second logarithm and obtain an approximated relation between the parameters (having fixed $H_I \lesssim 3 \times 10^{14}$ GeV)

$$\log \Omega_\phi^{\rm BBN} \approx -2\log T_I + C. \tag{5.36}$$

Hence, the free parameters we choose to employ are λ, T_I and $\Omega_\phi^{\rm BBN}$

After the beginning of the radiation era, the scalar field is said to be "frozen" by the Hubble friction and its evolution remains dominated by its kinetic energy density. This phase terminates at a temperature T_{KV}, when the potential energy density happens to be comparable with the kinetic energy density. After this stage, the field starts being dominated by its potential.

The final stage is the asymptotic approach to the late-time attractor solution, where $\rho_\phi = V(\phi)$ accounts for the totality of the energy budget of the Universe. As described in Section 3.2.3, one finds global-attractor and the late-time attractor solutions, which are (we rewrite them for the sake of clarity):

- Global attractor for $\lambda > \sqrt{3(1+w_B)}$, with $w_\phi^\star = w_B$ and $\Omega_\phi^\star = 3(1+w_B)/\lambda^2$. This is the famous "self-tuning solution" (described in full details in [67]), where the scalar field mimics the scaling of the dominating background. However, as we said, experimental data show exactly the opposite: now, dark energy is dominating and the Universe is accelerating, leaving no room for meeting this kind of solutions.

- Late-time attractor for $\lambda < \sqrt{3(1+w_B)}$ with $w_\phi^\star = \lambda^2/3 - 1$ and $\Omega_\phi^\star = 1$. This configuration is still in good agreement with observations, even though we do not know what will be the precise evolution of the Universe in the future. For different values of λ one may obtain a variety of late-time scenarios: for $\lambda = \sqrt{2}$, $w_\phi^\star = -1/3$, meaning that the Universe will be asymptotically expand at constant velocity; for $\lambda < \sqrt{2}$, $w_\phi^\star < -1/3$, hence eternal acceleration cannot be avoided. The Universe will eventually start to decelerate only if $\lambda > \sqrt{2}$ (and $\lambda < \sqrt{3}$) with $w_\phi^\star > -1/3$ (and $w_\phi^\star < 0$). Observations suggest that $\lambda \lesssim 0.6$, implying an eternally accelerating Universe in the exponential potential scenario.

The various phases are illustrated in Fig. 5.9 where we plot the change of the energy densities of Quintessence, radiation and pressureless matter during the expansion of the Universe. The parameters set for the numerical integration (and for satisfying the constraints) are $T_I = 10^9$ GeV (equivalent to $\tau_I = -50.6$), $\Omega_\phi^{\rm BBN} = 0.002$ (equivalent to $H_I \simeq 2 \times 10^{11}$ GeV and to $T_r \simeq 20$ MeV), $\lambda = 0.5$ (late-time attractor), by which $w_\phi^\star = -0.9167$ (the observed density parameter of dark energy is obtained with $\hat{V}_0 = 4.8 \times 10^{13}$).

The evolution of the parameter densities of Quintessence, radiation and matter are shown in Fig. 5.10 as a function of the logarithmic scale factor along with the equation-of-state parameter w_ϕ of Quintessence. It can be noticed that the scalar field remains dominated by its kinetic energy density until $\tau_{KP} = -9.82$, corresponding to $z_{KP} \simeq 18400$ (or $T_{KP} \sim$ eV). However, the abundance of ϕ is completely suppressed after the Quintessence-radiation equality, happening at $\tau_r = -25.36$ (or $T_r \sim 21$ MeV, what we have required at the beginning), hence its effects are completely negligible. Dark energy starts to dominate over matter at $\tau_{\phi m} = -0.26$, equivalent to $z_{\phi m} = 0.3$, but we find that the acceleration parameter (see Eq. (A.10)) becomes zero and then turns to be negative at $\tau_t = -0.46$, or $z_t = 0.59$, in perfect agreement with experimental indications by Planck [1]. The barotropic equation-of-state at present time is $w_\phi(0) = -0.96$, consistent with Eq. (5.25), while at late-time we find $w_\phi(\tau = 10) = -0.917$, which perfectly matches the fixed-point equation-of-state parameter.

5.2.3 FHPO freeze-in with Quintessence

We now insert the Hubble rate found with the previous analysis into the Boltzmann equation for freeze-in production of the fermionic dark matter candidate through the Higgs portal. We have already shown in Section 5.1 that, if DM is produced during a KD scenario with a five-dimensional operator, the extremes of integration appear in the final yield in the logarithmic form, so that the dependence on the initial and final conditions is very weak. On the contrary, the relic abundance is more subject to the precise moment in which radiation overcomes the kination-like field, i.e. T_r (or $\Omega_\phi^{\rm BBN}$). The equations of motion for Quintessence have been solved imposing a KD initial condition, with T_I taking the role of the reheating temperature; if we keep $T_r \simeq 20$ MeV ($\Omega_\phi^{\rm BBN} = 0.002$), we do expect precisely the same behavior found in Eq. (5.7) and in Fig. 5.5.

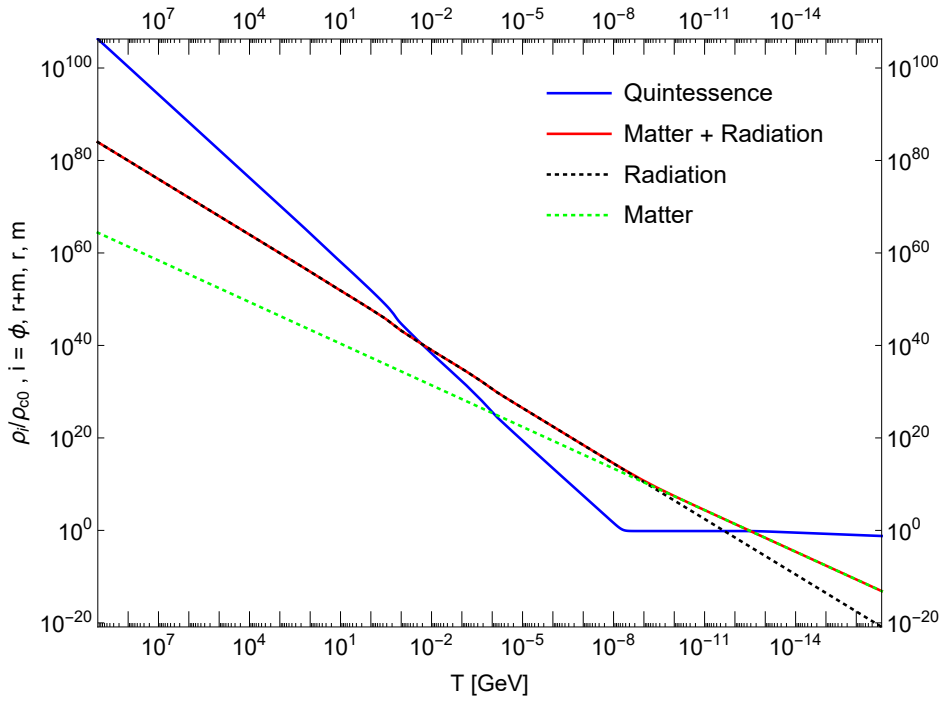

Figure 5.9: The evolution of the energy densities of Quintessence (blue line), the matter+radiation background (red line), radiation only (black dotted line) and matter only (Green dotted line) normalized to the critical density today. The parameters are set to $T_I = 10^9$ GeV, $\Omega_\phi^{\rm BBN} = 0.002$, and $\lambda = 0.5$ (equivalent to $H_I \simeq 2 \times 10^{11}$ GeV, $T_r \simeq 20$ MeV and $w_\phi^\star = -0.9167$).

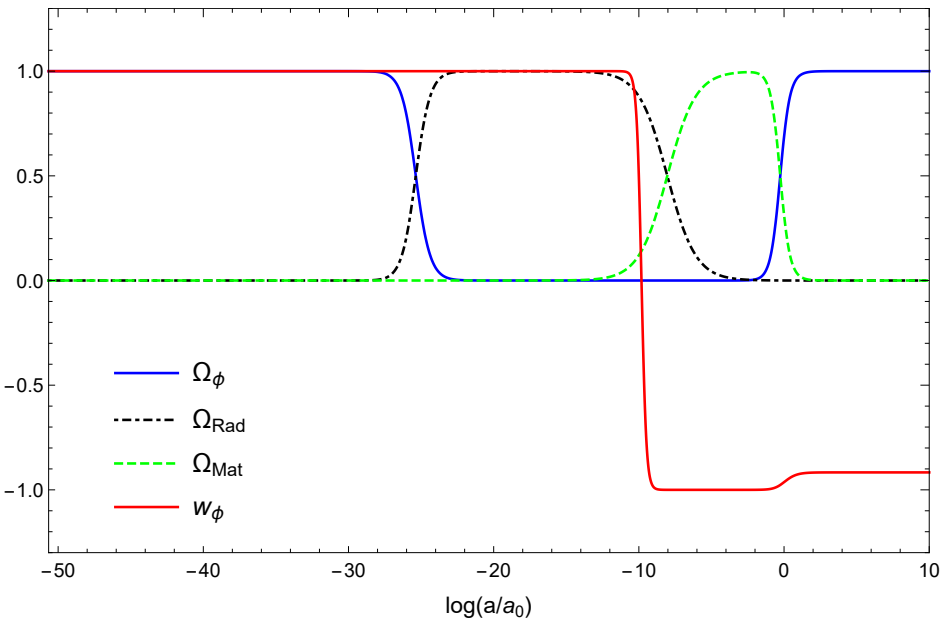

Figure 5.10: The equation-of-state parameter for Quintessence (red line), its density parameter (blue line) and those of radiation (black dotted line) and matter (Green dotted line) plotted as functions of logarithmic time. The set of parameters is $T_I = 10^9$ GeV, $\Omega_\phi^{\rm BBN} = 0.002$, and $\lambda = 0.5$ (equivalent to $H_I \simeq 2 \times 10^{11}$ GeV, $T_r \simeq 20$ MeV and $w_\phi^\star = -0.9167$).

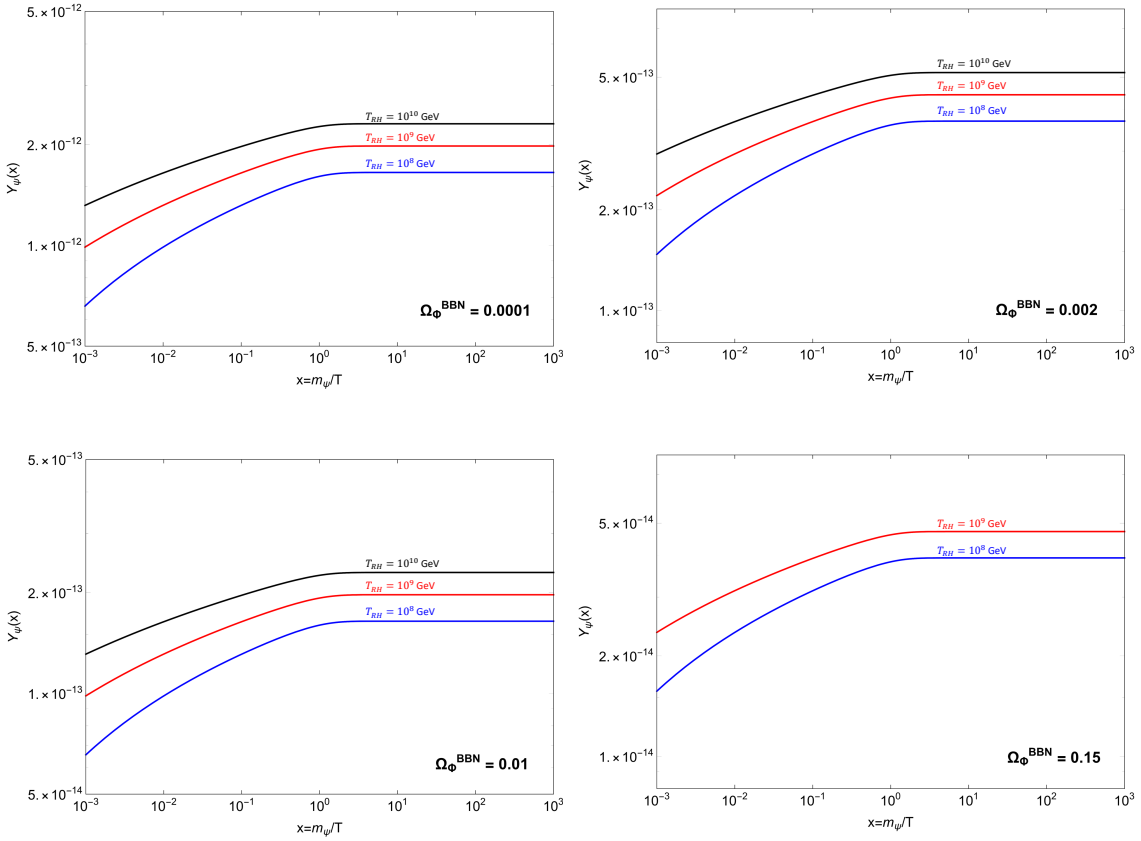

Figure 5.11: Comoving density of the fermionic FIMP with $m_\psi = 1$ TeV produced via the FHPO with a reference scale $\Lambda = 1.6 \times 10^{12}$ GeV, during an early KD phase set by a Quintessential field (with exponential potential and $\lambda = 0.5$, even though it does not contribute in the early Universe). The four panels correspond to four values of $\Omega_\phi^{\rm BBN}$: 0.0001, 0.002, 0.01 and 0.15. The colors refer to three different initial (reheating) temperatures: black for $T_I = 10^{10}$ GeV, red for $T_I = 10^9$ GeV, blue for $T_I = 10^8$ GeV (the $\Omega_\phi^{\rm BBN} = 0.15$ case is constrained by $T_I < 5 \times 10^9$ GeV).

The yield for ψ particles of mass 1 TeV is completely established by the initial evolution of the scalar field, so that the effective cosmological background is not different from Equations (3.31)–(3.32) and the result here found are fully comparable with those found in Section 3.3 for $n = 2$.

This is illustrated in Fig. 5.11, where we plot the comoving abundance of the FIMP with different values of $\Omega_\phi^{\rm BBN}$ (0.0001, 0.002, 0.01, 0.15) and of T_I (10^{10}, 10^9 and 10^8 GeV), with the only exception of $\Omega_\phi^{\rm BBN} = 0.15$ (equivalent to $T_r = 2.4$ MeV), for which $T_I \lesssim 5 \times 10^9$ GeV, as discussed previously. We choose $\Lambda = 1.6 \times 10^{12}$ GeV and $\lambda = 0.5$, but only for the purpose of the numerical calculation, since the precise value of the steepness parameter only affects the late-time behavior of the field. The logarithmic growth is evident from the figure; in scenarios with a greater abundance of Quintessence at the onset of BBN (hence a lower Φ-radiation equality temperature T_r), the Universe has stopped the fast-expanding period at a later stage than in less

Φ-abundant scenarios. This implies that the number density of DM particles had time to become more diluted. The relic density suppression factor for this range of values varies from to 2.7×10^8 when $T_I = 10^8$ GeV and $\Omega_\phi^{\rm BBN} = 0.0001$ ($T_r = 100$ MeV) to 2×10^{11} when $T_I = 10^{10}$ GeV and $\Omega_\phi^{\rm BBN} = 0.01$ ($T_r = 10$ MeV). These numbers encourage coupling constant boosts of order $10^4 - 10^6$, which, compared to the usual 10^{-12} values found in the standard RD, renormalizable freeze-in scenario, could have dramatic consequences on DM phenomenology, possibly opening new observable windows in the parameter space for direct, indirect and perhaps also collider searches

T_I [GeV]	$\Omega_\phi^{\rm BBN}$	$\mathcal{F}^{-1}$	$\Lambda \times 10^{12}$ [GeV]
10^{10}	0.0001	1.9×10^{10}	3.75
10^9	0.0001	2.3×10^9	3.5
10^8	0.0001	2.7×10^8	3.2
10^{10}	0.002	8.7×10^{10}	1.8
10^9	0.002	1×10^{10}	1.6
10^8	0.002	1.2×10^9	1.5
10^{10}	0.01	2×10^{11}	1.2
10^9	0.01	2.3×10^{10}	1.1
10^8	0.01	2.8×10^9	1.0
10^9	0.15	9.5×10^{10}	0.5
10^8	0.15	1.1×10^{10}	0.5

Table 5.2: Parameters utilized in Fig. 5.11 with the relative relic density suppression factor and the Λ needed to reproduce the observed yield.

As regards the mass scale of the EFT interaction here utilized, we can see that it does not vary very much within a cluster, as we already knew from Fig. 5.6; the small changes arise when altering the $\Omega_\phi^{\rm BBN}$ parameter, but these modifications are of order unity, since the two quantities depend on each other very mildly: $\Lambda \sim 1/(\Omega_\phi^{\rm BBN})^{1/4}$ when $\Omega_\phi^{\rm BBN}$ is small, that is almost always (very small differences arise when it takes the maximum value of 0.15). Even more negligible is the contribution of the initial temperature (and also the final one, though it is fixed at m_ψ in our case), since, from Eq. (5.3), we clearly see that during kination one obtains $\Lambda \propto \sqrt{\log(T_I/m_\psi)}$, which is an almost flat dependence.

Conclusions and outlooks

In this thesis, we investigated to what extent non-renormalizable operators affect the freeze-in production of a dark matter candidate, when the background cosmological scenario expands with a rate different from a standard radiation era. In particular, we numerically solved the Boltzmann equation for the number density of a Dirac fermion dark matter particle ψ, when the collisional term is ruled by a five-dimensional Higgs portal; the typical center-of-mass energies of interest stand above the EWSB scale, so that we retained the full complex massless Higgs doublet, while the scattering processes we were interested in were the pair annihilations of the neutral components $H_0\overline{H}_0 \to \overline{\psi}\psi$ and the charged components $H^+H^- \to \overline{\psi}\psi$, both giving the same contribution. The feeble coupling between the dark and visible sectors was replaced by the UV-cutoff interaction scale Λ of the portal operator.

The cosmological histories we analyzed were split into three categories: an early, non-adiabatic matter-dominated epoch, a generic, adiabatic faster-than-radiation era and the quintessential kination scenario. The general output is that, when the Universe is dominated by a fluid which makes it expand at a faster pace, the relic density of dark matter is suppressed by a wide rage of possible values.

Within the first cosmological epoch (see Section 4.3), this reduction depends on the value of the reheating temperature after inflation, when the Universe enters the radiation era. In fact, if $T_{RH} > m_\psi$, the majority of dark matter is generated after the matter field has decayed, so that the yield is UV-dominated by T_{RH}. The dependence of the codensity on T_{RH} is linear, so that it decreases by an order of magnitude when the reheating temperature lowers by a factor of ten.

More interesting was the case with $T_{RH} < m_\psi$; in fact, the extreme IR behavior of the non-adiabatic expansion makes the production mechanism stop at m_ψ, while the field, still oscillating around its minimum, injects entropy in the Universe, which in turns depletes the comoving density by a factor of $(T/T_{RH})^5$. We found that the yield is proportional to $T_{RH}^7/(m_\psi^6\Lambda^2)$, so that a small variation of T_{RH} is able to seriously drop the final relic abundance. In contrast, the interaction scale needs to be lowered by a large factor, in order to match the observed relic density; hence, the coupling with the complex Higgses gets boosted. In Fig. 5.6, we showed that the difference in Λ between a 1 GeV and a 10^6 GeV reheating temperature spans more than ten orders. The comoving number density reaches thermal equilibrium when T_{RH} approaches 2.4 GeV; after that, the freeze-in mechanism is no longer reliable.

The second analysis we employed was an extension of [39] to the fermionic Higgs

portal operator. Thus, we modeled the cosmological histories with n and T_r, i.e., respectively, the index parameterizing the faster redshifting of the Hubble rate and the temperature when the energy densities of ϕ and radiation are equal (see Section 3.3 and Section 5.1). The higher n, the faster the expansion, whereas the lower T_r, the longer this exotic epoch lasts, enhancing the relic density depletion. The freeze-in mechanism is IR-dominated for operators whose mass dimension satisfies $d < 4.5+n/4$; we computed the evolution of the yield for the fermionic Higgs portal, for which we confirmed a UV dominance for $n < 2$, a logarithmic dependence on the extremes of integration in the kination regime ($n = 2$) and again an IR-dominance for $n > 2$.

We calculated the relic density suppression with different n and T_r, as shown in Figures 5.7–5.8. The main result is that freeze-in production is even more suppressed with a non-renormalizable operator than in the renormalizable cases, with reductions spanning $1 - 10^{16}$ orders w.r.t. a standard radiation scenario. This implies that, to produce enough dark matter to match observations, a lower interaction scale, hence a larger coupling (up to $7 - 8$ orders of magnitude), is needed.

Finally, we incorporated the case with $n = 2$ into a more physical situation: quintessential kination. Alongside the radiation and matter component, we added a stable, spatially homogeneous and minimally coupled scalar field Φ, rolling down its potential. The theory behind Quintessence is rich and controversial, but its main employment has always been trying to solve (or at least mitigate) the cosmological constant problems. Hence, we decided to set the parameter space in such a way that this field was dominating in the early Universe with its kinetic energy density, then evolved as a subdominant species and finally became responsible for the dark energy component $\Omega_{\Lambda 0}$ and the present acceleration of the Universe w_0. The potential we chose was the exponential form $V_0 \exp[-\lambda\Phi/M_P]$, where the only relevant parameter is λ, describing the steepness of the potential, while V_0 was tuned to match the observed $\Omega_{\Lambda 0}$. Also, the involved parameter space became narrower than previous results in the literature, simply because cosmological observations have continuously put tighter constraints on a number of relevant quantities, such as w_0, $\Omega_{\Lambda 0}$, H_I (the initial Hubble rate) and N_{eff} (the effective number of neutrino species). For instance, we used $\lambda \lesssim 0.6$, i.e. a late-time attractor solution, favouring eternal acceleration and complete Quintessence domination in the future.

We solved the Boltzmann equation for dark matter coupled with the equation of motion for Quintessence and we found results compatible with a simple $n = 2$, generic cosmology. In fact, the role of Quintessence becomes different from pure kination only after T_r, when dark matter is supposed to have already been created. For this reason, λ does not play any role in the early Universe, but, for consistency, we kept its value within its phenomenological bound. The remaining free parameters were T_I (supposing instantaneous reheating) and $\Omega_\Phi^{\rm BBN}$ (the abundance of Φ at BBN), taking the place of T_r. We found that, once the interaction scale was fixed, the codensity slightly varied with T_I and $\Omega_\phi^{\rm BBN}$. Scenarios with a larger presence of Φ at BBN (a lower T_r) implied a greater suppression; at the same time, lowering T_I activates the Higgs portal at a later time, producing less dark matter. However, while $\Lambda^{-1} \propto (\Omega_\Phi^{\rm BBN})^{1/4}$, we also

found $\Lambda^{-1} \propto 1/\sqrt{\log T_I}$, so that, actually, the initial temperature gives a very small contribution. The parameter space investigated clearly show a relic density suppression of order $10^8 - 10^{11}$, leaving room for coupling enhancements of order $10^4 - 10^6$, in order to obtain the observed abundance. The phenomenological implications of this result are promising and need to be studied.

This analysis paves the way for deeper studies on the role of the fermionic Higgs portal in modified cosmological histories and, in general, on how non-renormalizable operators with dimension five (or greater) relates to theories with a kination domination. The possibilities in this sense are manifold. On the particle physics side, an important step is to frame the EFT of the Higgs portal within a UV-complete theory; an example could be freeze-in of singlet-doublet dark matter models [98, 99]; a follow-up along this line is left for future works. New degrees of freedom could introduce novel signatures, like displaced vertices at colliders, a new branch of collider physics which is facing an increasing interest, with proposed experiments such as the MATHUSLA surface detector concept for LHC [100], which could hunt ultra-long-lived-particles possibly produced in exotic Higgs decays or more general production modes. Also, the enhancements of coupling constants could have an important impact on direct and indirect detection searches.

On the cosmological side, a detailed inspection of the physics of inflation and the reheating phase could certainly help give a more comprehensive knowledge of the history of the Universe and when the various degrees of freedom had a role, or if they put any kind of imprint on dark matter. These, in turn, may give rise to isocurvature perturbations, which are however strongly constrained by CMB data. Also, five-dimensional operators are typical for production of gravitinos and axinos (two well-motivated DM candidates), but their freeze-in generation during kination has not yet been addressed; the phenomenological implications are left for future studies.

In this respect, the CMB may reserve surprises in its finest structure and the next-generation CMB-S4 experiment [101] aims at reaching an unprecedented precision for what regards B-mode polarization, inflationary parameters and the number and masses of neutrinos in particular. Dark energy, dark matter and the initial conditions of the Universe will be also scrupulously investigated by the EUCLID satellite [102], soon to be launched, which will better measure the expansion history and the large scale structure of the Universe.

To conclude, alterations of the standard cosmological era could resurrect constrained dark matter theories and open new parameter windows to be surveyed with forthcoming experiments. Also, effective interactions might leave their mark on the phenomenology explored with next-generation colliders and direct/indirect detection experiments, where higher statistics and improved sensitivity and energy could reveal hints of New Physics. Perhaps, we are entering a new thrilling era for dark matter searches (and BSM physics in general), in which old-fashioned theoretical prejudices might be reversed and new fundamental paradigms be considered, in a way that also detection strategies could be dramatically affected.

Appendices

Appendix A

Rudimentary Cosmology and Thermal History of the Universe

A.1 The FLRW Universe

The standard theory for describing the cosmos is the (Inflationary) Hot Big Bang model, nowadays better referred to as the ΛCDM cosmological model of the Universe, which is based on few simple assumptions [2, 8]. First, the Large Scale Structure (LSS) of the Universe is spatially homogeneous and isotropic on average. This implies that we can restrict ourselves to the Friedmann-Lemâitre-Robertson-Walker metric [103],

$$\mathrm{d}s^2 = \mathrm{d}t^2 - a^2(t)\,(\mathrm{d}x^2 + \mathrm{d}y^2 + \mathrm{d}z^2), \tag{A.1}$$

where $a(t)$ is the scale factor, affecting the spatial hypersurfaces at constant time coordinate and we made use of a mostly negative signature and natural units ($c = 1$). The usual normalization for $a(t)$ utilizes $a(t_0) = 1$, with t_0 the present time.

Second, the matter-energy content throughout the entire history of the Universe is exclusively made of radiation, pressureless matter and a cosmological constant, whose dynamics is governed by the Friedmann equations,

$$\left(\frac{\dot{a}}{a}\right)^2 \equiv H^2 = \frac{8\pi G}{3}\rho - \frac{k}{a^2}, \tag{A.2}$$

$$\frac{\ddot{a}}{a} = -\frac{4\pi G}{3}(\rho + 3P). \tag{A.3}$$

Here, $H = \dot{a}/a$ is the Hubble parameter, ρ and P represent the sum of all the contributions to the *energy density* and *isotropic pressure* in the Universe, whereas $G = 6.67408(31) \times 10^{-11}\,\mathrm{m^3\,kg^{-1}\,s^{-2}}$ [9] is the gravitational constant, k is the spatial curvature and the dots stand for derivatives with respect to the time coordinate. Ex-

perimental data seem to point to a flat Universe with very high precision, so that we can safely neglect the curvature term in our equations.

In order to solve them, one has to close the system with the additional *equation of state* for the barotropic fluids

$$P = w\rho, \tag{A.4}$$

where w is a constant and discriminate the different types of matter:

$$\begin{cases} w = 0 & \text{pressureless matter} \\ w = 1/3 & \text{radiation} \\ w = -1 & \text{vacuum energy} \end{cases} . \tag{A.5}$$

The solutions to Eq. (A.2) scale as

$$\rho \propto a^{-3(1+w)}, \tag{A.6}$$

hence we have different scalings for the various types of matter,

$$\rho = \begin{cases} a^{-3} & \text{pressureless matter} \\ a^{-4} & \text{radiation} \\ const & \text{vacuum energy} \end{cases} . \tag{A.7}$$

Consequently, in a single-component universe the time dependence of the scale factor differs case by case, since Eq. (A.2) reduces to

$$\frac{\dot{a}}{a} \propto a^{-\frac{3}{2}(1+w)}, \tag{A.8}$$

whose solutions scale as $a(t) \propto t^{\frac{2}{3(1+w)}}$ and we end up with a variety of expansion behaviors, depending on the specific value of w. In particular,

$$a(t) \propto \begin{cases} t^{2/3} & \text{pressureless matter} \\ t^{1/2} & \text{radiation} \\ e^{Ht} & \text{vacuum energy} \end{cases} , \tag{A.9}$$

where in the last case we used the fact that $H = const$ when $w = -1$. We notice that, from Eq. (A.3), if the dominant fluid has $w < -1/3$, the Universe undergoes a period of accelerated expansion. The quantity that measures cosmic acceleration is the *deceleration parameter* q, defined by

$$q = -\frac{\ddot{a}\dot{a}}{\dot{a}^2} = -1 - \frac{\dot{H}}{H^2} = \frac{1}{2}\sum \Omega_i(1 + 3w_i). \tag{A.10}$$

If we were to consider a multi-component universe, things would become more complicated, since we should take into account the sum of all contributions

$$\rho_{TOT} = \rho_r + \rho_m + \rho_\Lambda,$$

with $\rho_\Lambda = \Lambda/8\pi G$. Analytical solutions are not so straightforward to obtain, but, thanks to the different scaling, we can easily infer at which period of the cosmic history the various components dominate the energy budget of the universe. In fact, at early times, the energy density is completely ruled by radiation, but, as the time passes, pressureless matter overcomes until it gets completely subdued by the constant contribution of the vacuum energy, which does not feel the red-shifting of the scale factor.

If we put $k = 0$, we can define the *critical density* ρ_c as

$$\rho_c = \frac{3H^2}{8\pi G}, \tag{A.11}$$

which is the energy density the Universe should have to be spatially flat. Today its value is $\rho_{c0} = 1.87840(9) \times 10^{-29} h^2\,\mathrm{g\,cm^{-3}} = 1.05371(5) \times 10^{-5} h^2\,(\mathrm{GeV}/c^2)\,\mathrm{cm^{-3}} \simeq 8 \times 10^{-47} h^2\,\mathrm{GeV}^4$.

The natural way to compare present day energy densities with ρ_{c0} is by defining the *density parameter* as

$$\Omega_i = \frac{\rho_{i0}}{\rho_{c0}} = \frac{8\pi G \rho_{i0}}{3H_0^2}, \tag{A.12}$$

so that, dividing Eq. (A.2) by H^2, one finds

$$1 = \frac{\sum_i \rho_i}{\rho_c} - \frac{k}{a^2 H^2} = \sum_i \Omega_i - \frac{k}{a^2 H^2}.$$

Observing how $\Omega_{\mathrm{TOT}} = \sum_i \Omega_i$ differs from 1 tells us what is the spatial curvature of the Universe. In fact, the latter addend is usually rewritten as $\Omega_k = -k/a^2H^2$ and Planck data suggest this to be consistent with zero, hence a spatially-flat Universe.

A.2 The ΛCDM model

Overall, the best way we have to describe the Universe is the spatially-flat ΛCDM model, which is based on few parameters, such as the Hubble parameter today (or the age of the Universe), the matter density parameter Ω_c, the baryon density parameter Ω_b and other quantities which refer to various important stages of the cosmic evolution, like Inflation, Recombination and Reionization, although we are not interested in the details of these epochs. The important thing to remember is that Inflation, a primordial, very rapid exponential growth of the scale factor, arises in its primitive form mainly as a tool for solving two experimental evidences: the Universe is too flat today for not having very special fine tuning initial conditions (remember that the energy density of spatial curvature redshifts as a^{-2}, so that it should dominate today, unless in the first epochs it was extremely negligible) and the CMB looks very smooth, i.e. homogeneous and isotropic with a precision of one part over 10^{-5} (actually, the very first motivation was why we do not observe magnetic monopoles). An early exponential expansion driven by the vacuum energy density of an inflaton field would be able to solve these and other

shortcomings. Soon, inflationary physics became more than this; the quantum nature of the inflaton field, in fact, is regarded as the origin of all the macroscopic structure we observe on the largest scale, since the first quantum fluctuations impressed their sign on the local spacetime fabric, e.g. gravity, and then were frozen with the expansion of the Universe. These perturbations were transferred through gravity onto the local distribution of matter, which then evolved into largest structures.

The first observation of an expanding Universe dates back to the '30s, when Edwin Hubble found that galaxies were receding from us with a velocity proportional to their distance: $v = H_0\, d$, with H_0 the Hubble parameter (not a constant in fact) today. Nowadays, this experimental evidence has been brought to extraordinary precision by an enormous quantity of astrophysical and cosmological surveys and we know that the value of the Hubble parameter today is

$$H_0 = 100h\,\mathrm{km\,s^{-1}\,Mpc^{-1}}, \tag{A.13}$$

where h was historically introduced to take into account the variation of the experimental determination of H_0 and its value is around 0.7. Actually, the two most accurate measurements of H_0 come from Planck 2018 [1] and Riess et al. 2018 [37] results,

$$H_0^{\text{Planck 2018}} = 67.3 \pm 1.2\,\mathrm{km\,s^{-1}\,Mpc^{-1}}, \tag{A.14}$$

$$H_0^{\text{Riess et al.}} = 74.03 \pm 1.42\,\mathrm{km\,s^{-1}\,Mpc^{-1}}, \tag{A.15}$$

with $4.4\,\sigma$ discrepancy between the two. This is what is now called the H_0 *tension*, which has seen a continuous dramatic strengthening in these years.

The two measurements, however, refer to two different cosmological epochs, being Planck a CMB experiment and the analysis conducted by Riess et al. being focused on nearby Cepheid stars. In fact, the tension is increasingly becoming a regular feature between late time and early time experiments [37]. For these reasons, understanding this mismatch is becoming crucial, because, in the case decisive experimental errors were ruled out, we would need to rethink all the cosmological evolution, eventually including new exotic scenarios such as those with a time-varying cosmological constant.

As regards the density parameters of the relevant matter-energy fractions, the best measurements come again from Planck 2018, which gives $\Omega_c h^2 = 0.1200 \pm 0.0012$ for cold dark matter and $\Omega_b = 0.0224 \pm 0.0001$ for baryons, leading to a total matter density today of $\Omega_m h^2 = 0.1430 \pm 0.0011$. Conversely, assuming a flat Universe, this constraint is translated into a value for the dark energy density parameter $\Omega_\Lambda h^2 = 0.3107 \pm 0.0082$. In particular, from this estimate one derives the experimental value for the cosmological constant, which is

$$\Lambda = (2.846 \pm 0.076) \times 10^{-122} M_P^2,$$

while its natural value would be *of order* the Planck mass squared. This is the so-called *fine-tuning problem*, also discussed in Section 3.2.1.

A.3 Thermodynamics in the early universe

Studying the history of the Universe to varying temperature is of priority interest. But what do we mean with the word "temperature" in cosmology? This concept makes sense only if the considered system is at thermal equilibrium, a condition which can be achieved if particles inside that system are tightly interacting, sharing thermodynamic properties, including temperature. Hence, the crucial aspect one has to face with is to evaluate the key players in the interactions among particles and for the contribution to the energy budget of the Universe.

To quantify these properties, one needs to give a proper definition to some thermodynamic variables and, therefore, we give a quick review on basic equilibrium thermodynamics in an expanding universe [2]. The momentum eigenstates of particles are assigned following their phase space distribution function $f(\mathbf{x}, \mathbf{p}, t) = f(p, T, \mu)$, where we used the homogeneity and isotropy assumption to rewrite f solely as a function of $p = |\mathbf{p}|$, the temperature T and the chemical potential μ, having in mind an expression already averaged over positions. The *number density*, *energy density* and *isotropic pressure* of particles are defined as

$$\begin{aligned} n(T,\mu) &= \frac{g}{(2\pi)^3}\int \mathrm{d}^3\vec{p}\, f(p,T,\mu), \\ \rho(T,\mu) &= \frac{g}{(2\pi)^3}\int \mathrm{d}^3\vec{p}\, E(p) f(p,T,\mu), \\ P(T,\mu) &= \frac{g}{(2\pi)^3}\int \mathrm{d}^3\vec{p}\, \frac{|\vec{p}|^2}{3E(p)} f(p,T,\mu), \end{aligned} \tag{A.16}$$

where $E^2 = p^2 + m^2$ and the factor 3 accounts for the isotropy property.

Usually, we assume particles to be in *kinetic equilibrium*, so that we can use Bose-Einstein (BE) or Fermi-Dirac (FD) statistics,

$$f(p,T,\mu) = \left[\exp\left(\frac{E-\mu}{T}\right) \pm 1\right]^{-1}, \tag{A.17}$$

where the $-$ holds for bosons and the $+$ for fermions.

Neglecting the chemical potentials in the early universe[1], our thermodynamic variables can be rewritten in the relativistic regime ($T \gg m$) as

$$n(T) = g\frac{\zeta(3)}{\pi^2}T^3 \begin{cases} 1 & \text{BE} \\ 3/4 & \text{FD} \end{cases} \tag{A.18}$$

[1]See Section 6 of Chapter 15 of the book of S. Weinberg for an explanation [104]. The reason we can do so is basically the fact that the Universe is electrically neutral, the baryon density is estimated to be less than a billionth of the photon density and the lepton density is also thought to be very small, on the same order as the baryon number. Actually, precise calculations must involve non-vanishing chemical potentials, but they lie beyond the scope of this thesis work.

$$\rho(T) = g\frac{\pi^2}{30}T^4 \begin{cases} 1 & \text{BE} \\ 7/8 & \text{FD} \end{cases}, \tag{A.19}$$

where ζ is the Riemann's zeta function and $\zeta(3) \approx 1.2$; instead, in the non-relativistic regime ($T \ll M$), we recover the Maxwell-Boltzmann (MB) distribution

$$n(T) = g\left(\frac{mT}{2\pi}\right)^{3/2} e^{-m/T} \tag{A.20}$$

and

$$\rho(T) = mn(T). \tag{A.21}$$

If some process occurs at thermal equilibrium, then the particles involved share the same temperature. On the contrary, there are cases in which some species i are not in equilibrium with the others and possess their own T_i. In that case, the total energy density of relativistic particles can be written as

$$\rho(T) = \frac{\pi^2}{30}g_*(T)T^4, \tag{A.22}$$

where

$$g_*(T) = \sum_{i=BE} g_i\left(\frac{T_i}{T}\right)^4 + \frac{7}{8}\sum_{i=FD} g_i\left(\frac{T_i}{T}\right)^4 \tag{A.23}$$

is the *effective number of relativistic degrees of freedom*, which takes into account the fact that with the diminishing of T, the contribution of particles that are no longer relativistic disappears.

The last ingredient we need for tracking the thermal history is the *entropy of a comoving volume*,

$$S(a,T) = a^3\,\frac{\rho(T)+P(T)}{T}, \tag{A.24}$$

which is a conserved quantity in the expanding universe as long as the particles species are in thermal equilibrium. If we consider relativistic particles, $P = \rho/3$, this quantity can be rewritten as

$$S(a,T) = \frac{2\pi^2}{45}gT^3a^3 \tag{A.25}$$

for a single species; if there were many species with different equilibrium temperatures (a typical situation when describing the early Universe) the employed expression is given by

$$S(a,T) = \frac{2\pi^2}{45}g_{*S}(T)\,T^3a^3 \tag{A.26}$$

where

$$g_{*S}(T) = \sum_{i=BE} g_i\left(\frac{T_i}{T}\right)^3 + \frac{7}{8}\sum_{i=FD} g_i\left(\frac{T_i}{T}\right)^3 \tag{A.27}$$

is the *entropic effective number of relativistic degrees of freedom.*

The key aspect of Eq. (A.26) is the fact that all along the expansion history of the universe we can assume $g_{*S}^{1/3}\,Ta = const$, anytime thermal equilibrium is assured. Another very commonly used quantity is the entropy density, namely the entropy per comoving volume, which is

$$s(a,T) = \frac{2\pi^2}{45} g_{*S}(T)\,T^3. \tag{A.28}$$

Consequently, one can write an equation for the evolution of the temperature with cosmic time as

$$\mathrm{d}\left(g_{*S}^{1/3} Ta\right) = 0 \implies \frac{1}{T}\frac{\mathrm{d}T}{\mathrm{d}t} = -H\left(1 + \frac{1}{3}\frac{\mathrm{d}\ln g_{*S}}{\mathrm{d}\ln T}\right)^{-1}, \tag{A.29}$$

or, by employing the conformal time $\tau = \ln(a/a_0)$, as

$$\frac{1}{T}\frac{\mathrm{d}T}{\mathrm{d}\tau} = -\left(1 + \frac{1}{3}\frac{\mathrm{d}\ln g_{*S}}{\mathrm{d}\ln T}\right)^{-1}. \tag{A.30}$$

A.3.1 Effective number of relativistic degrees of freedom

The key functions for determining the magnitude of the thermodynamic variables and so their contribution inside the Boltzmann equations for the number or energy densities are precisely those which model the effective number of relativistic degrees of freedom. An excellent review on this topic is given by [105], of which we report only some results, relevant for the numerical calculations carried out in this thesis work.

	Flavors	Part. + Antip.	Colors	Spins	Total
Quarks (u, d, c, s, t, b)	6	2	3	2	72
Charged leptons (e, μ, τ)	3	2	1	2	12
Neutrinos (ν_e, ν_μ, ν_τ)	3	2	1	1	6
Gluons (g)	1	1	8	2	16
Photon (γ)	1	1	1	2	2
Massive gauge bosons ($W^\pm$, Z^0)	2	2, 1	1	3	9
Higgs boson (H^0)	1	1	1	1	1
All elementary particles	17				118

Table A.1: The elementary particles of the SM and their internal degrees of freedom and degeneracy.

At the highest energies, all the possible Standard Model (SM) particles are present, with a total of 28 degrees of freedom for the bosons and 90 for the fermions, leading to an effective number $g_* = g_{*S} = 28 + 7/8 \times 90 = 106.75$.
Actually, it is very useful to track the behavior of the effective degrees of freedom analytically. To do so, let us rewrite the variables in Eq. (A.16), setting out the energy dispersion relation and integrating over the solid angle:

$$n(T) = \sum_j \frac{g_j}{2\pi^2} \int_{m_j}^{\infty} \mathrm{d}E \, \frac{E\sqrt{E^2 - m_j^2}}{e^{E/T} \pm 1}, \quad \rho(T) = \sum_j \frac{g_j}{2\pi^2} \int_{m_j}^{\infty} \mathrm{d}E \, \frac{E^2\sqrt{E^2 - m_j^2}}{e^{E/T} \pm 1},$$
$$P(T) = \sum_j \frac{g_j}{6\pi^2} \int_{m_j}^{\infty} \mathrm{d}E \, \frac{(E^2 - m_j^2)^{3/2}}{e^{E/T} \pm 1}, \tag{A.31}$$

and the entropy density follows from $s(T) = (\rho(T) + P(T))/T$,

$$s(T) = \sum_j \frac{g_j}{2\pi^2} \int_{m_j}^{\infty} \mathrm{d}E \frac{\sqrt{E^2 - m_j^2}}{e^{E/T} \pm 1} \frac{4E^2 - m_j^2}{3}. \tag{A.32}$$

We can define the effective number of relativistic degrees of freedom of a given species j for a certain thermodynamic variable, by dividing it with the corresponding relativistic variable (with $g = 1$),

$$g_{*n_j}(T) = \frac{\frac{g_j T^3}{2\pi^2} \int_{z_j}^{\infty} \mathrm{d}u \, \frac{u\sqrt{u^2 - z_j^2}}{e^u \pm 1}}{\frac{T^3}{2\pi^2} \int_0^{\infty} \mathrm{d}u \frac{u^2}{e^u \pm 1}} = \frac{g_j}{2\zeta(3)} \int_{z_j}^{\infty} \mathrm{d}u \frac{u\sqrt{u^2 - z_j^2}}{e^u \pm 1},$$
$$g_{*\rho_j}(T) = \frac{\frac{g_j T^4}{2\pi^2} \int_{z_j}^{\infty} \mathrm{d}u \, \frac{u^2\sqrt{u^2 - z_j^2}}{e^u \pm 1}}{\frac{T^4}{2\pi^2} \int_0^{\infty} \mathrm{d}u \frac{u^3}{e^u \pm 1}} = \frac{15 g_j}{\pi^4} \int_{z_j}^{\infty} \mathrm{d}u \frac{u^2\sqrt{u^2 - z_j^2}}{e^u \pm 1},$$
$$g_{*P_j}(T) = \frac{\frac{g_j T^4}{6\pi^2} \int_{z_j}^{\infty} \mathrm{d}u \, \frac{(u^2 - z_j^2)^{3/2}}{e^u \pm 1}}{\frac{T^4}{6\pi^2} \int_0^{\infty} \mathrm{d}u \frac{u^3}{e^u \pm 1}} = \frac{15 g_j}{\pi^4} \int_{z_j}^{\infty} \mathrm{d}u \frac{(u^2 - z_j^2)^{3/2}}{e^u \pm 1},$$
$$g_{*s_j}(T) = \frac{45}{2\pi^2 T^3} s_j(T) = \frac{3 g_{*\rho_j}(T) + g_{*P_j}(T)}{4} = \frac{45 g_j}{4\pi^4} \int_{z_j}^{\infty} \mathrm{d}u \frac{\sqrt{u^2 - z_j^2}}{e^u \pm 1} \frac{4u^2 - z_j^2}{3}. \tag{A.33}$$

If we want the total "$g_*(T)$" function, we need to sum over all the particle species

involved, hence obtaining

$$
\begin{aligned}
g_{*n}(T) &= \sum_j \frac{g_j}{2\zeta(3)} \int_{z_j}^{\infty} \mathrm{d}u \frac{u\sqrt{u^2 - z_j^2}}{e^u \pm 1}, \\
g_{*\rho}(T) &= \sum_j \frac{g_j}{15\pi^4} \int_{z_j}^{\infty} \mathrm{d}u \frac{u^2\sqrt{u^2 - z_j^2}}{e^u \pm 1}, \\
g_{*P}(T) &= \sum_j \frac{g_j}{15\pi^4} \int_{z_j}^{\infty} \mathrm{d}u \frac{(u^2 - z_j^2)^{3/2}}{e^u \pm 1}, \\
g_{*s}(T) &= \sum_j \frac{45 g_j}{4\pi^4} \int_{z_j}^{\infty} \mathrm{d}u \frac{\sqrt{u^2 - z_j^2}}{e^u \pm 1} \frac{4u^2 - z_j^2}{3}.
\end{aligned}
\tag{A.34}
$$

These are the thermodynamic functions we employ in our calculations and are shown in Fig. A.1; the functions here utilized have been extrapolated from [106].

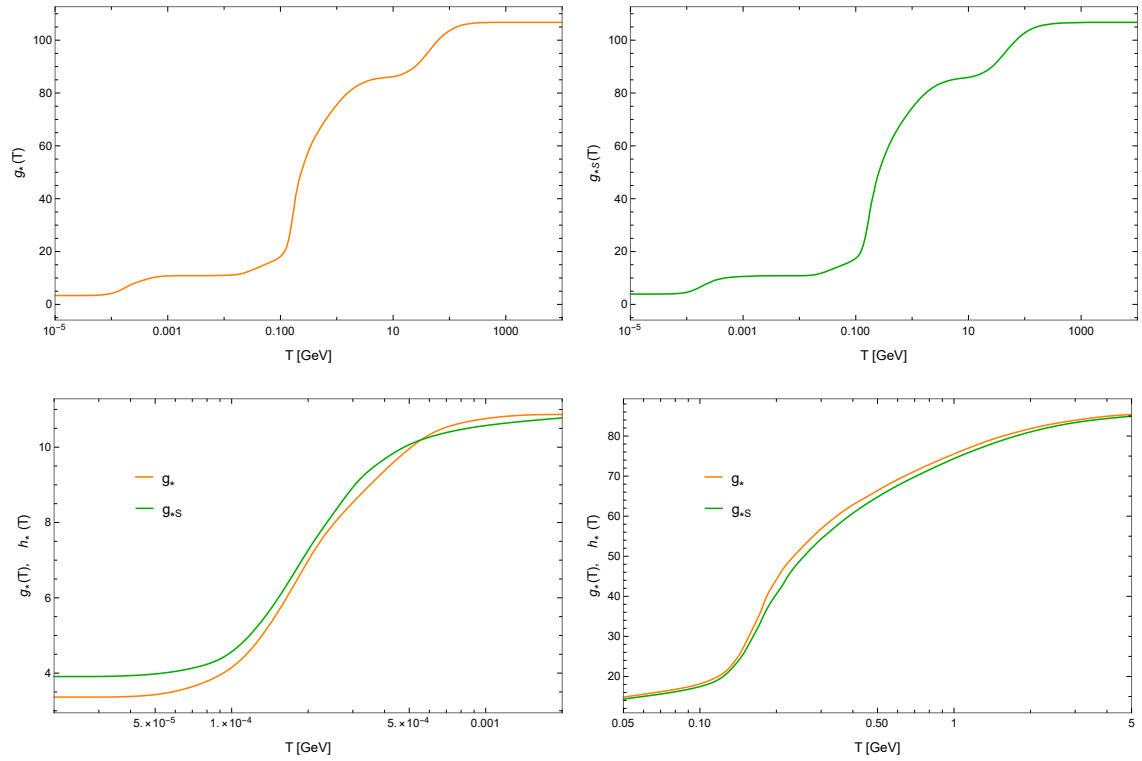

Figure A.1: In the top panels we show the number of degrees of freedom g_* (g_{*S}) for the energy (entropy) density as a function of the thermal bath temperature. The bottom panels draw attention to the small differences between the two quantities during the neutrino decoupling phase (bottom left) and the QCD phase (bottom right). The functions have been extrapolated from [106].

When dealing with the evolution of the cooling Universe, one has to pay attention

to the different epochs and their processes. For instance, in addition to the various particle species equilibrium departures as the temperature falls below their mass, which decrease the "$g_*(T)$" functions, there are at least a couple of relevant low-energy scales at which the physics involved is not so trivial: the QCD phase transition scale and neutrino decoupling.

Regarding the first one, the treatment is everything but trivial, since there is still no analytical solution to QCD in non-perturbative regimes, but only numerical ones, such as lattice QCD (LQCD). Literature is rich of discussions about how to treat the degrees of freedom in the early Universe when the temperature drops down to the QCD parton-to-hadron transition scale, e.g. when the strong force between colored particles becomes so powerful to be able to confine quarks and gluons into baryons and mesons. No result claims for sure what this energy scale is, but all searches concur that this should be around few hundreds of MeV. At the same time, the functional form of the equation-of-state of this polymorphic exotic fluid is not clear. In this thesis work, we have followed a recent analysis of [106], based on one of the latest major achievements with LQCD, namely the so-called ($N_f = 2 + 1$)-flavor QCD [107], where dynamical quarks are considered in the equation of state and, in particular, the u and d quarks are degenerate in mass, while the strange quark mass needs to be taken into account. The critical temperature is $T_c = 154$ MeV and the c quark contribution is also included around it. The bottom and the top quarks are too heavy, so that they have been regarded as essentially free particles during (de)confinement.

Weak interactions become ineffective at temperatures around 1 MeV, so that neutrinos decouple from the photons of the thermal bath and evolve as an independent thermal reservoir. The total entropy of the two baths (the photon and the neutrino ones) are separately conserved. However, the photon bath gets reheated by electron-positron annihilations at $T_\gamma \sim 0.5$ MeV, but neutrinos are not affected by this process and they keep on expanding with a lower temperature T_ν. Entropy conservation allows us to write a relation between the temperature immediately before (be) and after (af) electron-positron annihilations

$$T_{\rm be} = \left(\frac{g_{*_{\rm af}}}{g_{*_{\rm be}}}\right)^{1/3} T_{\rm af}.$$

The number of relativistic degrees of freedom before is given by photons, electrons and positrons, $g_{*_{\rm af}} = 2 + (7/8) \cdot 2 \cdot 2 = 11/2$, whereas, after the transitions, only photons contribute, $g_{*_{\rm be}} = 2$. Hence, the radiation temperature after annihilations is a factor $(11/4)^{1/3} \approx 1.4$ higher than before. The temperature of photons ahead of the transition is by the way equal to that of neutrinos, which means that

$$T_\nu \simeq \left(\frac{4}{11}\right)^{1/3} T_\gamma \simeq 0.71\, T_\gamma. \tag{A.35}$$

Since the CMB shows $T_{\gamma 0} = 2.725$ K, the cosmic neutrino background (CνB) should have $T_{\nu 0} = 1.938$ K. The colder particles (neutrinos) give a smaller contribution to the

effective number of relativistic degrees of freedom than the hotter (photons), so that one needs to recalculate the various g_* by inserting the factor $T(T_\nu/T)$ instead of T in the calculations. The final results for the number, energy and entropy densities are

$$g_{*n} = 2 + 6 \cdot 3/4 \cdot (T_\nu/T)^3 \approx 3.636,$$
$$g_{*\rho} = 2 + 6 \cdot 7/8 \cdot (T_\nu/T)^4 \approx 3.363,$$
$$g_{*s} = 2 + 6 \cdot 7/8 \cdot (T_\nu/T)^3 \approx 3.909.$$

These numbers should be adjusted with the effective number of active neutrinos $N_{eff} \simeq 3.045$ (accounting for the contribution of electron neutrinos and finite-temperature QED effects during electron-positron annihilation), also discussed in Section 1.4. The corrected numbers are

$$g_{*n} = 2 + 2 \cdot 3.045 \cdot 3/4 \cdot (T_\nu/T)^3 \approx 3.661,$$
$$g_{*\rho} = 2 + 2 \cdot 3.045 \cdot 7/8 \cdot (T_\nu/T)^4 \approx 3.383,$$
$$g_{*s} = 2 + 2 \cdot 3.045 \cdot 7/8 \cdot (T_\nu/T)^3 \approx 3.938.$$

The differences between $g_{*\rho}$ and g_{*s} both around the QCD phase and after neutrino decoupling are highlighted in the two bottom panels of Fig. A.1.

Appendix B

Useful formulae and Notation

Throughout this thesis work we have always made use of *natural units*, where

$$c = \hbar = k_B = 1,$$

unless we wanted to explicitly show the contribution of these fundamental constants in a given formula. These have the property of leaving all the dimensional quantities in units of energy (or mass), useful for extracting natural physical scale (like the Planck mass) and comparing very different physical processes.

B.1 Exact equilibrium abundances

We give here an exact formulation of the equilibrium number density of a species i in Eq. (2.21) (either bosonic or fermionic), which we write as

$$n_i^{eq} = \frac{g_i}{2\pi^2} \int_0^\infty \mathrm{d}p\, p^2\, e^{-E_i/T}.$$

We can use the relativistic dispersion relation $p^2 = E^2 - m^2$ twice, once to substitute $p\,\mathrm{d}p$ with $E\,\mathrm{d}E$ and another time in the remaining p factor. The result is

$$n_i^{eq} = \frac{g_i}{2\pi^2} \int_{m_i}^\infty \mathrm{d}E_i\, E_i \sqrt{E_i^2 - m_i^2}\, e^{-E_i/T}.$$

We pass to the integration variable $x = E_i/m_i$ and we define $z = m_i/T$, obtaining

$$\begin{aligned} n_i^{eq} &= \frac{g_i}{2\pi^2} m_i^3 \int_1^\infty \mathrm{d}x\, x\sqrt{x^2-1}\, e^{-zx} = \\ &= \frac{g_i}{2\pi^2} m_i^2\, T\, z \int_1^\infty \mathrm{d}x\, x\sqrt{x^2-1}\, e^{-zx} = \\ &= \frac{g_i}{2\pi^2} m_i^2\, T\, K_2[z] \end{aligned} \tag{B.1}$$

In the last passage we used the definition of *modified Bessel function of the second kind of order n*, which can be written in the following integral representation [108]

$$K_n[z] = \frac{\pi^{1/2}}{\Gamma[n+1/2]} \left(\frac{z}{2}\right)^n \int_1^\infty \mathrm{d}x\, e^{-zx}(x^2-1)^{n-1/2}, \tag{B.2}$$

valid only for $n > -1/2$. In particular, we have

$$K_1[z] = z \int_1^\infty \mathrm{d}x\, \sqrt{x^2-1}\, e^{-zx},$$
$$K_2[z] = z \int_1^\infty \mathrm{d}x\, x\sqrt{x^2-1}\, e^{-zx}.$$

The exact comoving equilibrium abundance follows immediately:

$$Y_i^{eq}(z) = \frac{n_i^{eq}}{s} = \frac{45\, g_i}{4\pi^4\, g_{*S}} z^2 K_2[z]. \tag{B.3}$$

B.2 Amplitudes and cross sections

The decay rate and the cross-section are the two main quantities of interest when dealing with scattering and decay processes. The first one measures the probability (or the average frequency) of decay of a given particle, the other accounts for the probability that a given flux of incident particles interact in a unit time interval. Their differential forms are defined as

$$\mathrm{d}\Gamma = V\, w \prod_f \frac{\mathrm{d}^3\mathbf{p'}_f}{(2\pi)^3}, \quad \mathrm{d}\sigma = \frac{V}{v_{rel}} w \prod_f \frac{\mathrm{d}^3\mathbf{p'}_f}{(2\pi)^3}, \tag{B.4}$$

where $w = |S_{fi}|^2/T$ is the transition probability per unit time, with S_{fi} the S-matrix element between the initial and final states $|i\rangle = |p_1\rangle \cdots |p_k\rangle$ and $|f\rangle = |p'_1\rangle \cdots |p'_j\rangle$, canonically normalized as $\langle i|i\rangle = \prod_k (2E_k V)$ and $\langle f|f\rangle = \prod_j (2E_j V)$. The incident flux has been written in terms of the relative velocity v_{rel} (see also Section B.2.1 for details)

Exploiting the form of w and performing few calculations, one finds [109]

$$\mathrm{d}\Gamma = (2\pi)^4\, \delta^{(4)}\left(\sum p'_f - p\right) \frac{1}{2E} \prod_f \frac{\mathrm{d}^3\mathbf{p'}_f}{(2\pi)^3 2E'_f} |\mathcal{M}|^2, \tag{B.5}$$

$$\mathrm{d}\sigma = (2\pi)^4\, \delta^{(4)}\left(\sum p'_f - \sum p_i\right) \frac{1}{4E_1 E_2 v_{rel}} \prod_f \frac{\mathrm{d}^3\mathbf{p'}_f}{(2\pi)^3 2E'_f} |\mathcal{M}|^2, \tag{B.6}$$

where $|\mathcal{M}|^2$ is the probability amplitude for the involved process. Notice that the Dirac delta ensures four-momentum conservation and that we used a single initial momentum for the decays. The integral over the final state is called (n-body) *Lorentz-invariant*

phase space (LIPS), usually denoted as $\mathrm{d}\Pi_n = \prod_j^n \mathrm{d}^3\mathbf{p'}_j/2E'_f(2\pi)^3$, which derives from the manifestly invariant form

$$\frac{\mathrm{d}^3\mathbf{p}}{2E} = \int \mathrm{d}^4p\,\delta(p^2 - m^2)\,\theta(p^0),$$

being $\theta(p^0)$ the Heaviside step function, ensuring the positivity of energy.

The factor $1/E_1E_2v_{rel}$ is invariant only for boosts along the z-direction, that is to say that, if we have two interacting particles, we recover a Lorentz-invariant expression if we consider the angle between the two incident momenta to be zero, obtaining $E_1E_2v_{rel} = \sqrt{(p_1\cdot p_2)^2 - m_1^2m_2^2}$.

If we put ourselves in the center-of-mass (CM) frame of reference, one can perform various simplifications from the fact that $\mathbf{p}_1+\mathbf{p}_2 = 0$. The final differential cross-section in the CM frame of reference is given by [109]

$$\left(\frac{\mathrm{d}\sigma}{\mathrm{d}\Omega}\right)_{cm} = \frac{1}{2E_1 2E_2}\frac{1}{v_{rel}}\frac{|\mathbf{p}_1|}{(2\pi)^2 4E_{cm}}|\mathcal{M}|^2, \tag{B.7}$$

which can be reworked in the following way:

$$\mathrm{d}\sigma = \frac{1}{4E_1E_2}\frac{1}{v_{rel}}\frac{1}{8\pi}\frac{2|\mathbf{p}_1|}{E_{cm}}|\mathcal{M}|^2\frac{\mathrm{d}\Omega_{cm}}{4\pi}. \tag{B.8}$$

In the ultrarelativistic limit, sometimes very useful for performing simplified calculations in the early Universe, this formula reduces to

$$\mathrm{d}\sigma = \frac{|\mathcal{M}|^2}{16\pi E_{cm}^2}\frac{\mathrm{d}\Omega_{cm}}{4\pi}. \tag{B.9}$$

A common interesting case is when the ingoing and outgoing colliding beams are unpolarized and the final polarization states are not measured. In this case, we must *average* over all initial $2j_i + 1$ polarization states and *sum* over all final polarization states, thus obtaining the unpolarized Feynman amplitude

$$|\overline{\mathcal{M}}|^2 = \left(\prod_i \frac{1}{2j_i+1}\right)\sum_{s_i}\sum_{s_f}|\mathcal{M}_{fi}|^2, \tag{B.10}$$

usually employed in cross-section calculations. Throughout this work, we have always denoted the number of polarization states with g, so that we can also write this formula with the product $\prod_i 1/g_i$.

For a generic $1 + 2 \to 3 + 4$ process, we can calculate the total cross-section from Eq. (B.6) as

$$\begin{aligned}\sigma_{1+2\to3+4}(s) = &\frac{1}{g_1g_2}\frac{1}{4(p_1\cdot p_2)\,v_{12}}\times\\ &\times\int \mathrm{d}\Pi_3\,\mathrm{d}\Pi_4\,|\mathcal{M}_{12\to34}|^2\,(2\pi)^4\,\delta^{(4)}(p_1+p_2-p_3-p_4),\end{aligned} \tag{B.11}$$

where we considered the amplitude squared only summed over the final polarization states (hence the factor of $1/g_1 g_2$) and we made use of the fully Lorentz-invariant relative velocity as defined in Eq. (B.12), which takes the place of the previous definition, valid only for boosts along the z-direction.

Notice that, in natural units in a four-dimensional spacetime, the mass dimension for a n-particle process is $[\mathcal{M}_n] = 4 - n$, hence for a $1 \to 2$ decay it has dimension 1, whereas for a $2 \to 2$ scattering it is dimensionless. The cross-section, having the dimension of an area, has $[\sigma] = -2$, namely $(\text{Energy})^{-2}$.

B.2.1 Velocity misconception

We saw that the r.h.s of the Boltzmann equation for a $2 \to 2$ scattering process (e.g. Eq. (2.14) and Eq. (2.24)) can be written as

$$\frac{g}{(2\pi)^3}\int \frac{\mathrm{d}^3\mathbf{p}}{E}\,\hat{\mathbb{C}}[f] = -\langle\sigma v\rangle(n_1 n_2 - n_1^{eq} n_2^{eq}),$$

where we usually refer to v as the "relative velocity" of the involved particles, namely $v_r = |\mathbf{v_1} - \mathbf{v_2}|$. Actually, this quantity is clearly not Lorentz-invariant and it is valid only in a fully non-relativistic regime, whereas the r.h.s of the Boltzmann equation is perfectly Lorentz-invariant, since it is derived from a covariant quantity. We would like to use a better definition for a relative velocity in a generic relativistic context. A famous paper by Gondolo and Gelmini [42] pointed out this problem, where the authors re-calculated the collisional part of the Boltzmann equation with a fully relativistic approach. They used the so-called *Møller velocity*, given by $v_{\text{Møl}} = \mathcal{F}/E_1 E_2$ [110], where $\mathcal{F} = \sqrt{(p_1 \cdot p_2)^2 - m_1^2 m_2^2}$ is the Lorentz-invariant flux of particles. There, the statement that $v_{\text{Møl}} n_1 n_2$ is invariant under Lorentz transformations is certainly true, since the canonical normalization for one-particle states[1] allows us to write $n = 2E$ and then

$$v_{\text{Møl}}\, n_1 n_2 = v_{\text{Møl}}\, 4E_1 E_2 = 4\mathcal{F} \equiv F,$$

which is a Lorentz-invariant quantity. This Lorentz scalar can be rearranged in another popular version [112],

$$F = n_1 n_2 \frac{\mathcal{F}}{E_1 E_2} = n_1 n_2 \sqrt{(\mathbf{v_1} - \mathbf{v_2})^2 - (\mathbf{v_1} \times \mathbf{v_2})^2},$$

where $\mathbf{v} = \mathbf{p}/E$ and which clearly reduces to a collinear flux in the particular case $\mathbf{v_1} \times \mathbf{v_2} = 0$. This makes the differences between v_r and $v_{\text{Møl}}$ clearer.

In the literature, the Møller velocity is the one usually inserted inside the angular parentheses for computing relic densities, even though it is not a Lorentz scalar and is not directly related to a physical relative velocity. As discussed in [112], a correct,

[1] $\langle \mathbf{p}|\mathbf{p}'\rangle = (2\pi)^3\, 2E\, \delta^{(3)}(\mathbf{p} - \mathbf{p}')$.

relativistic and Lorentz-invariant expression for such a relative velocity is given by [111] and reads

$$v_{rel} = \frac{\sqrt{(p_1 \cdot p_2)^2 - m_1^2 m_2^2}}{p_1 \cdot p_2}, \tag{B.12}$$

which is equivalent to

$$v_{rel} = \frac{\sqrt{(\mathbf{v_1} - \mathbf{v_2})^2 - (\mathbf{v_1} \times \mathbf{v_2})^2}}{1 - \mathbf{v_1} \cdot \mathbf{v_2}},$$

or to

$$v_{B_1 B_2} = \frac{\lambda^{1/2}(s, m_{B_1}, m_{B_2})}{2(p_{B_1} \cdot p_{B_2})}. \tag{B.13}$$

where we introduced the *Källén (or triangular) function*

$$\lambda(x, y, z) \equiv [x - (y + z)^2][x - (x - y)^2].$$

Accordingly, the invariant flux F must be rearranged in the following form:

$$F = n_1 n_2 \frac{p_1 \cdot p_2}{E_1 E_2} v_{rel},$$

We notice that in the collinear case the relative velocity is not $|\mathbf{v_1} - \mathbf{v_2}|$, but instead

$$v_{rel}^{col.} = \frac{|\mathbf{v_1} - \mathbf{v_2}|}{1 - \mathbf{v_1} \cdot \mathbf{v_2}},$$

which can never overcome the speed of light. In [112], the author comments the fact that $v_{\text{Møl}}$ is just v_{rel} times $(1 - \mathbf{v_1} \cdot \mathbf{v_2})$ and that it has no physical meaning by itself. The correct line of reasoning always starts from the invariant flux, which is directly related to the rate equation. In this thesis, we use Eq. (B.12) in our calculations.

B.2.2 What do we mean by $\langle \sigma v \rangle$?

With the definition for the relative velocity in mind, we can give a meaning to $\langle \sigma v \rangle$. The thermally averaged cross section times the relative velocity was first calculated in [42]. If we consider our particle species at the equilibrium, with initial negligible chemical potential, we can use $f_i \sim \exp[-E_i/T]$ in the comoving frame. Thus, the definition of the thermal average of the quantity σv is straightforward:

$$\langle \sigma v \rangle = \frac{\int \mathrm{d}^3 p_1 \, \mathrm{d}^3 p_2 \, e^{-E_1/T} e^{-E_2/T} \, \sigma v}{\int \mathrm{d}^3 p_1 \, \mathrm{d}^3 p_2 \, e^{-E_1/T} e^{-E_2/T}}. \tag{B.14}$$

After some calculations, we would have, in the simpler case with $m_1 = m_2 = m$,

$$\int \mathrm{d}^3 p_1 \, \mathrm{d}^3 p_2 \, e^{-E_1/T} e^{-E_2/T} = (4\pi m^2 \, T K_2[m/T])^2,$$

$$\int \mathrm{d}^3 p_1 \, \mathrm{d}^3 p_2 \, e^{-E_1/T} e^{-E_2/T} \, \sigma v = 2\pi^2 \, T \int_{4m^2}^{\infty} \mathrm{d}s \, \sigma(s)(s - 4m^2)\sqrt{s} K_1[\sqrt{s}/T].$$

Otherwise, if $m_1 \neq m_2$, we would obtain

$$\begin{aligned}\int \mathrm{d}^3p_1\,\mathrm{d}^3p_2\,e^{-E_1/T}e^{-E_2/T} &= 16\pi^2\int_{m_1}^{\infty}\mathrm{d}E_1\,E_1\sqrt{E_1^2-m_1^2}\,e^{-E_1/T}\times\\ &\quad\times\int_{m_2}^{\infty}\mathrm{d}E_2\,E_2\sqrt{E_2^2-m_2^2}\,e^{-E_2/T} =\\ &= 16\pi^2 m_1^2\,m_2^2\,T^2K_2[m_1/T]K_2[m_2/T],\end{aligned}$$

$$\int \mathrm{d}^3p_1\,\mathrm{d}^3p_2\,e^{-E_1/T}e^{-E_2/T}\,\sigma v = 2\pi^2 T\int_{s_{12}^{min}}^{\infty}\mathrm{d}s\,\frac{\lambda^{1/2}(s,m_1,m_2)}{s^{1/2}}\,\sigma(s)K_1[\sqrt{s}/T],$$

where $s_{12}^{min} = (m_1+m_2)^2$. In both cases, we made use of Eq. (B.13), exploiting the denominator for the case of interest. Hence, in the most general case, our thermally averaged cross-section times the relative velocity will be given by

$$\boxed{\langle\sigma v\rangle = \frac{1}{8m_1^2m_2^2\,TK_2[m_1/T]K_2[m_2/T]}\int_{s_{12}^{min}}^{\infty}\mathrm{d}s\,\frac{\lambda^{1/2}(s,m_1,m_2)}{s^{1/2}}\,\sigma(s)K_1[\sqrt{s}/T].} \tag{B.15}$$

B.2.3 Fermionic Higgs Portal

The interaction we are interested in is described by the EFT encoded in the Fermionic Higgs Portal Operator (FHPO), which we have written as a SM part with the Higgs fields times a dark-sector part with the FIMP fields:

$$\mathcal{O}_{FHP} = (\text{SM operator})\otimes(\text{FIMP operator}).$$

This allows us to easily derive the matrix element $\mathcal{M}$ for the $h_1h_2 \to \overline{\psi}\psi$ process, since the two contributions are separately factorized. Notice that, as described in [88], one may assume a linear combination of different fermionic bilinears which are responsible for the vertex interaction of the FIMPs with the Higgses; in that case, one should account for interference terms to the total $|\mathcal{M}|^2$ and CP-violating contributions (e.g. from a pseudoscalar vertex like $\overline{\psi}i\gamma_5\psi\,H^\dagger H$), which is beyond the scope of this thesis.

The matrix element is simply given by

$$\mathcal{M} = \frac{1}{\Lambda}\,\overline{u}_{s'}(p')\,v_s(p), \tag{B.16}$$

where $v_s(p)$ is the spinor field of the final DM anti-fermion with spin polarization s and 4-momentum p, while $\overline{u}'_s(p')$ is the spinor field of the final DM fermion with spin polarization s' and 4-momentum p'. The modulus squared of $\mathcal{M}$, summed over the final polarization states, reads as

$$\begin{aligned}|\mathcal{M}|^2 =& \frac{1}{\Lambda^2}\sum_{s,s'}\overline{u}_{s'}(p')\,v_s(p)\,\overline{v}_s(p)\,u'_s(p') = \frac{1}{\Lambda^2}\,\mathrm{Tr}\{(\not{p}-m_\psi)(\not{p}'+m_\psi)\}\\ =& \frac{1}{\Lambda^2}\,4\,(p\cdot p'-m_\psi^2),\end{aligned} \tag{B.17}$$

where we made use of the spinors completeness relations and of the trace properties of Dirac's gamma matrices.

We can put ourselves in the center-of-mass (CM) frame of reference, in which we have that $\mathbf{p}_{h_1} = -\mathbf{p}_{h_2}$ and $\mathbf{p} = -\mathbf{p}'$, so that $E_{h_1} = E_{h_2} = E_\psi = E_{\overline{\psi}} = E_{cm}/2 = \sqrt{s}/2$. Now, since $p \cdot p' - m_\psi^2 = E_\psi^2 + |\mathbf{p}|^2 - m_\psi^2 = 2E_\psi^2 - 2m_\psi^2 = \frac{1}{2}(s - 4m_\psi^2)$, the amplitude reduces to

$$|\mathcal{M}|^2 = \frac{1}{\Lambda^2} 2(s - 4m_\psi^2). \tag{B.18}$$

Having this in mind, we can compute the cross section in Equations (B.11)–(4.11):

$$\begin{aligned}
\sigma_{\overline{\psi}\psi\to h_1 h_2}(s) &= \frac{1}{g_\psi^2} \frac{1}{2\,\lambda^{1/2}(s, m_\psi, m_\psi)} \int \frac{\mathrm{d}^3\mathbf{p}_{h_1}}{2E_{h_1}(2\pi)^3} \frac{\mathrm{d}^3\mathbf{p}_{h_2}}{2E_{h_2}(2\pi)^3} \frac{1}{\Lambda^2} 2(s - m_\psi^2) \times \\
&\quad \times (2\pi)^4 \delta^{(3)}(\mathbf{p}_{\overline{\psi}} + \mathbf{p}_\psi - \mathbf{p}_{h_1} - \mathbf{p}_{h_2})\, \delta(E_{\overline{\psi}} + E_\psi - E_{h_1} - E_{h_2}) = \\
&= \frac{1}{g_\psi^2} \frac{1}{2\,\lambda^{1/2}(s, m_\psi, m_\psi)} \frac{1}{\Lambda^2} 2(s - 4m_\psi^2) \frac{1}{16\pi^2 E_{h_1} E_{h_2}} \times \\
&\quad \times \int \mathrm{d}^3\mathbf{p}_{h_1} \mathrm{d}^3\mathbf{p}_{h_2}\, \delta^{(3)}(\mathbf{p}_{\overline{\psi}} + \mathbf{p}_\psi - \mathbf{p}_{h_1} - \mathbf{p}_{h_2})\, \delta(E_{h_1} + E_{h_2} - \sqrt{s}) = \\
&= \frac{1}{16\pi^2 g_\psi^2 \Lambda^2} \frac{s - 4m_\psi^2}{\lambda^{1/2}(s, m_\psi, m_\psi)} \frac{1}{E_{h_1} E_{h_2}} \int \mathrm{d}^3\mathbf{p}_{h_1}\, \delta(E_{h_1} + E_{h_2} - \sqrt{s}),
\end{aligned} \tag{B.19}$$

where we have integrated over $\mathrm{d}^3\mathbf{p}_{h_2}$ to eliminate the delta of the linear momenta and put $E_{\overline{\psi}} + E_\psi = \sqrt{s}$.

The last integration can be performed with a standard calculation, whose details are reported in the following box. The result, valid for massless h_1 and h_2 particles, is

$$\int \mathrm{d}^3\mathbf{p}_{h_1}\, \delta(E_{h_1} + E_{h_2} - \sqrt{s}) = 2\pi E_{h_1} E_{h_2}. \tag{B.20}$$

Inserting this expression into Eq. (B.19), the cross section for the annihilation (pair-production) process reads as follows:

$$\sigma_{\overline{\psi}\psi\to h_1 h_2}(s) = \frac{1}{8\pi g_\psi^2 \Lambda^2} \frac{(s - 4m_\psi^2)}{s} \frac{\lambda^{1/2}(s, m_{h_1}, m_{h_2})}{\lambda^{1/2}(s, m_\psi, m_\psi)}, \tag{B.21}$$

or, opening up the triangular functions and considering the Higgs field as massless,

$$\boxed{\sigma_{\overline{\psi}\psi\to h_1 h_2}(s) = \frac{1}{8\pi g_\psi^2} \frac{1}{\Lambda^2} \frac{\sqrt{s - 4m_\psi^2}}{\sqrt{s}},} \tag{B.22}$$

which is the cross section for annihilations $h_1 h_2 \to \overline{\psi}\psi$ of each the complex scalars in the Higgs doublet.

Let us develop the integral in Eq. (B.20) for two generic particles h_1 and h_2, which will be considered massive for the sake of generality. Putting $\sqrt{s} = E_{h_1} + E_{h_2}$, the one-dimensional integral becomes

$$\int \mathrm{d}^3\mathbf{p}_{h_1}\,\delta(E_{h_1}+E_{h_2}-\sqrt{s}) = \int \mathrm{d}p_{h_1}\mathrm{d}\Omega\, p_{h_1}^2\,\delta\left(\sqrt{m_{h_1}^2+\mathbf{p}_{h_1}^2}+\sqrt{m_{h_2}^2+\mathbf{p}_{h_1}^2}-\sqrt{s}\right),$$

where, in the second squared root, we used $\mathbf{p}_{h_2} = -\mathbf{p}_{h_1}$, valid in the CM frame. Using the usual properties of the Dirac's delta of a function $f(p_{h_1})$, with $p_{h_1} = |\mathbf{p}_{h_1}|$, we have that the integral is non-zero only for vanishing $f(p_{h_1})$. Here, the function we are interested in is

$$f(p_{h_1}) = \sqrt{m_{h_1}^2+\mathbf{p}_{h_1}^2}+\sqrt{m_{h_2}^2+\mathbf{p}_{h_1}^2}-\sqrt{s}.$$

After a short calculation, we can solve $f(p_{h_1}) = 0$ for p_{h_1} and find that this happens for those values $p_{h_1}^*$ satisfying

$$p_{h_1}^* = \frac{1}{2\sqrt{s}}\left[(s-(m_{h_1}+m_{h_2})^2)^2 - 4m_{h_1}^2 m_{h_2}^2\right]^{1/2} = \frac{\lambda^{1/2}(s,m_{h_1},m_{h_2})}{2\sqrt{s}}.$$

Finally, we make use of another property of the delta of a function, for which

$$\int \mathrm{d}x\,\delta(f(x)) = \int \mathrm{d}x \sum_i \frac{\delta(x-x_i^*)}{|f'(x_i^*)|},$$

with $f(x = x_i^*) = 0$.
In our case we have only one zero to take care of, hence the integrand becomes

$$\begin{aligned}\mathrm{d}p_{h_1}\,\mathrm{d}\Omega_{cm}\,p_{h_1}^2\delta(f(p_{h_1})) &= \mathrm{d}p_{h_1}\mathrm{d}\Omega_{cm}\frac{\delta(p_{h_1}-p_{h_1}^*)}{\left|\dfrac{p_{h_1}}{E_{h_1}}+\dfrac{p_{h_1}}{E_{h_2}}\right|}p_{h_1}^2 = \\ &= \mathrm{d}p_{h_1}\mathrm{d}\Omega_{cm}\,\delta(p_{h_1}-p_{h_1}^*)\,p_{h_1}\frac{E_{h_1}E_{h_2}}{E_{h_1}+E_{h_2}}.\end{aligned}$$

Integrating over the momentum and putting $E_{h_1} + E_{h_2} = \sqrt{s}$, we obtain

$$p_{h_1}^*\frac{E_{h_1}E_{h_2}}{E_{h_1}+E_{h_2}}\mathrm{d}\Omega_{cm} = \frac{E_{h_1}E_{h_2}}{\sqrt{s}}\frac{\lambda^{1/2}(s,m_{h_1},m_{h_2})}{2\sqrt{s}}\,\mathrm{d}\Omega_{cm}$$

and, finally integrating over the solid angle, we get

$$\int \mathrm{d}^3\mathbf{p}_{h_1}\,\delta(E_{h_1}+E_{h_2}-\sqrt{s}) = 2\pi\frac{E_{h_1}E_{h_2}}{s}\lambda^{1/2}(s,m_{h_1},m_{h_2}). \tag{B.23}$$

In the massless limit, the triangular function reduces to $\lambda(s,0,0) = s^2$ and that is why we obtain precisely the result of Eq. (B.20).

References

[1] Planck collaboration. "Planck 2018 results. VI. Cosmological parameters". In: (2018). arXiv: 1807.06209 [astro-ph.CO].

[2] E. Kolb and M. Turner. *The Early Universe*. Frontiers in physics. Avalon Publishing, 1994. ISBN: 9780201626742.

[3] M. Kuster, G. Raffelt, and B. Beltrán. *Axions: Theory, Cosmology, and Experimental Searches*. Lecture Notes in Physics. Springer Berlin Heidelberg, 2007. ISBN: 9783540735175.

[4] David J. E. Marsh. "Axion Cosmology". In: *Phys. Rept.* 643 (2016), pp. 1–79. DOI: 10.1016/j.physrep.2016.06.005. arXiv: 1510.07633 [astro-ph.CO].

[5] Lawrence J. Hall et al. "Freeze-In Production of FIMP Dark Matter". In: *JHEP* 03 (2010), p. 080. DOI: 10.1007/JHEP03(2010)080. arXiv: 0911.1120 [hep-ph].

[6] David E. Kaplan, Markus A. Luty, and Kathryn M. Zurek. "Asymmetric Dark Matter". In: *Phys. Rev.* D79 (2009), p. 115016. DOI: 10.1103/PhysRevD.79.115016. arXiv: 0901.4117 [hep-ph].

[7] Daniel J. H. Chung, Edward W. Kolb, and Antonio Riotto. "Superheavy dark matter". In: *Phys. Rev.* D59 (1999), p. 023501. DOI: 10.1103/PhysRevD.59.023501. arXiv: hep-ph/9802238 [hep-ph].

[8] Scott Dodelson. *Modern Cosmology*. Amsterdam: Academic Press, 2003. ISBN: 9780122191411.

[9] M. Tanabashi et al. "Review of Particle Physics". In: *Phys. Rev.* D98.3 (2018), p. 030001. DOI: 10.1103/PhysRevD.98.030001.

[10] Daniel J. H. Chung, Edward W. Kolb, and Antonio Riotto. "Production of massive particles during reheating". In: *Phys. Rev.* D60 (1999), p. 063504. DOI: 10.1103/PhysRevD.60.063504. arXiv: hep-ph/9809453 [hep-ph].

[11] Gian Francesco Giudice, Edward W. Kolb, and Antonio Riotto. "Largest temperature of the radiation era and its cosmological implications". In: *Phys. Rev.* D64 (2001), p. 023508. DOI: 10.1103/PhysRevD.64.023508. arXiv: hep-ph/0005123 [hep-ph].

[12] Raymond T. Co et al. "Freeze-In Dark Matter with Displaced Signatures at Colliders". In: *JCAP* 1512.12 (2015), p. 024. DOI: 10.1088/1475-7516/2015/12/024. arXiv: 1506.07532 [hep-ph].

[13] Stefano Profumo. *An Introduction to Particle Dark Matter*. World Scientific, 2017. ISBN: 9781786340016. DOI: 10.1142/q0001.

[14] Gianfranco Bertone, Dan Hooper, and Joseph Silk. "Particle dark matter: Evidence, candidates and constraints". In: *Phys. Rept.* 405 (2005), pp. 279–390. DOI: 10.1016/j.physrep.2004.08.031. arXiv: hep-ph/0404175 [hep-ph].

[15] Michael Klasen, Martin Pohl, and Günter Sigl. "Indirect and direct search for dark matter". In: *Prog. Part. Nucl. Phys.* 85 (2015), pp. 1–32. DOI: 10.1016/j.ppnp.2015.07.001. arXiv: 1507.03800 [hep-ph].

[16] Nicolás Bernal et al. "The Dawn of FIMP Dark Matter: A Review of Models and Constraints". In: *Int. J. Mod. Phys.* A32.27 (2017), p. 1730023. DOI: 10.1142/S0217751X1730023X. arXiv: 1706.07442 [hep-ph].

[17] Jonathan L. Feng and Jason Kumar. "The WIMPless Miracle: Dark-Matter Particles without Weak-Scale Masses or Weak Interactions". In: *Phys. Rev. Lett.* 101 (2008), p. 231301. DOI: 10.1103/PhysRevLett.101.231301. arXiv: 0803.4196 [hep-ph].

[18] Benjamin W. Lee and Steven Weinberg. "Cosmological Lower Bound on Heavy Neutrino Masses". In: *Phys. Rev. Lett.* 39 (1977). [,183(1977)], pp. 165–168. DOI: 10.1103/PhysRevLett.39.165.

[19] C. Boehm and Pierre Fayet. "Scalar dark matter candidates". In: *Nucl. Phys.* B683 (2004), pp. 219–263. DOI: 10.1016/j.nuclphysb.2004.01.015. arXiv: hep-ph/0305261 [hep-ph].

[20] Kim Griest and Marc Kamionkowski. "Unitarity Limits on the Mass and Radius of Dark Matter Particles". In: *Phys. Rev. Lett.* 64 (1990), p. 615. DOI: 10.1103/PhysRevLett.64.615.

[21] Giorgio Arcadi et al. "The waning of the WIMP? A review of models, searches, and constraints". In: *Eur. Phys. J.* C78.3 (2018), p. 203. DOI: 10.1140/epjc/s10052-018-5662-y. arXiv: 1703.07364 [hep-ph].

[22] LUX collaboration. "Results from a search for dark matter in the complete LUX exposure". In: *Phys. Rev. Lett.* 118.2 (2017), p. 021303. DOI: 10.1103/PhysRevLett.118.021303. arXiv: 1608.07648 [astro-ph.CO].

[23] XENON collaboration. "Dark Matter Search Results from a One Ton-Year Exposure of XENON1T". In: *Phys. Rev. Lett.* 121.11 (2018), p. 111302. DOI: 10.1103/PhysRevLett.121.111302. arXiv: 1805.12562 [astro-ph.CO].

[24] ATLAS collaboration. "Search for dark matter and other new phenomena in events with an energetic jet and large missing transverse momentum using the ATLAS detector". In: *JHEP* 01 (2018), p. 126. DOI: 10.1007/JHEP01(2018)126. arXiv: 1711.03301 [hep-ex].

[25] ATLAS collaboration. "Constraints on mediator-based dark matter and scalar dark energy models using $\sqrt{s} = 13$ TeV pp collision data collected by the ATLAS detector". In: *JHEP* 05 (2019), p. 142. DOI: 10.1007/JHEP05(2019)142. arXiv: 1903.01400 [hep-ex].

[26] Frank Daniel Steffen. "Gravitino dark matter and cosmological constraints". In: *JCAP* 0609 (2006), p. 001. DOI: 10.1088/1475-7516/2006/09/001. arXiv: hep-ph/0605306 [hep-ph].

[27] James M. Cline. "Baryogenesis". In: *Les Houches Summer School - Session 86: Particle Physics and Cosmology: The Fabric of Spacetime Les Houches, France, July 31-August 25, 2006*. 2006. arXiv: hep-ph/0609145 [hep-ph].

[28] Riccardo Barbieri et al. "Baryogenesis through leptogenesis". In: *Nucl. Phys.* B575 (2000), pp. 61–77. DOI: 10.1016/S0550-3213(00)00011-0. arXiv: hep-ph/9911315 [hep-ph].

[29] Edward W. Kolb, Daniel J. H. Chung, and Antonio Riotto. "WIMPzillas!" In: *AIP Conf. Proc.* 484.1 (1999). [,592(1999)], pp. 91–105. DOI: 10.1063/1.59655. arXiv: hep-ph/9810361 [hep-ph].

[30] Fatemeh Elahi, Christopher Kolda, and James Unwin. "UltraViolet Freeze-in". In: *JHEP* 03 (2015), p. 048. DOI: 10.1007/JHEP03(2015)048. arXiv: 1410.6157 [hep-ph].

[31] John McDonald. "Warm Dark Matter via Ultra-Violet Freeze-In: Reheating Temperature and Non-Thermal Distribution for Fermionic Higgs Portal Dark Matter". In: *JCAP* 1608.08 (2016), p. 035. DOI: 10.1088/1475-7516/2016/08/035. arXiv: 1512.06422 [hep-ph].

[32] Daniel J. H. Chung, Edward W. Kolb, and Antonio Riotto. "Nonthermal supermassive dark matter". In: *Phys. Rev. Lett.* 81 (1998), pp. 4048–4051. DOI: 10.1103/PhysRevLett.81.4048. arXiv: hep-ph/9805473 [hep-ph].

[33] Edward W. Kolb and Andrew J. Long. "Superheavy dark matter through Higgs portal operators". In: *Phys. Rev.* D96.10 (2017), p. 103540. DOI: 10.1103/PhysRevD.96.103540. arXiv: 1708.04293 [astro-ph.CO].

[34] Miguel Escudero. "Neutrino decoupling beyond the Standard Model: CMB constraints on the Dark Matter mass with a fast and precise $N_{\rm eff}$ evaluation". In: *JCAP* 1902 (2019), p. 007. DOI: 10.1088/1475-7516/2019/02/007. arXiv: 1812.05605 [hep-ph].

[35] Christopher Brust, David E. Kaplan, and Matthew T. Walters. "New Light Species and the CMB". In: *JHEP* 12 (2013), p. 058. DOI: 10.1007/JHEP12(2013)058. arXiv: 1303.5379 [hep-ph].

[36] Richard H. Cyburt et al. "Big Bang Nucleosynthesis: 2015". In: *Rev. Mod. Phys.* 88 (2016), p. 015004. DOI: 10.1103/RevModPhys.88.015004. arXiv: 1505.01076 [astro-ph.CO].

[37] Adam G. Riess et al. "New Parallaxes of Galactic Cepheids from Spatially Scanning the Hubble Space Telescope: Implications for the Hubble Constant". In: *Astrophys. J.* 855.2 (2018), p. 136. DOI: 10.3847/1538-4357/aaadb7. arXiv: 1801.01120 [astro-ph.SR].

[38] Francesco D'Eramo, Nicolas Fernandez, and Stefano Profumo. "When the Universe Expands Too Fast: Relentless Dark Matter". In: *JCAP* 1705.05 (2017), p. 012. DOI: 10.1088/1475-7516/2017/05/012. arXiv: 1703.04793 [hep-ph].

[39] Francesco D'Eramo, Nicolas Fernandez, and Stefano Profumo. "Dark Matter Freeze-in Production in Fast-Expanding Universes". In: *JCAP* 1802.02 (2018), p. 046. DOI: 10.1088/1475-7516/2018/02/046. arXiv: 1712.07453 [hep-ph].

[40] M. E. Gomez et al. "Quintessential Kination and Thermal Production of Gravitinos and Axinos". In: *JCAP* 0901 (2009), p. 027. DOI: 10.1088/1475-7516/2009/01/027. arXiv: 0809.1859 [hep-ph].

[41] K. Huang. *Statistical Mechanics*. New York: John Wiley and Sons, 2000. ISBN: 9789971512958.

[42] Paolo Gondolo and Graciela Gelmini. "Cosmic abundances of stable particles: Improved analysis". In: *Nucl. Phys.* B360 (1991), pp. 145–179. DOI: 10.1016/0550-3213(91)90438-4.

[43] J. Bernstein. *Kinetic Theory in the Expanding Universe*. Cambridge Monographs on Mathematical Physics. Cambridge, U.K.: Cambridge University Press, 1988. ISBN: 9780511564185. DOI: 10.1017/CBO9780511564185.

[44] Robert J. Scherrer and Michael S. Turner. "On the Relic, Cosmic Abundance of Stable Weakly Interacting Massive Particles". In: *Phys. Rev.* D33 (1986). [Erratum: Phys. Rev.D34,3263(1986)], p. 1585. DOI: 10.1103/PhysRevD.33.1585,10.1103/PhysRevD.34.3263.

[45] Planck collaboration. "Planck 2018 results. X. Constraints on inflation". In: (2018). arXiv: 1807.06211 [astro-ph.CO].

[46] A.R. Liddle and D.H. Lyth. *Cosmological Inflation and Large-Scale Structure*. Cosmological Inflation and Large-scale Structure. Cambridge University Press, 2000. ISBN: 9780521575980. URL: https://books.google.it/books?id=XmWauPZSovMC.

[47] Daniel Baumann. "Inflation". In: *Physics of the large and the small, TASI 09, proceedings of the Theoretical Advanced Study Institute in Elementary Particle Physics, Boulder, Colorado, USA, 1-26 June 2009*. 2011, pp. 523–686. DOI: 10.1142/9789814327183_0010. arXiv: 0907.5424 [hep-th].

[48] Michael S. Turner. "Coherent Scalar Field Oscillations in an Expanding Universe". In: *Phys. Rev.* D28 (1983), p. 1243. DOI: 10.1103/PhysRevD.28.1243.

[49] Robert J. Scherrer and Michael S. Turner. "Decaying Particles Do Not Heat Up the Universe". In: *Phys. Rev.* D31 (1985), p. 681. DOI: 10.1103/PhysRevD.31.681.

[50] David H. Lyth and Ewan D. Stewart. "Thermal inflation and the moduli problem". In: *Phys. Rev.* D53 (1996), pp. 1784–1798. DOI: 10.1103/PhysRevD.53.1784. arXiv: hep-ph/9510204 [hep-ph].

[51] Bobby Samir Acharya et al. "A Non-thermal WIMP Miracle". In: *Phys. Rev.* D80 (2009), p. 083529. DOI: 10.1103/PhysRevD.80.083529. arXiv: 0908.2430 [astro-ph.CO].

[52] Gordon L. Kane et al. "Dark matter production mechanisms with a nonthermal cosmological history: A classification". In: *Phys. Rev.* D93.6 (2016), p. 063527. DOI: 10.1103/PhysRevD.93.063527. arXiv: 1502.05406 [hep-ph].

[53] Adrienne L. Erickcek. "The Dark Matter Annihilation Boost from Low-Temperature Reheating". In: *Phys. Rev.* D92.10 (2015), p. 103505. DOI: 10.1103/PhysRevD.92.103505. arXiv: 1504.03335 [astro-ph.CO].

[54] Francesca Rosati. "Quintessential enhancement of dark matter abundance". In: *Phys. Lett.* B570 (2003), pp. 5–10. DOI: 10.1016/j.physletb.2003.07.048. arXiv: hep-ph/0302159 [hep-ph].

[55] Pierre Salati. "Quintessence and the relic density of neutralinos". In: *Phys. Lett.* B571 (2003), pp. 121–131. DOI: 10.1016/j.physletb.2003.07.073. arXiv: astro-ph/0207396 [astro-ph].

[56] Stefano Profumo and Piero Ullio. "SUSY dark matter and quintessence". In: *JCAP* 0311 (2003), p. 006. DOI: 10.1088/1475-7516/2003/11/006. arXiv: hep-ph/0309220 [hep-ph].

[57] Luca Visinelli. "(Non-)thermal production of WIMPs during kination". In: *Symmetry* 10.11 (2018), p. 546. DOI: 10.3390/sym10110546. arXiv: 1710.11006 [astro-ph.CO].

[58] S. Perlmutter et al. "Measurements of Omega and Lambda from 42 high redshift supernovae". In: *Astrophys. J.* 517 (1999), pp. 565–586. DOI: 10.1086/307221. arXiv: astro-ph/9812133 [astro-ph].

[59] Adam G. Riess et al. "Observational evidence from supernovae for an accelerating universe and a cosmological constant". In: *Astron. J.* 116 (1998), pp. 1009–1038. DOI: 10.1086/300499. arXiv: astro-ph/9805201 [astro-ph].

[60] Sean M. Carroll. "The Cosmological constant". In: *Living Rev. Rel.* 4 (2001), p. 1. DOI: 10.12942/lrr-2001-1. arXiv: astro-ph/0004075 [astro-ph].

[61] P. J. E. Peebles and Bharat Ratra. "The Cosmological constant and dark energy". In: *Rev. Mod. Phys.* 75 (2003). [,592(2002)], pp. 559–606. DOI: 10.1103/RevModPhys.75.559. arXiv: astro-ph/0207347 [astro-ph].

[62] Edmund J. Copeland, M. Sami, and Shinji Tsujikawa. "Dynamics of dark energy". In: *Int. J. Mod. Phys.* D15 (2006), pp. 1753–1936. DOI: %%10.1142/S021827180600942X%%. arXiv: hep-th/0603057 [hep-th].

[63] Bharat Ratra and P. J. E. Peebles. "Cosmological Consequences of a Rolling Homogeneous Scalar Field". In: *Phys. Rev.* D37 (1988), p. 3406. DOI: 10.1103/PhysRevD.37.3406.

[64] P. J. E. Peebles and Bharat Ratra. "Cosmology with a Time Variable Cosmological Constant". In: *Astrophys. J.* 325 (1988), p. L17. DOI: 10.1086/185100.

[65] Christof Wetterich. "The Cosmon model for an asymptotically vanishing time dependent cosmological 'constant'". In: *Astron. Astrophys.* 301 (1995), pp. 321–328. arXiv: hep-th/9408025 [hep-th].

[66] Ivaylo Zlatev, Li-Min Wang, and Paul J. Steinhardt. "Quintessence, cosmic coincidence, and the cosmological constant". In: *Phys. Rev. Lett.* 82 (1999), pp. 896–899. DOI: 10.1103/PhysRevLett.82.896. arXiv: astro-ph/9807002 [astro-ph].

[67] Paul J. Steinhardt, Li-Min Wang, and Ivaylo Zlatev. "Cosmological tracking solutions". In: *Phys. Rev.* D59 (1999), p. 123504. DOI: 10.1103/PhysRevD.59.123504. arXiv: astro-ph/9812313 [astro-ph].

[68] Edmund J. Copeland, Andrew R Liddle, and David Wands. "Exponential potentials and cosmological scaling solutions". In: *Phys. Rev.* D57 (1998), pp. 4686–4690. DOI: 10.1103/PhysRevD.57.4686. arXiv: gr-qc/9711068 [gr-qc].

[69] Pedro G. Ferreira and Michael Joyce. "Cosmology with a primordial scaling field". In: *Phys. Rev.* D58 (1998), p. 023503. DOI: 10.1103/PhysRevD.58.023503. arXiv: astro-ph/9711102 [astro-ph].

[70] J. J. Halliwell. "Scalar Fields in Cosmology with an Exponential Potential". In: *Phys. Lett.* B185 (1987), p. 341. DOI: 10.1016/0370-2693(87)91011-2.

[71] John D. Barrow. "String-Driven Inflationary and Deflationary Cosmological Models". In: *Nucl. Phys.* B310 (1988), pp. 743–763. DOI: 10.1016/0550-3213(88)90101-0.

[72] F. Lucchin and S. Matarrese. "Power Law Inflation". In: *Phys. Rev.* D32 (1985), p. 1316. DOI: 10.1103/PhysRevD.32.1316.

[73] C. Wetterich. "Kaluza-Klein Cosmology and the Inflationary Universe". In: *Nucl. Phys.* B252 (1985), pp. 309–320. DOI: 10.1016/0550-3213(85)90445-6.

[74] P. K. Townsend. "Quintessence from M theory". In: *JHEP* 11 (2001), p. 042. DOI: 10.1088/1126-6708/2001/11/042. arXiv: hep-th/0110072 [hep-th].

[75] E. Cremmer et al. "Naturally Vanishing Cosmological Constant in N=1 Supergravity". In: *Phys. Lett.* 133B (1983), p. 61. DOI: 10.1016/0370-2693(83)90106-5.

[76] John R. Ellis et al. "No-Scale Supersymmetric Standard Model". In: *Phys. Lett.* 134B (1984), p. 429. DOI: 10.1016/0370-2693(84)91378-9.

[77] Edward Witten. "Dimensional Reduction of Superstring Models". In: *Phys. Lett.* 155B (1985), p. 151. DOI: 10.1016/0370-2693(85)90976-1.

[78] Edmund J. Copeland, Andrew R. Liddle, and James E. Lidsey. "Steep inflation: Ending brane world inflation by gravitational particle production". In: *Phys. Rev.* D64 (2001), p. 023509. DOI: 10.1103/PhysRevD.64.023509. arXiv: astro-ph/0006421 [astro-ph].

[79] Urbano França and Rogerio Rosenfeld. "Fine tuning in quintessence models with exponential potentials". In: *JHEP* 10 (2002), p. 015. DOI: 10.1088/1126-6708/2002/10/015. arXiv: astro-ph/0206194 [astro-ph].

[80] Christopher F. Kolda and William Lahneman. "Exponential quintessence and the end of acceleration". In: (2001). arXiv: hep-ph/0105300 [hep-ph].

[81] James M. Cline. "Quintessence, cosmological horizons, and self-tuning". In: *JHEP* 08 (2001), p. 035. DOI: 10.1088/1126-6708/2001/08/035. arXiv: hep-ph/0105251 [hep-ph].

[82] C. Pallis. "Quintessential kination and cold dark matter abundance". In: *JCAP* 0510 (2005), p. 015. DOI: 10.1088/1475-7516/2005/10/015. arXiv: hep-ph/0503080 [hep-ph].

[83] Justin Khoury et al. "The Ekpyrotic universe: Colliding branes and the origin of the hot big bang". In: *Phys. Rev.* D64 (2001), p. 123522. DOI: 10.1103/PhysRevD.64.123522. arXiv: hep-th/0103239 [hep-th].

[84] Laura Lopez-Honorez, Thomas Schwetz, and Jure Zupan. "Higgs portal, fermionic dark matter, and a Standard Model like Higgs at 125 GeV". In: *Phys. Lett.* B716 (2012), pp. 179–185. DOI: 10.1016/j.physletb.2012.07.017. arXiv: 1203.2064 [hep-ph].

[85] Michael A. Fedderke et al. "The Fermionic Dark Matter Higgs Portal: an effective field theory approach". In: *JHEP* 08 (2014), p. 122. DOI: 10.1007/JHEP08(2014)122. arXiv: 1404.2283 [hep-ph].

[86] Xiaoyong Chu, Thomas Hambye, and Michel H. G. Tytgat. "The Four Basic Ways of Creating Dark Matter Through a Portal". In: *JCAP* 1205 (2012), p. 034. DOI: 10.1088/1475-7516/2012/05/034. arXiv: 1112.0493 [hep-ph].

[87] Mattias Blennow, Enrique Fernandez-Martinez, and Bryan Zaldivar. "Freeze-in through portals". In: *JCAP* 1401 (2014), p. 003. DOI: 10.1088/1475-7516/2014/01/003. arXiv: 1309.7348 [hep-ph].

[88] Jing-Yuan Chen, Edward W. Kolb, and Lian-Tao Wang. "Dark matter coupling to electroweak gauge and Higgs bosons: an effective field theory approach". In: *Phys. Dark Univ.* 2 (2013), pp. 200–218. DOI: 10.1016/j.dark.2013.11.002. arXiv: 1305.0021 [hep-ph].

[89] Thomas Hambye. "On the stability of particle dark matter". In: *PoS* IDM2010 (2011), p. 098. DOI: 10.22323/1.110.0098. arXiv: 1012.4587 [hep-ph].

[90] Yann Mambrini, Stefano Profumo, and Farinaldo S. Queiroz. "Dark Matter and Global Symmetries". In: *Phys. Lett.* B760 (2016), pp. 807–815. DOI: 10.1016/j.physletb.2016.07.076. arXiv: 1508.06635 [hep-ph].

[91] Gian F. Giudice and Matthew McCullough. "A Clockwork Theory". In: *JHEP* 02 (2017), p. 036. DOI: 10.1007/JHEP02(2017)036. arXiv: 1610.07962 [hep-ph].

[92] A. Jeffrey and D. Zwillinger. *Table of Integrals, Series, and Products*. Elsevier Science, 2000. ISBN: 9780080542225.

[93] T. Moroi, H. Murayama, and Masahiro Yamaguchi. "Cosmological constraints on the light stable gravitino". In: *Phys. Lett.* B303 (1993), pp. 289–294. DOI: 10.1016/0370-2693(93)91434-O.

[94] R. R. Caldwell, Rahul Dave, and Paul J. Steinhardt. "Cosmological imprint of an energy component with general equation of state". In: *Phys. Rev. Lett.* 80 (1998), pp. 1582–1585. DOI: 10.1103/PhysRevLett.80.1582. arXiv: astro-ph/9708069 [astro-ph].

[95] Carl L. Gardner. "Quintessence and the transition to an accelerating universe". In: *Nucl. Phys.* B707 (2005), pp. 278–300. DOI: 10.1016/j.nuclphysb.2004.11.065. arXiv: astro-ph/0407604 [astro-ph].

[96] Konstantinos Dimopoulos and J. W. F. Valle. "Modeling quintessential inflation". In: *Astropart. Phys.* 18 (2002), pp. 287–306. DOI: 10.1016/S0927-6505(02)00115-9. arXiv: astro-ph/0111417 [astro-ph].

[97] Richard H. Cyburt et al. "New BBN limits on physics beyond the standard model from ^4He". In: *Astropart. Phys.* 23 (2005), pp. 313–323. DOI: 10.1016/j.astropartphys.2005.01.005. arXiv: astro-ph/0408033 [astro-ph].

[98] Francesco D'Eramo. "Dark matter and Higgs boson physics". In: *Phys. Rev.* D76 (2007), p. 083522. DOI: 10.1103/PhysRevD.76.083522. arXiv: 0705.4493 [hep-ph].

[99] Timothy Cohen et al. "Singlet-Doublet Dark Matter". In: *Phys. Rev.* D85 (2012), p. 075003. DOI: 10.1103/PhysRevD.85.075003. arXiv: 1109.2604 [hep-ph].

[100] David Curtin et al. "Long-Lived Particles at the Energy Frontier: The MATHUSLA Physics Case". In: *Rept. Prog. Phys.* 82.11 (2019), p. 116201. DOI: 10.1088/1361-6633/ab28d6. arXiv: 1806.07396 [hep-ph].

[101] CMB-S4 collaboration. "CMB-S4 Science Book, First Edition". In: (2016). arXiv: 1610.02743 [astro-ph.CO].

[102] Luca Amendola et al. "Cosmology and fundamental physics with the Euclid satellite". In: *Living Rev. Rel.* 21.1 (2018), p. 2. DOI: 10.1007/s41114-017-0010-3. arXiv: 1606.00180 [astro-ph.CO].

[103] Alexander Friedmann. "Über die krümmung des raumes". In: *Zeitschrift fur Physik* 10 (1922), pp. 377–386; Georges Lemaıtre. "Expansion of the universe, A homogeneous universe of constant mass and increasing radius accounting for the radial velocity of extra-galactic nebulae". In: *Monthly Notices of the Royal Astronomical Society* 91 (1931), pp. 483–490; Howard P Robertson. "Kinematics and World-Structure III." In: *The Astrophysical Journal* 83 (1936), p. 257; Arthur Geoffrey Walker. "On Milne's Theory of World-Structure". In: *Proceedings of the London Mathematical Society* 2.1 (1937), pp. 90–127.

[104] Steven Weinberg. *Gravitation and Cosmology*. New York: John Wiley and Sons, 1972. ISBN: 9780471925675.

[105] Lars Husdal. "On Effective Degrees of Freedom in the Early Universe". In: *Galaxies* 4.4 (2016), p. 78. DOI: 10.3390/galaxies4040078. arXiv: 1609.04979 [astro-ph.CO].

[106] Manuel Drees, Fazlollah Hajkarim, and Ernany Rossi Schmitz. "The Effects of QCD Equation of State on the Relic Density of WIMP Dark Matter". In: *JCAP* 1506.06 (2015), p. 025. DOI: 10.1088/1475-7516/2015/06/025. arXiv: 1503.03513 [hep-ph].

[107] A. Bazavov et al. "Equation of state in (2+1)-flavor QCD". In: *Phys. Rev.* D90 (2014), p. 094503. DOI: 10.1103/PhysRevD.90.094503. arXiv: 1407.6387 [hep-lat].

[108] Milton Abramowitz and Irene A Stegun. *Handbook of mathematical functions: with formulas, graphs, and mathematical tables*. Vol. 55. Courier Corporation, 1965.

[109] Michael E. Peskin and Daniel V. Schroeder. *An Introduction to quantum field theory*. Reading, USA: Addison-Wesley, 1995. ISBN: 9780201503975.

[110] S. R. De Groot. *Relativistic Kinetic Theory. Principles and Applications*. Ed. by W. A. Van Leeuwen and C. G. Van Weert. 1980.

[111] L. D. Landau and E. M. Lifshitz. *The Classical Theory of Fields*. Vol. 2. Course of Theoretical Physics. Oxford: Pergamon Press, 1975. ISBN: 9780080181769.

[112] M. Cannoni. "Relativistic $< \sigma v_{\rm rel} >$ in the calculation of relics abundances: a closer look". In: *Phys. Rev.* D89.10 (2014), p. 103533. DOI: 10.1103/PhysRevD.89.103533. arXiv: 1311.4494 [astro-ph.CO]; M. Cannoni. "Lorentz invariant relative velocity and relativistic binary collisions". In: *Int. J. Mod. Phys.* A32.02n03 (2017), p. 1730002. DOI: 10.1142/S0217751X17300022. arXiv: 1605.00569 [hep-ph].